Evaluation of five dry particle deposition parameterizations for incorporation into atmospheric transport models

Tanvir R. Khan, Judith A. Perlinger

Department of Civil and Environmental Engineering, Michigan Technological University, Houghton, Michigan 49931, United States

Correspondence to: Judith A. Perlinger (jperl@mtu.edu)

Abstract. Despite considerable effort to develop mechanistic dry particle deposition parameterizations for atmospheric transport models, current knowledge has been inadequate to propose quantitative measures of the relative performance of available parameterizations. In this study, we evaluated the performance of five dry particle deposition parameterizations developed by Zhang et al. (2001) (*Z01*), Petroff and Zhang (2010) (*PZ10*), Kouznetsov and Sofiev (2012) (*KS12*), Zhang and He (2014) (*ZH14*), and Zhang and Sao (2014) (*ZS14*), respectively. The evaluation was performed in three dimensions: model ability to reproduce observed deposition velocities, V_d (*accuracy*), the influence of imprecision in input parameter values on the modeled V_d (*uncertainty*), and identification of the most influential parameter(s) (*sensitivity*). The accuracy of the modeled V_d was evaluated using observations obtained from five land use categories (LUCs): grass, coniferous and deciduous forests, natural water, and ice/snow. To ascertain the uncertainty in modeled V_d, and quantify the influence of imprecision in key model input parameters, a Monte Carlo uncertainty analysis was performed. The Sobol' sensitivity analysis was conducted with the objective to determine the parameter ranking, from the most to the least influential. Comparing the normalized mean bias factors (indicator of accuracy), we find that the *ZH14* parameterization is the most accurate for all LUCs except for coniferous forest, for which it is second most accurate. From Monte Carlo simulations, the estimated mean normalized uncertainties in the modeled V_d obtained for seven particle sizes (ranging from 0.005 to 2.5 μm) for the five LUCs are 17%, 12%, 13%, 16%, and 27% for the *Z01*, *PZ10*, *KS12*, *ZH14*, and *ZS14* parameterizations, respectively. From the Sobol' sensitivity results, we suggest that the parameter rankings vary by particle size and LUC for a given parameterization. Overall, for d_p = 0.001 to 1.0 μm, friction velocity was one of the three most influential parameters in all parameterizations. For giant particles (d_p = 10 μm), relative humidity was the most influential parameter. Because it is the least complex of the five parameterizations, and it has the greatest accuracy and least uncertainty, we propose that the *ZH14* parameterization is currently superior for incorporation into atmospheric transport models.

1. Introduction

Dry deposition is a complex process that is influenced by the chemical properties of aerosols and their sources, meteorological conditions, and surface characteristic features. The transference of particles from the atmosphere to the earth's surface is controlled by forcings such as frictional drag and terrain induced flow modification (Giorgi, 1986; Stull, 1988). Understanding the processes and factors controlling dry deposition is necessary to estimate the residence time of atmospheric particles, which governs their atmospheric transport distance, trans-boundary fluxes, and potential climate effects (IPCC, 2001; Nemitz et al., 2002; Pryor et al., 2008). An accurate estimation of dry deposition is also needed to quantify the atmospheric loads of particles containing sulfate, nitrate, and ammonium that contribute to acidification and eutrophication of ecosystems, toxic elements such as Pb, Zn, and Cd, and base cations such as Na^+, K^+, Ca^{2+}, and Mg^{2+} that alter the nutrient cycling in soil (Ruijgrok et al., 1995; Petroff et al., 2008a).

Over the last three decades, several indirect and direct methods were developed to measure dry particle deposition (hereinafter referred to as dry deposition) flux to ecosystems (McMahon and Denisot, 1979; Sehmel, 1980; Gallagher et al., 1997;

Zhang and Vet, 2006; Pryor et al., 2008). Dry deposition velocity V_d at height z is defined as the ratio of the total flux $F(z)$ divided by the particle concentration at the same height $C(z)$ (Pryor et al., 2013; Rannik et al., 2016) and is mathematically expressed as:

$$V_d = -\frac{F(z)}{C(z)} \quad (1)$$

One of the major limitations of direct flux measurement is limited spatial coverage because the measurement stations are confined to only a limited number of sites (Nemitz et al., 2002). The application of spatially and temporally resolved 3-D atmospheric transport models, from regional to global scale, can produce estimates of dry deposition fluxes for a suite of atmospheric species over various natural surfaces such as bare soil, grass, forest canopies, water, and ice/snow. To predict the dry deposition fluxes using atmospheric transport models, a parameterization/scheme that can adequately account for the major physical processes of particle deposition (e.g., turbulent diffusion, gravitational settling, interception, impaction, and Brownian diffusion) must be embedded in the host model.

Many dry deposition models have been developed for scientific research and operational purposes (see model review by Petroff et al., 2008a). Significant advances in understanding the governing mechanisms of dry deposition were made through use of experimental deposition data on walls of vertical pipes in the developments of size-resolved parameterizations for atmospheric particle deposition on ground surface (Muyshondt et al., 1998; Noll et al., 2001; Feng et al., 2008). In mechanistic or process-based dry deposition models, an electrical resistance based approach is widely used to parameterize the dry deposition velocity (Venkatram and Pleim, 1999). In this approach, dry deposition occurs via two parallel pathways: turbulent diffusion (expressed as aerodynamic resistance) and gravitational settling (expressed as resistance due to gravitation). In addition, particle collection by surfaces via Brownian diffusion, interception, and impaction are represented using separate surface resistance terms (Slinn, 1982; Hicks et al., 1987; Wesely and Hicks, 2000; Zhang et al., 2001; Seinfeld and Pandis, 2006; Petroff and Zhang, 2010; Zhang and He, 2014). In all these models, the conventional resistance-based approach does not consider surface inhomogeneity or terrain complexity (i.e., deposition over flat terrain is assumed). However, Hicks (2008) argued about the importance of considering terrain complexity in dry deposition models because the assumption of surface homogeneity in existing deposition models limits the accuracy of pollutant load estimation in sensitive ecosystems that are located in complex terrain (e.g., on mountaintops or hills).

Despite considerable efforts in developing dry deposition parameterizations of varying complexity, there remain considerable gaps in systematic performance evaluation of existing schemes with reliable field measurements. We note that the evaluation of dry deposition parameterizations with field measurements is very limited and not up to date. Van Aalst (1986) evaluated the performance of six dry deposition parameterizations against field measurements, and reported large discrepancies in terms of the modeled deposition velocities. He reported that over water surfaces the modeled deposition velocities for 1.0-μm particles by the Williams (1982) scheme were factors of 10 to 50 higher than those predicted by the Sehmel and Hodgson (1978) scheme. For forest canopy, the Wiman and Agren (1985) model over-predicted the deposition velocities of the Slinn (1982) model by a factor of five. In a recent study, Hicks et al. (2016) compared five deposition models with measurements conducted over forests. They found that for particle sizes less than ca. 0.2 μm, the modeled deposition velocities agreed fairly well with measured velocities. The largest discrepancy was observed for particle sizes of 0.3 to ca. 5.0 μm. Studies also suggest that in many dry deposition parameterizations, the largest uncertainty exists for 0.1-1.0 μm particles because of the differing treatments of some key particle deposition processes such as Brownian diffusion (Van Aalst, 1986; Petroff and Zhang, 2010; Zhang and Sao, 2014).

Uncertainty in modeled dry deposition velocities is an area that requires a thorough investigation. Only a few studies have been conducted in quantifying the uncertainties in dry deposition parameterizations. Ruijgrok et al. (1992) performed an uncertainty evaluation of the Slinn (1982) model by assessing the variabilities in nine input parameters to the model outputs. Using

Slinn's model, Gould and Davidson (1992) determined the influence of uncertainties in the size of the collection elements, roughness length, canopy wind profile and wind speed on the modeled deposition velocities. As far as we know, a detailed uncertainty analysis to address the influence of varying particle size, meteorological conditions, and surface features has not been performed on existing dry deposition parameterizations. The results from an uncertainty analysis could be used as one of the model's performance indicators, and help guide the modeling community to adequately account for uncertainties in the modeled deposition fluxes of pollutants to ecosystems.

Sensitivity analysis is often performed to determine the most influential parameters to the model outputs. Typically, a dry deposition model incorporates a large number of input parameters, which are subject to variability. In addition to identifying the most sensitive parameter(s), a sensitivity analysis can provide important insight as to the processes that control the overall deposition process, and identify those that may require further improvement. However, a detailed sensitivity test that encompasses exploring the entire parameter spaces of the input parameters of a dry deposition parameterization has not yet been performed. Some researchers conducted one-at-a-time (OAT) sensitivity analysis (SA) (Ruijgrok et al., 1997; Zhang et al., 2001) of dry deposition models. In OAT-SA, the effect of varying one model input parameter is tested at a time while keeping all others fixed (Salteli and Annoni, 2010). Because in reality the variabilities in a set of model input parameters are expected to occur simultaneously, an OAT-SA is not a useful tool to determine the most influential parameter(s) in the deposition models. Rather, a variance-based global sensitivity test approach is needed. In global sensitivity analysis, the potential effects from simultaneous variabilities of model input parameters over their plausible range is considered (Lilburne and Tarantola, 2008).

In the present study, five dry deposition parameterizations, developed by Zhang et al. (2001), Petroff and Zhang (2010), Kouznetsov and Sofiev (2012), Zhang and He (2014), and Zhang and Sao (2014), are selected for an intercomparison of performance in terms of accuracy, uncertainty, and sensitivity. Throughout this paper, these models are referred to as *Z01*, *PZ10*, *KS12*, *ZH14*, and *ZS14*, respectively. The objectives of this study are threefold. The first objective is to evaluate the accuracy of five dry deposition parameterizations using measured dry deposition velocities obtained from field observations. Data of measured deposition velocities were collected from the literature, which comprised of measurements conducted over land use categories (LUCs) including grass, coniferous and deciduous forests, natural water, and ice/snow. The second objective is to perform an uncertainty analysis of the modeled dry deposition velocities related to imprecision in model input parameter values. The third objective is to quantify the most influential parameters in the modeled dry deposition velocities by applying a global variance-based sensitivity analysis.

2. Background

The five dry deposition schemes used in this paper are described briefly below. For each scheme, the major expressions/equations used to compute the dry deposition velocities are provided.

2.1. *Zhang et al. (2001) (Z01) scheme*

The *Z01* scheme estimates dry deposition velocity as a function of particle size and density, meteorological variables, and surface properties. In the *Z01* scheme, the dry deposition velocity (V_d) is expressed as:

$$V_d = V_g + \frac{1}{R_a + R_s}, \tag{2}$$

where V_g is the gravitational settling velocity, R_a is the aerodynamic resistance above the canopy, and R_s is the surface resistance. The expression for gravitational settling velocity (V_g) is given as:

$$V_g = \frac{\rho d_p^2 g C}{18\eta_V}, \tag{3}$$

where ρ is the dry density of the particle, d_p is the particle aerodynamic diameter, g is the gravitational acceleration, C is the Cunningham correction factor, and η_V is the temperature dependent viscosity coefficient of air. The correction factor C is applied to account for the molecular structure of the air and is expressed as:

$$C = 1 + \frac{2\lambda}{d_p}\left(1.257 + 0.4e^{-\frac{0.55 d_p}{\lambda}}\right), \quad (4)$$

where λ is the mean free path of air molecules.

The aerodynamic resistance (R_a) is calculated as:

$$R_a = \frac{\ln\left(\frac{z_R}{z_0}\right) - \psi_H}{\kappa u_*}, \quad (5)$$

where z_R is the reference height where V_d is typically computed, z_0 is the roughness height, κ is the von Kármán constant, u_* is the friction velocity, and ψ_H is the stability function for heat. The expression for ψ_H is: $\psi_H = 2ln[0.5(1 + (1 - 16x)^{0.5}]$ when $x \in [-2; 0]$, and $\psi_H = -5x$ when $x \in [0; 1]$. Here, $x = z/L_O$, where z is the measurement height and L_O is the Monin-Obukhov length.

The surface resistance term, R_s in Eq. 2, is a function of particle collection efficiencies due to Brownian diffusion (E_B), impaction (E_{IM}), and interception (E_{IN}). Accordingly, R_s is parameterized as:

$$R_s = \frac{1}{\varepsilon_0 u_* (E_B + E_{IM} + E_{IN}) R_1}, \quad (6)$$

where ε_0 is an empirical constant and its value is taken as 3 for all LUCs, and R_1 is the correction factor for particle rebound, which is included to modify the collection efficiencies at the surface. R_1 is parameterized as a function of Stokes number (St) as:

$$R_1 = \exp(-St^{-0.5}). \quad (7)$$

The parameterizations for E_B, E_{IM}, and E_{IN} are expressed by Eqs. (8), (10), and (14), respectively. The particle collection efficiency (E_B) is parameterized as a function of Schmidt number (Sc) as:

$$E_B = Sc^{-\gamma}, \quad (8)$$

where Sc is the ratio of kinematic viscosity of air (ν) to the particle Brownian diffusivity (D). γ is a LUC dependent variable, and the typical values of γ range from 0.54 to 0.56 for rough surfaces and from 0.50 to 0.56 for smooth surfaces. Brownian diffusivity (D) is calculated as:

$$D = \frac{C k_B T}{3\pi\mu d_p}, \quad (9)$$

where C is the Cunningham correction factor as expressed by Eq. (4), k_B is the Boltzmann's constant (1.38×10^{-23} J K^{-1}), and μ is the dynamic viscosity of air at temperature T.

For smooth surfaces, particle collection efficiency by impaction (E_{IM}) is parameterized as:

$$E_{IM} = 10^{-\frac{3}{St}}. \quad (10)$$

And, for rough surfaces,

$$E_{IM} = \left(\frac{St}{\alpha + St}\right)^{\beta}, \quad (11)$$

where α and β are constants; values of α are LUC dependent, and β is taken as 2. In Eqs. (10-11), the Stokes number (St) is expressed as:

$$St = \frac{V_g u_*}{gA} \quad \text{(for vegetative surfaces)}, \quad (12)$$

$$St = \frac{V_g u_*^2}{\nu} \quad \text{(for smooth surfaces)}, \quad (13)$$

where A is the characteristic radius of the surface collector elements. The values of A are given for different LUCs for various seasons by Zhang et al. (2001).

Collection efficiency by interception (E_{IN}) is calculated as:

$$E_{IN} = \frac{1}{2}\left(\frac{d_p}{A}\right)^2. \quad (14)$$

Growth of particles under humid conditions is considered in the *Z01* scheme by replacing the d_p with a wet particle diameter (d_w), which is calculated as:

$$d_w = \left[\frac{C_1\left(\frac{d_p}{2}\right)^{C_2}}{C_3\left(\frac{d_p}{2}\right)^{C_4} - logRH} + \left(\frac{d_p}{2}\right)^{C_3}\right]^{1/3}, \quad (15)$$

where C_1, C_2, C_3, and C_4 are the empirical constants (values given in Table 1 of Zhang et al., 2001), and RH is the relative humidity.

2.2. *Petroff and Zhang (2010) (PZ10) scheme*

Petroff and Zhang (2010) parameterized dry deposition velocity using an expression similar to Eq. (2) with some improvements of the surface resistance and collection efficiency terms. In the *PZ10* scheme, the effect of gravity and drift forces (e.g., phoretic effects) were taken into account by introducing the term drift velocity (V_{drift}). Thus, dry deposition velocity (V_d) at a reference height (z_R) is given as:

$$V_d = V_{drift} + \frac{1}{R_a + R_s}. \quad (16)$$

Here, the drift velocity V_{drift} is equal to the sum of gravitational settling velocity and phoretic velocity, and the expression of V_{drift} is:

$$V_{drift} = V_g + V_{phor}. \quad (17)$$

V_g is calculated using Eq. (3). The LUC dependent values of V_{phor} were given by Petroff and Zhang (2010).

Surface resistance (R_s) is commonly expressed as an inverse of the surface deposition velocity, V_{ds} (i.e., $R_s = 1/V_{ds}$). In the *PZ10* scheme, V_{ds} is parameterized as:

$$\frac{V_{ds}}{u_*} = E_g \frac{1 + \left[\frac{Q}{Q_g} - \frac{\alpha}{2}\right]\frac{\tanh(\eta)}{\eta}}{1 + \left[\frac{Q}{Q_g} + \alpha\right]\frac{\tanh(\eta)}{\eta}}. \quad (18)$$

The parameters (e.g., Q, Q_g, α, and η) used in Eq. (18) are dependent on the aerodynamic and surface characteristic features. The parameterization of the total particle collection efficiency on the ground below the vegetation (E_g) has two components: (i) collection by Brownian diffusion (E_{gb}) and (ii) collection by turbulent impaction (E_{gt}). In the *PZ10* scheme, formulation of E_{gb} is expressed as:

$$E_{gb} = \frac{Sc^{-2/3}}{14.5}\left[\frac{1}{6} ln\frac{(1+F)^2}{1-F+F^2} + \frac{1}{\sqrt{3}} Arctan\frac{2F-1}{\sqrt{3}} + \frac{\pi}{6\sqrt{3}}\right]^{-1}, \quad (19)$$

where F is a function of the Schmidt number (Sc) and is expressed as $F = Sc^{\frac{1}{3}}/2.9$.

Collection efficiency by turbulent impaction, E_{gt}, is a function of dimensionless particle relaxation time (τ_{ph}^+) and a coefficient C_{IT} (taken as 0.14). In the *PZ10* scheme, E_{gt} is parameterized as:

$$E_{gt} = 2.5 \times 10^{-3} C_{IT} \tau_{ph}^{+2}. \quad (20)$$

τ_{ph}^+ is calculated as $\tau_{ph}^+ = \tau_p u_f^2 / \nu$. The local friction velocity (u_f) is expressed as:

$$u_f = u_* e^{-\alpha}, \quad (21)$$

where α is the aerodynamic extinction coefficient and is expressed as:

$$\alpha = \left(\frac{k_x LAI}{12\kappa^2(1-\frac{d}{h})^2}\right)^{1/3} \Phi_m^{2/3}\left(\frac{h-d}{L_O}\right). \quad (22)$$

In Eq. (20), k_x is the inclination coefficient of canopy elements, LAI is the leaf area index, d is the zero-plane displacement height, h is the height of the canopy, L_O is the Monin-Obukhov length, and Φ_m is the non-dimensional stability function for momentum. The expressions for Φ_m is, $\Phi_m(x) = (1-16x)^{-1/4}$ when $x \in [-2{:}\,0]$ and $\Phi_m(x) = (1+5x)^{-1/4}$ when $x \in [0{:}\,1]$.

In Eq. (18), the non-dimensional time-scale parameter, Q, is defined as the ratio the turbulent transport time scale to the vegetation collection time scale. The magnitude of Q can be used to characterize the dominant mechanism of the vertical transport of particles to the surface. For particle deposition over a canopy, $Q \ll 1$ describes a condition in which homogeneous concentration of Aitken and accumulation mode particles prevails throughout the canopy. This condition occurs when turbulent mixing is very efficient and transfer of particles is limited by the collection efficiency on leaves. In contrast, $Q \gg 1$ characterizes a situation in which an inhomogeneous particle concentration within the canopy prevails, which is typical for coarse mode particles. Under such conditions, efficient collection of particles by leaves takes place and transfer to the surface is usually limited by the turbulent transport.

In the *PZ10* scheme, Q and Q_g are parameterized using Eqs. (23) and (24), respectively:

$$Q = \frac{LAI E_T h}{l_{mp}(h)}, \tag{23}$$

$$Q_g = \frac{E_g h}{l_{mp}(h)}, \tag{24}$$

where E_T is the total particle collection efficiency by various physical processes and $l_{mp}(h)$ is the mixing height for the particles. The mixing height for particles, $l_{mp}(h)$, is calculated as:

$$l_{mp}(h) = \frac{\kappa(h-d)}{\Phi_h\left(\frac{h-d}{L_O}\right)}, \tag{25}$$

where Φ_h is the stability function for heat and expressed as: $\Phi_h(x) = (1-16x)^{-1/2}$ when $x \in [-2; 0]$ and $\Phi_h(x) = 1+5x$ when $x \in [0; 1]$.

The total collection efficiency (E_T) is expressed as:

$$E_T = \frac{U_h}{u_*}(E_B + E_{IN} + E_{IM}) + E_{IT}, \tag{26}$$

where U_h is the horizontal wind speed at canopy height h, and E_B, E_{IN}, E_{IM}, and E_{IT} are the collection efficiencies by Brownian diffusion, interception, impaction, and turbulent impaction, respectively. Note that the physical meaning of the first three efficiency terms are similar to those of the *Z01* scheme. However, the parameterizations of these terms differ from the *Z01* scheme. The term describing turbulent impaction efficiency (E_{IT}) is absent in the *Z01* scheme.

Parameterization of deposition efficiencies (i.e., E_B, E_{IN}, E_{IM}, and E_{IT}) are given below according to the *PZ10* scheme:

Particle collection efficiency by Brownian diffusion (E_B):

$$E_B = C_B Sc^{-2/3} Re_h^{-1/2}. \tag{27}$$

In Eq. (27), C_B is the LUC dependent coefficient, Re_h is the Reynolds number of the horizontal air flow calculated at top of the canopy height h as $Re_h = \frac{U_h L}{\nu}$. Here, L is the LUC dependent characteristic length of the canopy obstacle elements.

Particle collection efficiency by interception (E_{IN}):

$$E_{IN} = C_B \frac{d_p}{L} \ (for\ needle-like\ obstacle), \tag{28}$$

$$E_{IN} = C_B \frac{d_p}{L}\left[2 + ln\frac{4L}{d_p}\right] \ (for\ leaf\ of\ plane\ obstacle). \tag{29}$$

In Eqs. 28-29, C_B is the LUC dependent coefficient.

Particle collection efficiency by impaction (E_{IM}):

$$E_{IM} = C_{IM}\left(\frac{St_h}{St_h+\beta_{IM}}\right)^2. \quad (30)$$

In Eq. (30), St_h is the Stokes number on top of the canopy, which is calculated as $St_h = \frac{\tau_p U_h}{L}$. τ_p is the particle relaxation time calculated as $\tau_p = V_g/g$. C_{IM} and β_{IM} are LUC dependent coefficients.

Particle collection efficiency by turbulent impaction (E_{IT}) is parameterized as:

$$E_{IT} = 2.5 \times 10^{-3} C_{IT} \tau_{ph}^{+2} \qquad if\ \tau_{ph}^{+} \le 20, \quad (31)$$

$$E_{IT} = C_{IT} \qquad if\ \tau_{ph}^{+} \ge 20, \quad (32)$$

In Eqs. (31-32), the dimensionless particle relaxation time, $\tau_{ph}^{+} = \tau_p u_*^2/\nu$.

The term η in Eq. (18) is taken as:

$$\eta = \sqrt{\frac{\alpha^2}{4}} + Q. \quad (33)$$

For non-vegetative surfaces, such as bare soil, natural water and ice/snow, a modified form of Eq. (16) is used in the form of Eq. (34), which is expressed as:

$$V_d = V_{drift} + \frac{1}{R_a + 1/(E_{gb} u_*)}. \quad (34)$$

2.3. Kouznetsov and Sofiev (2012) (*KS12)* scheme

Kouznetsov and Sofiev (2012) developed a dry deposition parameterization by extending the conventional resistance-based analogy using the exact solution of the steady-state equation for aerosol flux. According to the *KS12* scheme, for rough surfaces, dry deposition velocity (V_d) is computed as:

$$V_d = V_{diff} + V_{int} + V_{imp} + V_g, \quad (35)$$

where V_{diff}, V_{int}, V_{imp}, and V_g are the velocities for the depositing particles due to Brownian diffusion, interception, impaction, and gravitational settling, respectively. The parameterizations for these terms are provided below.

V_{diff} was parameterized as:

$$V_{diff} = 2u_* Re_*^{-1/2} Sc^{-2/3}, \quad (36)$$

where Re_* is the canopy Reynolds number given by

$$Re_* = \frac{u_* a}{\nu}, \quad (37)$$

where a is the length scale for different LUCs.

V_{int} is parameterized as:

$$V_{int} = u_* Re_*^{1/2}\left(\frac{d_p}{a}\right)^2, \quad (38)$$

V_{imp} is parameterized as:

$$V_{imp} = \frac{2u_*^2}{U_{top}} \eta_{imp}\left(St - \frac{u_*}{U_{top}} Re_*^{-1/2}\right), \quad (39)$$

where U_{top} is the mean horizontal wind speed on top of the canopy, η_{imp} is the particle collection efficiency due to impaction, and St is the Stokes number. Kouznetsov and Sofiev (2012) used Eq. (40) to parameterize $\frac{u_*}{U_{top}}$ as:

$$\frac{u_*}{U_{top}} = min\left[(C_s + C_R LAI/2)^2, \left(\frac{u_*}{U_{top}}\right)_{max}\right], \quad (40)$$

where C_s = 0.003, C_R = 0.3, and $\left(\frac{u_*}{U_{top}}\right)_{max}$ = 0.3 are constants.

The Stokes number St is expressed as:

$$St = \frac{\tau_p u_*}{a}, \quad (41)$$

where τ_p is the particle relaxation time calculated as $\tau_p = V_g/g$.

The expression for η_{imp} is given as:

$$\eta_{imp} = exp\left\{\frac{-0.1}{St_e - 0.15} - \frac{1}{\sqrt{St_e - 0.15}}\right\} \quad if\ St_e > 0.15, \quad (42)$$

$$\eta_{imp} = 0 \quad if\ St_e \leq 0.15, \quad (43)$$

where St_e is the effective Stokes number calculated as:

$$St_e = St - Re_c^{-\frac{1}{2}}, \quad (44)$$

where Re_c is the critical Reynolds number calculated as:

$$Re_c = \left(\frac{U_{top}}{u_*}\right)^2 Re_*. \quad (45)$$

The term V_g in Eq. (35) is parameterized using Eq. (3).

Note that in the *KS12* scheme, the parameterization of V_d over smooth surfaces requires solving the universal velocity profiles (either numerically or analytically) described by Kouznetsov and Sofiev (2012). We exclude the details of the solution procedure in this paper. We used the analytical solutions of the velocity profile obtained from the authors of the *KS12* scheme through personal communication.

2.4. Zhang and He (2014) (*ZH14*) scheme

Zhang and He (2014) developed an empirical resistance-based parameterization for dry deposition by modifying the *Z01* scheme. The overall structure of the *ZH14* scheme is similar to that of the *Z01* scheme (i.e., V_d is calculated using Eq. (2)). In the *ZH14* scheme, the parameterizations of R_a and R_g are similar to those of the *Z01* scheme. However, in the *ZH14* scheme, parametrizations for the surface resistance term R_s were modified for three bulk particle sizes (i.e., $PM_{2.5}$, $PM_{2.5\text{-}10}$, and PM_{10+}). Recalling, $R_s = 1/V_{ds}$, the parameterizations of V_{ds} are given below.

For particle sizes less than or equal to 2.5 μm ($PM_{2.5}$), V_{ds} is expressed as:

$$V_{ds(PM2.5)} = a_1 u_*, \quad (46)$$

where a_1 is an empirical constant derived by regression analysis. Values of a_1 are given by Zhang and He (2014) for five groups of 26 LUCs.

For particle sizes between 2.5 and 10 μm ($PM_{2.5\text{-}10}$), V_{ds} is expressed as:

$$V_{ds(PM2.5-10)} = (b_1 u_* + b_2 u_*^2 + b_3 u_*^3) e^{k1\left(\frac{LAI}{LAI_{max}} - 1\right)}, \quad (47)$$

where b_1, b_2, and b_3 are LUC dependent constants, LAI_{max} is the maximum leaf area index for a given LUC, and $k1$ is a constant, which is a function of u_*, and expressed as:

$$k1 = c_1 u_* + c_2 u_*^2 + c_3 u_*^3, \quad (48)$$

where c_1, c_2, and c_3 are the LUC dependent constants.

For particle sizes larger than 10 μm (PM_{10+}), V_{ds} is expressed as:

$$V_{ds(10+)} = (d_1 u_* + d_2 u_*^2 + d_3 u_*^3) e^{k2\left(\frac{LAI}{LAI_{max}} - 1\right)}, \quad (49)$$

where d_1, d_2, and d_3 are the LUC dependent constants, and LAI_{max} is the maximum leaf area index for a given LUC. The parameter $k2$ is a constant, which is a function of u_*, and is expressed as:

$$k2 = f_1 u_* + f_2 u_*^2 + f_3 u_*^3, \quad (50)$$

where f_1, f_2, and f_3 are the LUC dependent constants.

2.5. Zhang and Sao (2014) (*ZS14*) scheme

Zhang and Sao (2014) used an analytical solution of the steady-state flux equation to derive an expression to compute dry deposition velocity V_d as:

$$V_d = \left(R_g + \frac{R_s - R_g}{\exp(\frac{R_a}{R_g})} \right)^{-1}, \quad (51)$$

For neutral atmospheric stability conditions, the parameterizations of R_a for rough and smooth surfaces are given in Eqs. (52), and (53), respectively:

$$R_a = \frac{Sc_T}{\kappa u_*} ln\left(\frac{z-d}{h_c-d}\right), \quad (rough\ surfaces) \quad (52)$$

$$R_a = \frac{B_1 Sc_T}{\kappa u_*} ln\left(\frac{z}{z_0}\right), \quad (smooth\ surfaces) \quad (53)$$

where B_1 is an empirical constant (0.45), and Sc_T is the turbulent Schmidt number expressed as:

$$Sc_T = \left(1 + \frac{\alpha^2 V_g^2}{u_*^2}\right), \quad (54)$$

where α is a dimensionless coefficient taken as 1.

The gravitational resistance term R_g is calculated as $R_g = 1/V_g$. The parameterization of the surface resistance term R_s is given by Zhang and Sao (2014) as follows:

$$R_s = \left\{ RV_{dm} \left[\frac{E}{C_d} \frac{\tau_c}{\tau} + \left(1 + \frac{\tau_c}{\tau}\right) Sc^{-1} + 10^{\frac{-3}{T_{p,\delta}^+}} \right] + V_{g,w} \right\}^{-1}, \quad (55)$$

where $R = \exp(-b\sqrt{St})$ and where b is an empirical constant, E is the total collection efficiency, C_d is the drag partition coefficient, Sc is the Schmidt number, $T_{p,\delta}^+$ is the dimensionless particle relaxation time near the surface, and $V_{g,w}$ is the gravitational settling velocity of particle after humidity correction. $\frac{\tau_c}{\tau}$ is the ratio of the drag on the roof of the roughness element (τ_c) to the total shear stress (τ) and is calculated as:

$$\frac{\tau_c}{\tau} = \frac{\beta \lambda_e}{1 + \beta \lambda_e}, \quad (56)$$

where β is the ratio of the pressure-drag coefficient to friction-drag coefficient, and λ_e is the effective frontal area index. The parameter λ_e is a function of frontal area index or roughness density (λ), and plane area index (η). The expression of λ_e is

$$\lambda_e = \frac{\lambda}{(1-\eta)^{c_2}} exp\left(-\frac{c_1 \lambda}{(1-\eta)^{c_2}}\right), \quad (57)$$

where $c_1 = 6$ and $c_2 = 0.1$.

Eq. (56) is used to compute $T_{p,\delta}^+$ as:

$$T_{p,\delta}^+ = \frac{T_{p,\delta} u_*^2}{\nu}, \quad (58)$$

where $T_{p,\delta}$ is the particle relaxation time near the surface ($T_{p,\delta} = V_g/g$).

V_{dm} is calculated using two separate expressions for rough and smooth surfaces, as expressed in Eqs. (59) and (60), respectively:

$$V_{dm} = \frac{u_*}{u_a h_c} \quad (for\ \text{rough surfaces}), \quad (59)$$

where u_a is the horizontal air speed and h_c is the height of the roughness element.

$$V_{dm} = B_2 u_* \quad (\text{for smooth surfaces}), \quad (60)$$

where B_2 is an empirical constant taken as 3.

In Eq. (55), the total collection efficiency (E) is comprised of collection efficiencies by Brownian diffusion (E_B), impaction (E_{IM}), and interception (E_{IN}). The parameterizations for each of these three terms are given below:

$$E_B = C_B Sc^{-2/3} Re^{n_B - 1}, \quad (61)$$

where C_B and n_B are empirical parameters function of flow regimes, and are given by Zhang and Sao (2014).

$$E_{IM} = \left(\frac{St}{0.6+St}\right)^2, \quad (62)$$

where St is the Stokes number and is expressed as $St = \tau_p u_* / d_c$. Here, d_c is the diameter of the surface collection element. Values of d_c are given by Zhang and Sao (2014) for various surfaces.

$$E_{IN} = A_{in} u_* 10^{-St \frac{2d_{p,w}}{d_c}}, \quad (63)$$

where A_{in} is a surface dependent micro-roughness characteristic element, and $d_{p,w}$ is the wet diameter of the particle.

3. Methods

3.1. An evaluation of the dry deposition parameterizations

To assess the accuracy of the five parameterizations, the modeled dry deposition velocities were compared with field measurements from both rough and smooth surfaces. The measurement studies conducted on various natural surfaces were collected from the literature. More specifically, the studies citied in the review article on particle flux measurements by Pryor et al. (2008) were collected to acquire the meta-data on particle deposition. The availability of the measured and/or reported parameters (e.g., particle size and density, air temperature, relative humidity, horizontal wind speed, friction velocity, atmospheric stability parameter, canopy height, roughness height, zero-plane displacement height, and leaf area index) from these measurement studies was thoroughly investigated and compiled. It was found that the many (ca. 50%) of the studies citied by Pryor et al. (2008) did not report most of the aforementioned parameters necessary to run the parameterizations to perform a valid comparison between the model output and measurements. To reduce uncertainty, those studies were excluded from the parametrization accuracy evaluation. In addition, a literature search was performed in Web of Science® to find measurement studies published after 2008, and those studies were thoroughly assessed to determine the availability of required input parameters to run the dry deposition models. Finally, 29 measurement studies covering five land use categories (LUCs) were selected to evaluate the accuracy of the five parameterizations. The five LUCs include grass, deciduous, and coniferous forests (rough surfaces), and natural water and ice/snow (smooth surfaces). Table 1 summarizes information related to sampling location, latitude, longitude, elevation above mean sea level (AMSL), sampling periods, and particle sizes reported in the measurement studies. The global spatial distribution of these measurement studies is shown in Figure 1 according to the five LUCs.

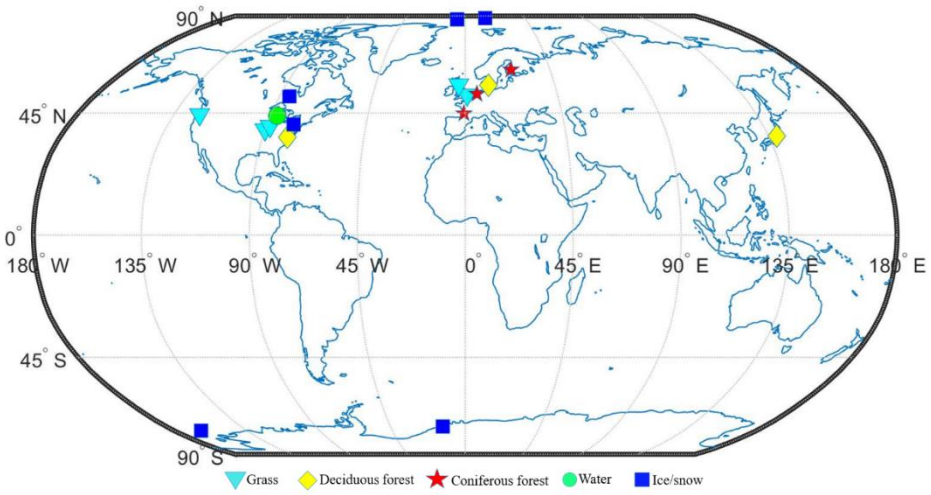

Figure 1. Global distribution of dry deposition measurement locations (listed in Table 1) used to evaluate the *Z01*, *PZ10*, *KS12*, *ZH14*, and *ZS14* parameterizations. Note that for multiple measurement campaigns conducted in one location, only one data point is shown. Two wind tunnel studies on water surfaces are not shown.

Measurements conducted over grass by Wesely et al. (1977), Neumann and den Hartog (1985), Allen et al. (1991), Nemitz et al. (2002), and Vong et al. (2004) were used to evaluate the performance of the five parameterizations. For coniferous forest, modeled deposition velocities were compared with measurements from Lamaud et al. (1994), Wyzers and Duyzer (1996), Gallagher et al. (1997), Ruijgrok et al. (1997), Buzorius et al. (2000), Rannik et al. (2000), Gaman et al. (2004), Pryor et al. (2007), and Grönholm et al. (2009). Experiments conducted over deciduous forest are limited, and only three studies (Wesely et al., 1983; Pryor, 2006; Matsuda et al., 2010) were used in the present paper.

To evaluate the performance of the parameterizations over water surfaces, studies by Möller and Schumann (1970), Sehmel et al. (1974), Zufall et al. (1998) and Caffrey et al. (1998) were used. We note that the studies by Möller and Schumann, and Sehmel et al. were conducted in the wind tunnels, and thus the observed deposition does not necessarily reflect deposition under natural conditions. Particle deposition measurements on ice/snow pack were collected from eight studies: Ibrahim (1983); Duan et al. (1987); Nilsson and Rannik (2001); Gronlund et al. (2002); Contini et al. (2010); Held et al. (2011a); Held et al. (2011b); and Donateo and Contini (2014). The parametrizations were fed using reported values of particle properties (diameter and density), meteorological conditions (stability parameter, temperature, wind speed, etc.), and surface properties (canopy height, roughness length, leaf area index, etc.). However, reasonable values of the missing parameters were used when needed.

In the present study, the accuracy of the dry deposition parameterizations was evaluated using the normalized mean bias factor (B_{NMBF}). The B_{NMBF} provides a statistically robust and unbiased symmetric measure of the factor by which the modeled dry deposition velocities differ from the measured ones, and the sense of that factor (i.e., the positive and negative values imply the ovepredictionand underprediction by models, respectively). The interpretation of the B_{NMBF} is simple (i.e., average amount by which the ratio of modeled and measured quantities differ from unity), and it avoids any inflation that may be caused by low values of measured quantities (Yu et al., 2006).

To quantify the disagreement between the modeled and observed quantities, the normalized mean bias factors were calculated for the pairs of modeled ($V_{d(modeled),i}$) and measured dry deposition velocities ($V_{d(measured),i}$), respectively. In this study, the expressions for computing B_{NMBF} used in two different forms, which are:

For the $V_{d(modeled),i} > V_{d(measured),i}$ case (i.e., overestimation):

$$B_{NMBF} = \frac{\sum V_{d(modeled),i}}{\sum V_{d(measured),i}} - 1 \quad (64)$$

For the $V_{d(modeled),i} < V_{d(measured),i}$ case (i.e., underestimation):

$$B_{NMBF} = 1 - \frac{\sum V_{d(measured),i}}{\sum V_{d(modeled),i}} \quad (65)$$

The step-wise derivation of the Eqs. (64-65) and their application on training air quality datasets are illustrated by Yu et al. (2006).

3.2. Uncertainty analysis of the dry deposition parameterizations

To quantify the influence of imprecision in the model input parameter values on the modeled velocities, a classical Monte Carlo uncertainty analysis was applied. The Monte Carlo techniques have been widely used to evaluate the propagated uncertainty in the modeled outputs in many geophysical models (e.g., Alcamo and Bartnickj, 1987; Derwent and Hov, 1988; Chen et al., 1997; Tatang et al., 1997; Hanna et al., 1998, 2001; Bergin et al., 1999; Bergin and Milford, 2000; Beekman et al., 2003; Mallet and Sportisse, 2006). Monte Carlo uncertainty evaluation techniques are relatively straightforward and flexible means for incorporating probabilistic values in the modeled dry deposition velocities. Indeed, the techniques are less reliant on assumptions about distributions of the input parameters (Hanna et al., 2002).

In this study, we define uncertainty in the parameterizations as the inability to confidently specify single-valued quantities because of the imprecision in the model input parameters. A classical Monte Carlo uncertainty method was applied to assess the overall uncertainty of a dry deposition parameterization with regard to the uncertainties in the following input parameters: *RH*, *h*, z_0, *d*, *LAI*, *U*, u_*, and L_O. The uncertainty estimates for those input parameters were obtained from the literature and are presented in Table 2. Using the uncertainty ranges for each of these parameters, uniform probability distribution functions were assigned since information on their actual distributions are lacking. It is noted that a constant dry particle density of 1500 kg m^{-3} (Petroff et al., 2012) was used in all Monte Carlo simulations. Because of the inhomogeneous nature of ambient particles, accurate measurement of particle density is challenging. In their work, Oskouie et al. (2003) developed methods using a time-of-flight instrument to minimize the effect of uncertainties in density estimation in particle size characterization.

The Monte Carlo simulations were performed using R statistical software (version 3.2.4). Each simulation was run by randomly drawing 100 samples from the assigned uniform probability density function (PDF). The simulations were repeated 10,000 times. Frequency distributions or the PDFs of the modeled dry deposition velocity are the basic results of the Monte Carlo simulations. These PDFs were approximated assuming normal distributions, and then the 5th, 50th, and 95th percentile dry deposition velocities were computed. We use the range of the central 90% (the difference between 95^{th} and 5^{th} percentiles) of the PDFs as a convenient measure of uncertainty in the modeled deposition velocity. These steps were repeated for all five parameterizations using seven different particle sizes: 0.005, 0.05, 0.5, 1.0, 1.5, 2.0, and 2.5 μm on the five selected five LUCs (i.e., grass, deciduous and coniferous forests, water, and ice/snow). These particle sizes were selected to represent four distinct particle modes: nucleation (<0.01 μm), Aitken (0.01-0.1 μm), accumulation (0.1-1.0 μm), and coarse (>1.0 μm), respectively.

3.3. Sensitivity analysis

In this study, the Sobol' sensitivity method (Sobol' 1990) was applied to identify the most influential input parameter or the set of parameters of a dry deposition parameterization, and to characterize the relative contribution of the parameters to the overall variability in the modeled V_d. As opposed to the local sensitivity analysis (e.g., OAT approach), the Sobol' method is a global sensitivity approach, in which a set of input parameters of a model can be varied simultaneously over their entire parameter value space to identify their relative contributions to the overall model output variance. The Sobol' method has been applied in environmental modeling applications (Tang et al., 2007; Pappenberger et al., 2008; van Werkhoven et al., 2008; Yang, 2011), but has not yet been applied in dry deposition modeling research. Given that in most of the dry deposition parameterizations, model inputs can span a wide range within their physical realms, the application of a global sensitivity analysis used in this study should be viewed as a critical step toward the understanding of different sub-physical processes of particle deposition.

In the Sobol' method, the variance contributions to the total output variance of individual parameters and parameter interactions can be determined. These contributions are characterized by the ratio of the partial variance (V_i) to the total variance (V) as expressed in Eq. 66. This ratio is commonly termed as Sobol' first order index (S_i) (Saltelli et al., 2010; Nossent et al., 2011). The first order indices represent the fractions of the unconditional model output variance. In this study, Sobol' first order sensitivity indices were calculated as:

$$S_i = \frac{V_i}{V} = \frac{V_{X_i}(E_{\boldsymbol{X}_{\sim i}}(V_d|X_i))}{V(V_d)}, \tag{66}$$

where X_i is the *i*-th input parameter and $\boldsymbol{X}_{\sim i}$ denotes the matrix of all input parameters but X_i. The meaning of the inner expectation operator is that the mean of V_d is taken over all possible values of $X_{\sim i}$ while keeping X_i fixed. The outer variance is taken over all possible values of X_i. The variance $V(V_d)$ in the denominator is the total (unconditional) variance.

The numerator in Eq. (66) can be interpreted as follows: $V_{X_i}(E_{\boldsymbol{X}_{\sim i}}(V_d|X_i))$ is the expected reduction in variance that would be obtained if X_i could be fixed. In regard to the variability of the model input parameters in dry deposition schemes, S_i provides a means to quantity the effect of parameter X_i by itself. A higher order (S_{ij}) or total order (S_{Ti}) can be computed when the total effect of a parameter, inclusive of all its interaction with other model input parameters, are of interest. In this paper, we confine the sensitivity analysis to Sobol' first order indices only.

For each of the five parameterizations evaluated here, four to nine input parameters were selected for determining the first order Sobol' sensitivity indices. An exception to applying the Sobol' method was made for the *KS12* parameterization while evaluating the parameter sensitivity for smooth surfaces. Due to the complex nature of *KS12* smooth surface parameterization, it was not computationally feasible to apply the Sobol' method. Instead, the OAT approach was applied for water and ice/snow surfaces. Note that the total number of input parameters that go into each model varies between parameterizations, and LUC types. For each parameterization, five particle sizes (d_p = 0.001, 0.01, 0.1, 1.0, and 10 μm) were assessed for Sobol' analysis. The sensitivity of each parameterization was tested for the following three sets of input parameters for five LUCs: (i) particle properties, (ii) aerodynamic parameters, and (iii) surface characteristics of particle deposition. First, the sensitivity of particle deposition to particle properties (aerodynamic diameter and density) was tested. Sensitivity indices were calculated for the particle size range of 0.001 μm to 10 μm. Second, the sensitivity of the schemes was tested for aerodynamic parameters (friction velocity, wind speed, and stability condition) for different particle sizes one-at-a-time. Third, the sensitivity of the schemes to surface characteristics was tested. Surface characteristics include *h*, z_0, *d*, and *LAI*. The sensitivity ranges for the parameter values used for Sobol' analysis are reported in Table 3.

The Sobol 2007 package in R statistical software package (version 3.2.4) was used to perform the Sobol' sensitivity analysis. In the Sobol' method, the Monte Carlo simulations were performed by drawing samples from the assigned parameter value distribution. In this study, all the selected parameters were approximated using uniform PDFs. To assert uncertainty in the simulations, bootstrapping (Efron and Tibshirani, 1993) with re-sampling was used to achieve 95% confidence intervals on the Sobol' first order indices. For a fixed particle size, the simulations were run 100,000 times and samples were bootstrapped 1,000 times. To identify the most important parameters in each of the five dry deposition models with respect to particle size and LUC, a parameter ranking (e.g., from most to least influential) was conducted.

The results section is organized in the following manner. First, the accuracy of five dry deposition parameterizations (i.e., *Z01*, *PZ10*, *KS12*, *ZH14*, and *ZS14*) are compared with measured dry deposition velocities obtained from five LUCs. Second, the uncertainties in modeled dry deposition velocities due to the imprecision in the model input parameter values quantified using Monte Carlo simulation techniques are presented. Third, the sensitivity analysis results for modeled dry deposition velocities by the five parameterizations are presented.

4. Results

4.1. Evaluation of the dry deposition parameterizations

Field measurements conducted on five LUCs: grass, coniferous forest, deciduous forest, water surfaces, and ice/snow were used to evaluate the agreement between measured and modeled dry deposition velocity (V_d). The parameterizations were run using reported values of the meteorological (e.g., U, u_*, T, RH, and L_O) and canopy (e.g., h, z_0, d, and LAI) parameters, and particle properties (e.g., d_p and ρ) from the measurement studies. Reasonable parameter values were assumed for any missing or unreported parameters. Normalized mean bias factors (B_{NMBF}) were used as an indicator of the agreement between measured and modeled V_d. B_{NMBF} is a signed quantity-its magnitude indicates the factor by which the modeled and observed V_d differ from each other, and its sign provides an indicator as to whether the modeled V_d is greater or less than the measured V_d. It is to be noted that uncertainties in the measured dry deposition velocities were not considered while evaluating the performance of the five parameterizations in terms of accuracy.

4.1.1. Evaluation of dry deposition to grass

Five measurement studies conducted on grass (Wesely et al., 1977; Allen et al., 1991; Neumann and den Hartog, 1985; Nemitz et al., 2002; and Vong et al., 2004) were used to evaluate the accuracy of the parameterizations. In those studies, reported values of meteorological parameters, canopy properties, and particle size vary widely. For example, the u_* varies from 0.05 to 0.70 m/s, wind speed (U) varies from 0.67 to 6.20 m/s, particle size (d_p) varies from 0.05 to 2.28 µm, and LAI varies from 2 to 4 m^2/m^2. The parameterizations were fed with reported values from each of the studies to reduce any uncertainty in the accuracy comparison, however, for any missing parameter value(s), the assumed input parameter values typically fell within the aforementioned ranges.

Table 4 summarizes the B_{NMBF} for modeled V_d computed against five measurement studies on grass. The B_{NMBF} is interpreted as follows: for example, if B_{NMBF} is positive, the parameterization overestimates the measured V_d by a factor of $B_{NMBF}+1$. If B_{NMBF} is negative, the model underestimates the measured V_d by a factor of $1-B_{NMBF}$. For the case using the observations from Allen et al. (1991), the B_{NMBF} values of -17.61, -18.12, -0.55, and -5.13 indicate that the *Z01*, *KS12*, *ZH14*, and *ZS14* parameterizations underestimated the measured V_d by factors of 18.61, 19.12, 1.55, and 6.13, respectively, whereas, the B_{NMBF} value of +15.96 indicates that the *PZ10* parameterization overestimated the observations by a factor of 16.96.

These results provide means for a relative comparison of the parameterizations' accuracy. For instance, the B_{NMBF} values corresponding to the Allen et al. study suggest that the *ZH14* parameterization is the most accurate and the *KS12* parameterization is least accurate. Similar comparison between the modeled and observed V_d can be made using the B_{NMBF} values for the remaining four studies in Table 4. Nonetheless, it is evident that none of the parameterizations performed best in terms of accuracy for all of the five studies since the B_{NMBF} values show high variability both in terms of the magnitude and direction of the bias (i.e., positive or negative) when assessed against all the five studies listed in Table 4.

The characteristics of a parameterization (e.g., *Z01*) to simultaneously over-predict (i.e., the positive B_{NMBF} for Neumann and den Hartog, and Nemitz et al.) and under-predict (i.e., the negative B_{NMBF} for Allen et al. 1991, Wesely et al. 1977, and Vong et al., 2004) the measurements could be misleading, resulting in erroneous judgement of the performance of the parameterizations. To address this limitation, an ensemble approach was taken, in which B_{NMBF} was calculated for each of the parameterizations using all the observations reported in the five studies. The results from this ensemble analysis indicate that, except for the *Z01* parameterization, the other four parameterizations underestimated the measured V_d by factors ranging from 1.54 to 10.37. In contrast, the *Z01* parameterization overestimated the observation by a factor of 6.45 (Table 4). Overall, these results indicate that the *ZH14* parameterization provided the best agreement between the measured and modeled V_d of the five parameterizations.

4.1.2. Evaluation of dry deposition to coniferous forest

Nine studies conducted on coniferous forest (Lamaud et al., 1994; Wyer and Duyzers, 1996; Gallagher et al., 1997; Ruijgrok et al., 1997; Rannik et al., 2000; Buzorious et al., 2000; Gaman et al., 2004; Pryor et al., 2007; and Grönholm et al., 2009) were used to evaluate the accuracy of the parameterizations. In these studies, the largest variations (ranges are given in the parentheses) were associated with u_* (0.06-1.30 m/s), U (0.60-6.19 m/s), LAI (6-10 m^2/m^2), and d_p (0.01-0.60 μm). For any missing parameter value(s), the assumed input parameter values typically fell within the aforementioned ranges.

Comparison of the computed B_{NMBF} values for coniferous forest (Table 5) shows that the majority of the simulations performed using the five parameterizations underestimated the measured V_d. For example, the *PZ10* parameterization underestimated observed V_d by factors ranged from 1.51 to 27.98 (B_{NMBF} values varied from -0.51 to -26.98) for eight of the nine studies on coniferous forest. Table 5 also illustrates that both the magnitude and sign of the B_{NMBF} values varied widely when the accuracy of the five parameterizations was evaluated against only one study (e.g., Pryor et al., 2007). Of the B_{NMBF} values associated with the Rannik et al. (2000) study, the *Z01* and *KS12* parameterizations overestimated the measured V_d by factors of 4.16 and 1.51, respectively, whereas the *PZ10*, *ZH14*, and *ZS14* parameterizations underestimated the measured V_d by factors of 3.54, 2.13, and 19.75, respectively. The bias factors for the *Z01* parameterization for the following studies: Lamaud et al. (1994), Gallagher et al. (1997), Buzorious et al. (2000), and Gaman et al. (2004), were +0.77, -1.74, +0.75, and -0.90, respectively. Comparing these values with the corresponding B_{NMBF} values of the other four parameterizations, it can be deduced that the *Z01* parameterization is the most accurate against those observations reported in these four studies. However, the accuracy of the *Z01* parameterization is not the best for the other five studies, as can be seen from Table 5.

An ensemble approach similar to the one described in the previous section was used to determine the most and the least accurate parameterizations. From this analysis, the bias factors for the *Z01*, *PZ10*, *KS12*, *ZH14*, and *ZS14* parameterizations are -2.35, -3.93, -1.75, -2.31, and -3.67, respectively, suggesting that the *KS12* is the most accurate parameterization (i.e., under-predicted the observations by a factor of 2.75), and the *PZ10* is the least accurate parameterization (i.e., under-predicted the observations by a factor of 4.93) for coniferous forest. It can be noted that the performance of the *Z01* and *ZH14* parameterizations are nearly identical, while the *ZH14* is the second most accurate (i.e., under-predicted the observations by a factor of 3.31).

4.1.3. Evaluation of dry deposition to deciduous forest

A similar comparison between measured and modeled V_d was performed using three studies (Wesely et al., 1983; Pryor, 2006; and Matsuda et al., 2012) for deciduous forest. In these studies, the largest variations (ranges are given in the parentheses) were associated with u_* (0.12-1.13 m/s), U (1.20-6.00 m/s), LAI (0.20-10 m^2/m^2), and d_p (0.05-2.50 μm). For any missing parameter value(s), the assumed input parameter values typically fell within the aforementioned ranges.

Computed B_{NMBF} values for deciduous forest are presented in Table 6. For the Wesely et al. (1983) study, comparison of the B_{NMBF} values between the parameterizations show that the performance of the *ZS14* parameterization was the most accurate (i.e., B_{NMBF} = -2.28; under-predicted the observations by a factor of 3.28). The B_{NMBF} values associated with the *PZ10* parameterization showed strong variation between the studies (e.g., two orders of magnitude discrepancy between the Wesely et al. (1983) and Pryor (2006) or Matsuda et al. (2012) studies).

Evidently, none of the parameterizations performed consistently better for all the three studies. Overall, the results from the ensemble approach show that all the parameterizations overestimated the observations reported in three studies. Considering the B_{NMBF} values obtained by this approach, it is apparent that the *ZH14* is the most accurate parameterization (i.e., B_{NMBF} = -3.75, underestimated the observed V_d by a factor of 4.75), and the *ZS14* is the least accurate of the five parameterizations (i.e., B_{NMBF} = -10.93, underestimated the observed V_d by a factor of 11.93) for deciduous forest.

4.1.4. Evaluation of dry deposition to water surfaces

Only a limited number of measurement studies on size-segregated dry deposition over natural water surfaces are available in the literature. In this research, four studies (Möller and Schumann, 1970; Sehmel et al., 1974; Zuffal et al., 1998; and Caffery et al., 1998) conducted over water surfaces were used to evaluate the parameterizations' accuracy. From these studies, the reported values of the parameters that show the largest variations (ranges are given in the parentheses) are u_* (0.11-0.40 m/s) and d_p (0.03 to 48 μm).

Table 7 shows that the *PZ10* parameterization performed best for two studies (i.e., Möller and Schumann, 1970; and Caffery et al., 1998), in which B_{NMBF} values were -1.65 and +0.35, respectively. Comparison of the B_{NMBF} values between the *Z01* and *ZH14* parameterizations reveal that the accuracy of the two parameterizations varied widely among the studies (e.g., B_{NMBF} ranged from -0.144 to +18.87 and -0.33 to +10.28, respectively). Nevertheless, none of the five parameterizations was able to reproduce the measured V_d satisfactorily for all the four studies. Comparison of the B_{NMBF} values obtained by the ensemble approach showed that the *ZH14* parameterization is the most accurate, which underestimated the measured V_d by a factor of 1.25 (i.e., B_{NMBF} = -0.25), and the *PZ10* is the least accurate parameterization (i.e., B_{NMBF} = -0.89).

4.1.5. Evaluation of dry deposition to snow and ice surfaces

Two studies over snow (Ibrahim, 1983; and Duan et al., 1987), and six studies over ice surfaces (Nilsson and Rannik, 2001; Gronlund et al., 2002; Contini et al., 2010; Held et al., 2011a; Held et al., 2011b; and Donateo and Contini, 2014) were used to evaluate the accuracy of the four parameterizations (*Z01*, *PZ10*, *KS12*, and *ZH14*) for smooth surfaces. The *ZS14* parameterization was not included here because it does not allow prediction of deposition over ice/snow surfaces. The B_{NMFB} values for the parameterizations are presented in Table 8.

Of the four parameterizations, agreement between the modeled and measured V_d is not satisfactory for the *PZ10* and *KS12* parameterizations because they significantly underestimated the measured V_d (e.g., the bias factors from ensemble approach are -53.03 and -21.80, respectively). In contrast, the *Z01* and *ZH14* parameterizations predicted the measured V_d with reasonable

accuracy (e.g., the bias factors from ensemble approach were +1.98 and +0.26, respectively). Table 8 also shows that the *ZH14* parameterization performed best for six of the eight measurements in which the B_{NMBF} varied between -0.74 to 3.98. Overall, for the nine studies combined (i.e., ensemble measurements), the *ZH14* parameterization is the most accurate (overestimated the measured V_d by a factor of 1.26), and the *PZ10* is the least accurate parameterization (underestimated the measured V_d by a factor of 54.03).

To summarize, the results from the ensemble evaluation of the parameterizations are graphically shown in Figs. 2(A-B) for the five LUCs. The horizontal dotted-dashed line in the plots indicates 100% agreement between modeled and measured V_d, whereas any dispersion from this line either above (i.e., over-estimation) or below (i.e., under-estimation) indicates the degree of the model's accuracy.

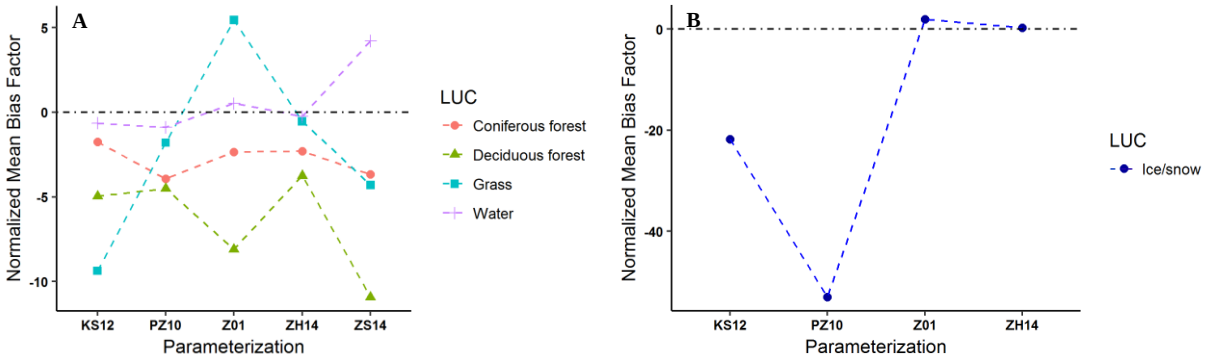

Figure 2. Ensemble averaged, normalized mean bias factors for the five parameterizations: a) three rough surfaces and water, b) Ice/snow.

4.2. Uncertainty analysis results from the Monte Carlo simulations

The overall uncertainty in the modeled V_d due to imprecision in the model inputs was assessed by performing a set of Monte Carlo simulations on the five dry deposition parameterizations. Uncertainties (in terms of imprecision) in the following model input parameters: *RH*, *U*, u_*, L_O, *h*, z_0, *d*, and *LAI* were approximated using uniform distributions. Note that not all of the five parameterizations require an identical number of input parameters. For example, Monte Carlo simulations performed on rough surfaces (i.e., grass, coniferous, and deciduous forests) for the *Z01*, *PZ10*, *KS12*, *ZH14*, and *ZS14* parameterizations, imprecision in four (*RH*, *L*, u_*, and z_0), eight (*RH*, *L*, u_*, *U*, z_0, *h*, *d*, and *LAI*), four (*RH*, u_*, *U*, and *LAI*), four (*RH*, *L*, u_*, and z_0), and two (*RH*, u_*) input parameters, respectively, were assessed to evaluate the overall uncertainty in modeled dry deposition velocities.

The results from the Monte Carlo simulations are summarized in Table 9 and are presented and discussed in two steps. First, the uncertainty estimates that are shown in Table 9 for five parameterizations on five LUCs are used to elucidate the models' precision, which is one of the indicators of overall performance of the parametrization (Sections 3.2.1-3.2.5). Second, the size-dependent uncertainty ranges (i.e., the difference between the 95th and 5th percentiles) was divided by the 50th percentile V_d, which can be treated as a normalized measure of uncertainty. This approach was taken to make reasonable comparison between different particle sizes for different parameterizations (Section 3.2.6). Note that the *ZS14* parameterization does not treat different vegetative covers separately; therefore, inter-comparison of the Monte Carlo simulation results is confined to the first four parameterizations listed in Table 9.

4.2.1. Uncertainties in the modeled V_d for grass

The uncertainties in simulated V_d (i.e., differences between 95th and 5th percentiles of distribution) for the given range of d_p (i.e., 0.005-2.5 µm) on grass varied widely (Table 9). In the *Z01* parameterization, the estimated uncertainty for nucleation mode particles (0.0038 m s^{-1} for d_p = 0.005 µm) was larger than that of coarse mode particles (0.0001 m s^{-1} for d_p > 1.0 µm). Overall, in

the *Z01* parameterization, the trend was that as the particle size increased from 0.005 to 2.5 µm, uncertainties in modeled V_d decreased considerably. In the *PZ10* parameterization, the range of uncertainty for the simulated particle sizes is narrower as compared to those of the *Z01* parameterization. Although not consistent, a decreasing trend in uncertainties can be seen for all the particle sizes in the *PZ10* parameterization. Of the simulated particle sizes, the uncertainty for d_p = 0.005 µm is the largest (0.0016 m s^{-1}) in the *KS12* parameterization. As particle size increased from 0.005 to 2.5 µm, significant decrease in uncertainties is observed. For d_p = 0.05 to 1.5 µm, the 5th and 95th percentile V_d were nearly identical (Table 9), suggesting that the *KS12* parameterization is the most precise of five parameterizations specifically for those particle sizes. From Table 9, it can be deduced that the uncertainties associated with the *ZH14* parameterization, which is an improved and simplified version of the *Z01* parameterization, were fairly constant (ca. 00003 m s^{-1}) for the seven particle sizes simulated here for grass.

4.2.2. Uncertainties in the modeled V_d for coniferous forest

For nucleation mode particles (i.e., d_p = 0.005 µm), the largest uncertainty (0.0036 m s^{-1}, median V_d = 0.0180 m s^{-1}) was associated with the *Z01* parameterization (Table 9). Overall, the uncertainties in the *Z01* parameterization showed a decreasing trend as the particle size increased from 0.005 to 2.5 µm. We note that in the *PZ10* parameterization, the relative magnitude of the uncertainties associated with 0.005, 1.0, 1.5, 2.0, and 2.5 µm particles were of the same order (i.e., varied between 0.0010 to 0.0031 m s^{-1}). In comparison, uncertainties in modeled V_d for 0.05 and 0.5 µm particles were smaller by factors of ca. 10. In the *KS12* parameterization, the largest uncertainty was found for the nucleation mode particles (i.e., 0.0027 m s^{-1}; median V_d = 0.0299 m s^{-1}), and the uncertainties in modeled V_d decreased substantially as d_p increased. The uncertainties in modeled V_d in the *ZH14* parameterization were constant (0.0002 m s^{-1}) for all seven particle sizes indicating the model's ability to reproduce dry deposition velocities with high precision.

4.2.3. Uncertainties in the modeled V_d for deciduous forest

A similar comparison of the uncertainties in modeled V_d can be made for deciduous forest. It is seen from Table 9 that, for all the parameterizations except for *ZH14*, the largest uncertainties were associated with nucleation mode particles. That is, *Z01* and *KS12* parameterizations showed substantially greater uncertainties for d_p = 0.005 µm (0.0030 and 0.0027 m s^{-1}, respectively) as compared to the Aitken or coarse mode particles, for which the relative magnitude of the uncertainties were smaller by factors of ca. 13-30. In the *KS12* parameterization, the identical values of the 5th and 95th percentile V_d resulted in uncertainty values of zero for each simulated particle size of 0.5 to 2.0 µm, which indicates that it is the most precise of all four parameterizations. In addition, the uncertainties in the modeled V_d in the *ZH14* parameterization were constant (0.0004 m s^{-1}) for all seven particle sizes.

4.2.4. Uncertainties in the modeled V_d for water surfaces

For water surfaces, the uncertainties in modeled V_d varied largely for the *Z01* parameterization (Table 9). That is, the largest uncertainty (0.0021 m s^{-1}) was associated with d_p = 0.005 µm (median V_d = 0.0099 m s^{-1}), and as d_p increased to 2.5 µm, the uncertainty decreased to 0.0001 m s^{-1} (for 2.5 µm particles, median V_d = 0.0009 m s^{-1}). Relatively narrower ranges in the uncertainties in modeled V_d for the *PZ10* and *KS12*, and constant uncertainties in the *ZH1*4 parameterizations with regard to changes in particle size suggest their higher precision as compared to the *Z01* parameterization under similar model input parameter uncertainties. Overall, as compared to the simulated uncertainties in the modeled V_d by the *Z01*, *PZ10*, *KS12*, and *ZH14* parameterizations, uncertainties in the *ZS14* parameterization are larger for d_p = 0.05 to 2.5 µm.

4.2.5. Uncertainties in the modeled V_d for ice/snow surfaces

Comparison between the simulated uncertainties in modeled V_d revealed that the uncertainties vary significantly for the *Z01* and *KS12* parameterizations as d_p changes. For example, uncertainties estimated from Table 9 for these two parametrizations decreased from 0.0023 to 0.0003 m s^{-1} and 0.0027 to 0.0008 m s^{-1}, respectively, as particle size increased from 0.005 to 2.5 µm. Note that the median V_d by the *PZ10* parameterization is an order of magnitude lower than that of other three parameterizations,

which results in close to zero uncertainties for all seven particle sizes. Also revealed in Table 9, the uncertainties in the *ZH14* parameterization are constant (0.0002 m s^{-1}) with regard to changes in the particle size.

4.2.6. Normalized uncertainties in the modeled V_d

An extended analysis of the results presented in the previous sections are summarized here. The normalized uncertainties presented in the Table 10 can be interpreted as follows: any value that is closer to zero indicates higher model precision (i.e., less uncertainty). As shown in Table 10, the normalized uncertainties for grass and d_p = 0.005 µm associated with the *Z01*, *PZ10*, *KS12*, *ZH14*, and *ZS14* parameterizations are 0.20, 0.11, 0.09, 0.20, and 0.20, respectively. These results suggest that *KS12* is the least uncertain (i.e., most precise) parameterization for nucleation mode particles, whereas, the *Z01*, *ZH14*, and *ZS14* are the most uncertain (i.e., least precise) parameterizations. Similar comparisons can be made for other particle sizes, as well as between the different LUCs. For example, the uncertainties associated with d_p = 0.05 µm is greater for the *PZ10* parameterization for deciduous forest as compared to grass (0.20 > 0.13).

Comparison of the normalized uncertainties in modeled V_d over smooth surfaces (i.e., water and ice/snow) also reveals interesting findings. For example, for d_p = 0.5 µm, the normalized uncertainties over water surfaces for the *Z01*, *PZ10*, *KS12*, and *ZH14* parameterizations are 0.20, 0.00, 0.50, and 0.17, respectively. These results suggest that the *PZ10* parameterization is the least uncertain (i.e., most precise), whereas, the *KS12* is the most uncertain (i.e., least precise) parameterization for accumulation mode particles. Over ice/snow surfaces, with d_p = 0.005 µm, both the *Z01* and *ZH14* parameterizations have large uncertainties (normalized uncertainties are 0.18 and 0.17). In contrast, *PZ10* is the most precise parameterization with close to zero normalized uncertainty value.

The normalized uncertainties presented in Table 10 also reveal interesting findings about the relative magnitude of imprecision for a given particle size on various LUCs by one parameterization. For example, with d_p = 0.005 µm, the range in normalized uncertainties varies from 0.18-0.20 and 0.09-0.20 for all the five LUCs for the *Z01* and *KS12* parameterizations, respectively.

Figs. 3(A-E) show the relative comparison between uncertainties in modeled V_d by five parameterization for seven particle sizes across five LUCs. For LUC grass, Fig. 3A shows that in the uncertainties in the *Z01* and *ZH14* parameterizations show nearly identical trends, which are relatively narrow. That is, the uncertainties for particle sizes from 0.005 to 2.5 µm varied from 12-22% and 11-20% in the *Z01* and *ZH14* parameterizations, respectively. In contrast, uncertainties in the *PZ10* and *KS12* parameterizations exhibit large dispersion (i.e., uncertainty ranges from ~0-13% in the *PZ10*, and ~0-14% in the *KS12* parameterizations). The largest uncertainties in the simulated V_d are associated with the *ZS14* parameterization, in which the range of uncertainty varied from ~0-34% for the seven particle sizes. We note that the minimum V_d produced by the *KS12* parameterization is at d_p = 0.5 µm for grass, coniferous and deciduous forest, and ice/snow surfaces, which can be confirmed from the Fig. 3(A-C and E). In addition, Fig. 3(D-E) show that the position of this minimum V_d in the *PZ10* parameterization ranged from d_p = 0.5-1.0 µm for water and ice/snow surfaces.

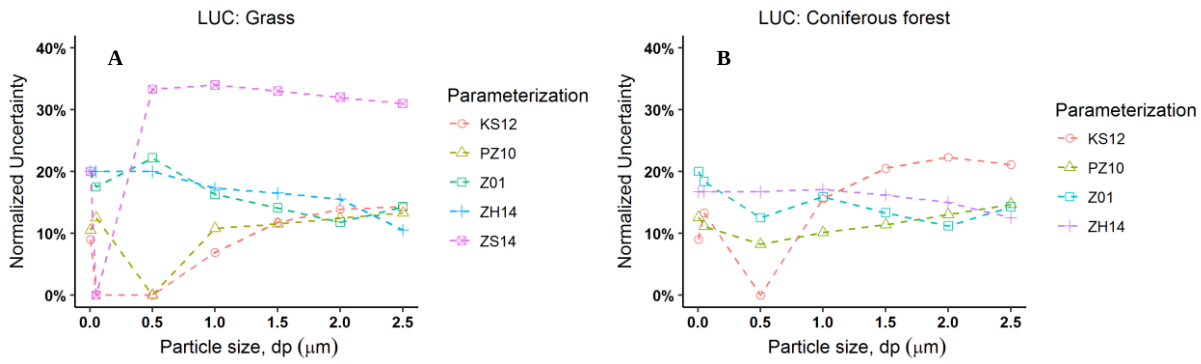

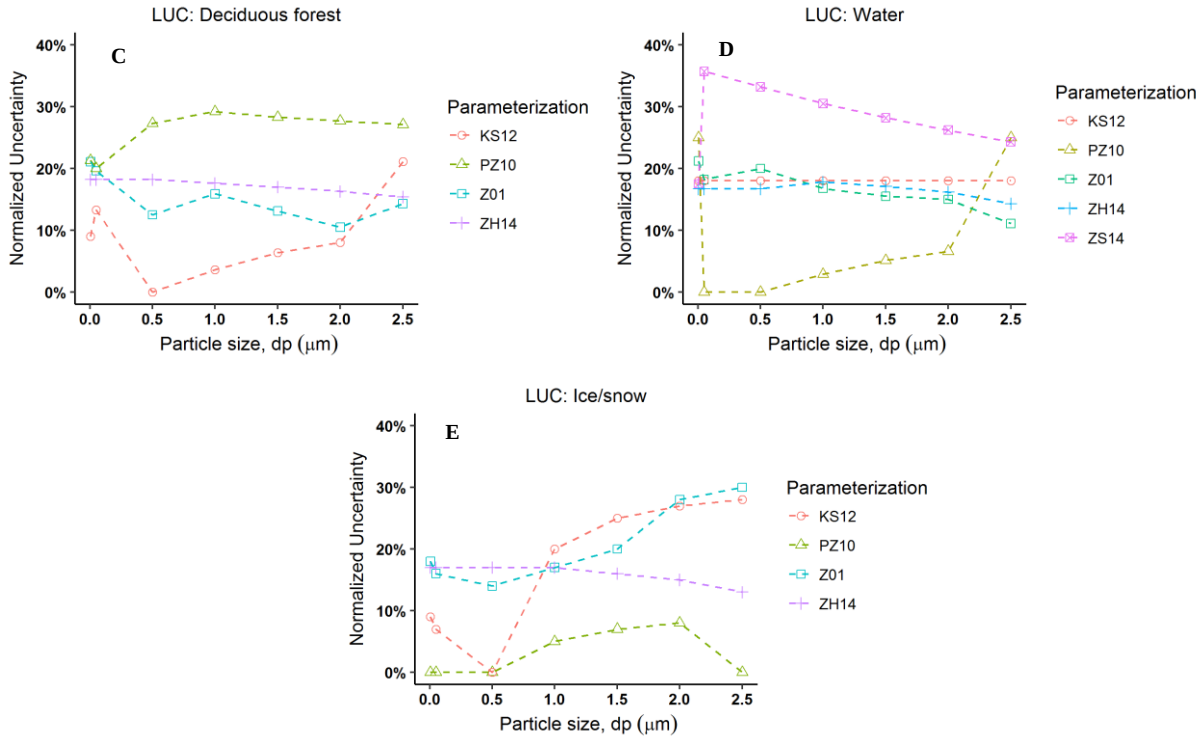

Figure 3. Comparison of the simulated uncertainties in the modeled dry deposition velocities as a function of particle size in five parameterizations for five LUCs.

Similar comparison can be made to evaluate the relative magnitude of the uncertainties in the modeled V_d predicted by the parameterizations over other LUCs from Figs. 3(B-E). In Fig. 3B, uncertainties in modeled V_d for coniferous forest ranged from 11-20%, 8-15%, ~0-21%, and 13-17%, in the *Z01*, *PZ10*, *KS12*, and *ZH14* parameterizations, respectively. In Fig. 3C, uncertainties in modeled V_d for deciduous forest ranged from 10-21%, 20-29%, ~0-21%, and 15-18% in the *Z01*, *PZ10*, *KS12*, and *ZH14* parameterizations, respectively. In Fig. 3D, uncertainties in modeled V_d for water surfaces ranged from 11-21%, ~0-25%, 18%, 14-18%, and 18-36% in the *Z01*, *PZ10*, *KS12*, *ZH14*, and *ZS14* parameterizations, respectively. In Fig. 3E, uncertainties in modeled V_d for ice/snow surfaces ranged from 14-30%, ~0-8%, ~0-28%, and 13-17% in the *Z01*, *PZ10*, *KS12*, and *ZH14* parameterizations, respectively.

4.3. Sensitivity analysis results: Sobol' first order sensitivity index

For Sobol' first order sensitivity analysis, five particle sizes (i.e., d_p = 0.001, 0.01, 0.1, 1.0, and 10 μm) were selected. A sample size (n) of 100,000 was used for model evaluations for each of the five particle sizes. To assess the confidence intervals for the first order Sobol' sensitivity index, bootstrapping resampling was used. In the bootstrapping method, the n samples used for the sensitivity simulations were sampled 1,000 times with replacement. In the following sections, the results from the Sobol' sensitivity analysis, and evolution of the parameter rankings are presented.

The Sobol' sensitivity analysis performed here is used to achieve a ranking of the model input parameters. The ranking of the parameters from most to least sensitive of the five particle sizes for the five parameterizations is shown in Table 11. Tables S1-S5 show the first order Sobol' indices of the various input parameters used in five dry deposition parameterizations for five LUCs. In these tables, particle size-dependent first order Sobol' index (S_i) for different model input parameters are presented with 95% confidence intervals (*CI*) obtained by bootstrap sampling. For example, the results of the first order Sobol' indices for the

Z01 parameterization on five LUCs are presented in Table S1. It is important to note that the number of parameters tested for Sobol' analysis varied between different LUCs, mainly because the number of parameters required for modeling V_d for one LUC may be more or less as compared to another LUC.

As shown in Table S1, for the *Z01* parameterization on grass, the importance of the most influential parameters on the modeled dry deposition velocities for five particles sizes can be compared using the corresponding S_i values of the model input parameters (e.g., $i = RH, \rho, L_O, u_*$, etc.). For example, with $d_p = 0.001$ µm, it can be clearly seen that the u_* is by far the single most sensitive parameter with an S_i value of 0.918, which indicates that 91.8% of the variation in the modeled V_d can be attributed to variations in u_*. The other parameters that have significant effect on the modeled V_d are z_0 and L_O. These two parameters have S_i values of 0.044 and 0.009, respectively. As compared to the first order Sobol' value of u_*, these values are significantly smaller; however, the lower limits of the corresponding 95% C.I. intervals for z_0 and L_O are greater than zero, indicating that they have a significant effect on the modeled velocities. The S_i values for the other two parameters, *RH* and particle ρ, were approximately zero for $d_p = 0.001$ µm (Table S1), and indicate that these variables have no influence on the modeled V_d.

Comparison between the first order Sobol' indices for different particle sizes for grass shows strong variations for certain input parameters, which reveals interesting findings about the relative importance (from the most to the least) of the model input parameters to the modeled dry V_d. For example, as seen from Table S1, as d_p increases from 0.001 to 10 µm, S_i values of u_* decrease from 0.918 to 0.245, which indicates that deposition of coarse particles is not strongly influenced by variations in friction velocity. From Table S1 it is also seen that parameters that influence particle properties (i.e., *RH* and ρ_P) have higher S_i values for the coarse particles as compared to the fine or accumulation mode particles. Similar comparisons between size-dependent behavior of parameter sensitivity for other rough surfaces (i.e., coniferous and deciduous forests) can be made using the S_i values reported in Table S1.

The results of the first order Sobol' indices for the *Z01* parameterization on two smooth surfaces: water and ice/snow are also presented in Table S1. Over liquid water surfaces, variation in u_* values has the largest influence modeled V_d for $d_p = 0.001$ to 10.0 µm. As is seen from Table S1, the S_i values of u_* can alone explain 98.3-99.5% of the variations in modeled V_d for particle sizes up to fine mode (i.e., 0.001-0.01 µm). For coarse mode particles (e.g., $d_p = 10$ µm), u_* is also the most influential parameter, contributing ca. 56% of the total variation in modeled V_d, while relative humidity is the second most influential/sensitive parameter with an S_i value of 0.393. The influence of u_* also tends to dominate the modeled V_d over ice/snow surfaces. This theory can be confirmed by comparing the size-dependent S_i values of u_* shown in Table S1, which suggest that u_* is the single most sensitive parameter ($S_i = 0.978$) for $d_p = 1.0$ µm. As the particle size increased to 10 µm, *RH* and u_* can explain 92.7% of the total variation in modeled V_d in the *Z01* parameterization.

The results of the first order Sobol' indices for the *PZ10* parameterization on five LUCs are presented in Table S2. The size-dependent S_i values on coniferous forest can be compared here to elucidate the contribution of different input parameters on the modeled V_d. It can be noted that, on rough surfaces, the *PZ10* parameterization was tested for the most number of input parameters (i.e., nine) among the five parameterizations. Some canopy properties such as *h*, *d*, *LAI*, and meteorological properties such as *U* were tested for their influence on modeled V_d in addition to those parameters that were tested for the rough surfaces in the *Z01* parameterization. As seen from Table S2, for coniferous forest, for $d_p = 0.001$ µm, u_* and L_O are the two most influential parameters (S_i values of 0.492 and 0.462, respectively). Although *LAI* is not the most influential parameter for the range of d_p tested here, its influence on the overall variability in the modeled V_d increase from 0.5 to 31.3% as particle size increases from 0.001 to 0.1 µm. Similarly, wind speed tends to show an increasing influence as d_p increases from 0.001 to 1.0 µm (overall

contribution of U in the variability in V_d shows an increase from 0.1% to 27.7%). For coarse particles (i.e., d_p = 10 um), u_* and L_O are the two most influential parameters with S_i values of 0.372 and 0.350, respectively. Together with *RH*, the three parameters can explain 92% of the variation in the modeled V_d. Results from the first order Sobol' indices for the other LUCs for the *PZ10* parameterization presented in Table S2 can be explained in a manner similar to that used to explain the contribution of the most sensitive parameters to the modeled dry deposition velocities. For the water surface, u_* is the most influential parameter for d_p = 0.001 µm as 99.4% of the total variance on the modeled V_d is attributed to its variability. Indeed, for particle sizes up to 0.1 µm, the u_* itself is most sensitive parameter. As seen from Table 11, *RH* becomes the most influential model parameter for d_p = 1.0 and 10.0 µm, which alone contribute to 69.5% and 95.6% of the total variabilities in the modeled V_d, respectively.

Table S3 shows the first order Sobol' indices for the *KS12* parameterization on five LUCs. For brevity, the results of the first order sensitivity indices for deciduous forest are discussed herein. It is seen that u_* is the single most influential parameter for d_p = 0.001 to 0.1 µm (e.g., total contribution on the modeled V_d attributable to u_* ranges from 94.4 to 96.7%). For d_p = 1.0 and 10 µm, *RH* is the most influential parameter with S_i values of 0.629 and 0.934, respectively.

Table S4 shows the first order Sobol' indices for the *ZH14* parameterization on five LUCs. The results show a strong influence of u_* on the modeled V_d. As shown in Table S4, the S_i values alone can explain nearly 100% of the variation in the modeled V_d for d_p = 0.001 to 1.0 µm. For large particles (e.g., d_p = 10 µm), *RH* is the most influential parameter, however, the contributions of other parameters as listed in Table S4 vary with regard to changes in LUCs.

5. Discussion

The accuracy of the parameterizations should be interpreted within the context of the field measurements used in this study assuming that they were accurate. In addition, the inter-comparison of the parameterizations' accuracy is subject to uncertainties with regard to the assumed values of missing meteorological parameters, particle properties, or surface features. Evidently, the normalized mean bias factors obtained using the ensemble approach is a useful measure to inter-compare the parameterizations' performance against a sub-set of field measurements for a given LUC. Extending the comparison of the normalized mean bias factors across the five LUCs for the five parameterizations investigated in this study provides a relative assessment of their accuracy. However, the *ZH14* parameterization is most accurate for all parameterizations except coniferous forest, where it is a close second to the *KS12* parameterization.

For rough surfaces, our results suggest that *ZH14* is the most accurate parameterization for grass and deciduous forest, and it is the second most accurate parameterization for coniferous forest. In contrast, *KS12*, *PZ10*, and *ZS14* are the least accurate parameterizations for grass, coniferous, and deciduous forests, respectively. It is interesting that in most cases the models under-predicted the measured dry deposition velocities (negative bias factors in Tables 4-8). Indeed, for grass, except for the *Z01* parameterization, the other four parameterizations under-predicted the measured V_d by factors of 1.54 to 10.37 (B_{NMBF} varied from -0.54 to -9.37). With regard to deciduous and coniferous forests, all of the five models (from the most to the least accurate: *ZH14*, *PZ10*, *KS12*, *Z01*, and *ZS14; KS12*, *ZH14*, *Z01*, *ZS14*, and *PZ10*) under-predicted the measured V_d by factors of 4.75 to 11.93, and 2.75 to 4.93, respectively.

A direct quantitative comparison of the accuracy of the five parameterizations with those reported in other studies is impossible because the metric used in the present study (B_{NMBF}) is not commonly used to evaluate the accuracy of the dry deposition models. However, qualitatively, our findings regarding the *PZ10* performance for coniferous forests are in accordance with those reported by Petroff and Zhang (2010). They reported that the *PZ10* parameterization under-predicted the measured deposition

765 velocities for the following subset of observations that we also investigated for coniferous forest: Lamaud et al. (1994), Gallagher et al. (1997), Buzorious et al. (2000), Gaman et al. (2004), and over-predicted for Grönholm et al. (2009).

The accuracy results over smooth surfaces suggest that, for the water surface, the best agreement between the measured and modeled V_d was found for the *ZH14* parameterization. Overall, the accuracy ranking from best to worst is as follows: *ZH14*, *Z01*, *KS12*, *PZ10*, and *ZS14*. Over ice/snow surface, the results suggest that the *ZH14* is the most accurate parameterization, and
770 *PZ10* is the least accurate. Qualitatively, this finding is consistent with Petroff and Zhang (2010), who reported that their model significantly underestimated the measured deposition velocities over ice/snow surface for the following studies: Ibrahim (1983), Duan et al. (1987), Nilsson and Rannik (2001), and Contini et al. (2010), which were also investigated in the present study. We also note that the *Z01* parameterization overestimated the measured V_d from the aforementioned studies. This finding is consistent with Petrofff and Zhang (2010), as they compared their model with *Z01* over the ice/snow surface. One possible explanation for a
775 large discrepancy between modeled and measured V_d by *PZ10* is an incorrect magnitude of the drift velocity applied, corresponding to phoretic effects on ice and snow.

Collectively for both rough and smooth surfaces, it is found that the *ZH14* scheme is the most accurate for these LUCs: grass, deciduous forest, water, and ice/snow surfaces. *KS12* performed slightly better for coniferous forest only. The performance of the *PZ10* scheme could be viewed as moderate. This finding is interesting considering that the *ZH14* is the simplest resistance-
780 based scheme of the five parameterizations. We emphasize that *Z01* and *ZH14* parameterizations share similar structural features, but simplifications of the particle collection processes by constant values by *ZH14* (see Eqs. (46-50)) could produce better agreement. In addition, we note that the *KS12* parametrization is based exclusively on wind tunnel measurements and its performance over forest canopies is not satisfactory, as reported by the model developers Kouznetsov and Sofiev (2012). However, we find that *KS12* performed the best over coniferous forests with the nine studies used in this research. However, Kouznetsov and
785 Sofiev (2012) did not use the same subset of studies to evaluate the model performance as we used.

Given the complex nature and incomplete knowledge of the dry deposition process, it is of importance to account for the uncertainties in the modeled deposition velocities in atmospheric transport models (Petroff and Zhang, 2010; Zhang et al., 2012). Although there have been many dry deposition models developed over the years, the information on the model output uncertainties is meager and not up-to-date. To assert uncertainty on the modeled dry deposition velocities, Gould and Davidson (1992) adopted
790 a step-wise uncertainty test of Slinn's (1982) model. However, in reality, the model parameters are subject to simultaneous variability, and a OAT test cannot adequately propagate the error to the overall model outputs. This limitation was partially overcome by Ruijgrok (1992), who performed a probabilistic uncertainty test of Slinn's model.

The Monte Carlo uncertainty analysis performed in this study assumes that in the five parameterizations all the major physical processes (e.g., turbulent diffusion, Brownian diffusion, impaction, interception, and gravitational settling) of dry
795 deposition are accounted for satisfactorily. Thus, the uncertainty analysis conforms to the uncertainties in the model input variables and their overall contribution to the propagated uncertainties in the modeled dry deposition velocities. Additional uncertainties in the modeled deposition velocities may arise from inadequate model formulation and/or inappropriate use of certain micrometeorological parameters. For example, in dry deposition models (such as *PZ10*), d and z_0 are often calculated as a fraction of h, and are often taken as $d \approx 2h/3$ and $z_0 \approx 0.1h$. These expressions are valid for dense canopies (Katul et al., 2010). If the leaf
800 area density is highly skewed or shows a bimodal distribution, such approximations cannot be used (Katul et al., 2010). In addition, the parameter values of d and z_0 are subject to large uncertainty and are very difficult to measure in urban areas (Cherin et al., 2015). Therefore, caution must be taken when using constant d and z_0 values from lookup tables. Also, current deposition models do not consider terrain complexity in their formulations. Hicks (2008) argued that conventional use of d and z_0 for non-flat terrain such as mountains is not appropriate for modeling deposition on complex terrain. In addition, experimentally derived values of d

and z_0 often represent local characteristics. Thus, it poses a challenge to scale those up in a model grid cell (Schaudt and Dickinson, 2000) in atmospheric transport models. Using remote sensing, robust scaling of these parameter values is achieved, which could be used to acquire representative values in a model grid cell (Tian et al., 2011). However, addressing the issue of a model's structural uncertainty in a detailed manner was outside the scope of this paper.

The values of the eight model parameters, covering four meteorological (U, u_*, L_O, and RH) and four canopy morphological (z_0, d, h, and LAI) properties, used in the Monte Carlo simulations were assumed to be uniformly distributed because their true distributions were unknown. It is emphasized that these parameters are not all necessarily independent; z_0 and d are functions of the surface characteristics (Zhang and Sao, 2014; Shao and Yang, 2005, 2008). Considering these underlying assumptions, the uncertainties in modeled V_d reported in this paper should be viewed as the effect of the chosen parameter PDFs on the output uncertainty. The uncertainty bounds (i.e., the central 90% values) reported in the Table 9 could be treated as a metric of the quality of the modeled outputs. The normalized uncertainties reported in this study are a useful indicator to assess the overall performance of a model for four particle modes (seven particle sizes) across five LUCs.

We applied Sobol' sensitivity analysis to identify the most influential parameter(s) of the five parameterizations. Parameter rankings achieved using the Sobol' first order indices for different models provide a robust evaluation of the models' sensitivity by varying a set of input parameters within their plausible ranges. It is emphasized that a local sensitivity analysis such as OAT could lead to incomplete or misleading inference of the parameter sensitivity on the model's output because assumptions of model linearity are not always justified for dry deposition parameterizations due to their complex formulations.

The Sobol' sensitivity rankings presented in Table 11 can be used for inter-comparison between models' parameter sensitivity. Over rough surfaces, for nucleation size particles (e.g., d_p = 0.001 μm), u_* is the most sensitive parameter for *Z01*, *PZ10*, *KS12*, and *ZH14* parameterizations. As particle size increases from 0.001 μm to 1.0 μm, except for the *PZ10* scheme and for 1.0 μm for grass in *KS12* scheme, u_* remains the most influential parameter. This finding is in accordance with previous studies (Zhang et al., 2001; Zhang and He, 2014) that show that dry deposition velocities for atmospheric particles are greatly influenced by friction velocity. We note that in the *PZ10* scheme, *LAI* and L_O are the two most commonly-found sensitive parameters for d_p = 0.001 to 1.0 μm for rough surfaces. As seen from the parameter rankings (Table 11), for d_p = 10 μm in the *Z01*, *PZ10*, *KS10*, *ZH14* schemes, *RH* is the most influential factor. We postulate that with particle growth, high humidity may have a significant effect on coarse mode particles, and as a result, other model input parameters become less sensitive. The parameter ranking of the *PZ10* scheme for deciduous forest shows that L_O is the most influential parameter. Similarly, for coniferous forest, L_O is found to be one of the most sensitive parameters for most particle sizes. One possible reason for this finding could be the interdependency of the particle mixing length parameter and L_O in the *PZ10* scheme. Indeed, the mixing length indirectly relates to particle collection efficiencies in the *PZ10* parameterization (see Eqs. 18, 25, and 26). The rankings of the *Z01* and *ZH14* parameters are nearly identical for rough and smooth surfaces. This finding is not surprising given that these two parameterizations were developed by applying similar assumptions.

In general, dry deposition parameterizations developed for different particle size ranges and surfaces vary widely in terms of their complexity in model structure. The complexity in their numerical formulations often depends on the purpose (e.g., operational or research) of the model development (Petroff et al., 2008a). Comparing two previously developed one-dimensional aerosol deposition models for broadleaf and coniferous canopies (see details in Petroff et al., 2008b; Petroff et al., 2009) with the *PZ10* parameterization, Petroff and Zhang (2010) argued that the mathematical formulations in those models are too complex and require numerous input parameters for implementation in aerosol transport models. Following this hypothesis, we attempt to qualitatively evaluate the relative complexity of the five dry deposition parameterizations tested in this study for incorporation into atmospheric transport models.

Of the five parameterizations, we note that the model structure of the *PZ10* is relatively more complex than those of the *Z01*, *ZH14*, and *ZS14* parameterizations. The complexity of the *KS12* parameterization tends to be different by a large degree between rough (i.e., vegetative canopies and snow) and smooth (i.e., water) surfaces. The *ZS14* formulation (Eqs. (51-63)) is of comparable complexity to the rough surface formulation in the *KS12* parameterization (Eqs. (35-45)), and these parameterizations can be viewed as moderately complex. The formulation of the *Z01* parameterization can be viewed as moderately complex as well. In this parameterization, three processes (Brownian diffusion, interception, and impaction) were parameterized using Eqs. (8-14) to describe the particle deposition at the collection surface. We claim that the *KS12* parameterization for smooth surfaces is the most complex of the five models. This is mainly because it requires solving the dimensionless dry deposition velocity profiles over smooth surfaces using an analytical approach, which can be complex and computationally-expensive.

A direct qualitative comparison of the relative complexities of the major process terms in the *PZ10* and *Z01* parameterizations is possible because both of these parameterizations are resistance-based (i.e., expressions of V_d in Eqs. 2 and 6 are of similar forms). It is evident from Eqs. (19-31) that the formulations in the *PZ10* parametrization to compute the three surface collection process terms are relatively complex as compared to those in the *Z01* parameterization. In the *ZH14* parameterization (a resistance-based scheme as well), these process terms are not explicitly parameterized. Presumably, by incorporating a large number of LUC dependent constants to compute surface deposition velocity using Eqs. (46-50), simplifications were made possible to the *ZH14* parameterization. The use of fitting parameters to account for poorly understood dry deposition processes in parameterizations is not uncommon. Due to the complex nature and inadequate understanding of the particle collection processes to leaf surfaces, suggestions were made to treat particle deposition on vegetative surfaces in a simplified manner using empirically derived fitting parameters (Petroff et al., 2008a). Consequently, Petroff and Zhang (2010) also introduced a large number of artificial parameters to account for characteristic length and orientation of the canopy obstacle, and different LUCs to parameterize the particle collection efficiencies (e.g., due to Brownian diffusion, interception, turbulent and inertial impaction). Based on these considerations and those in the previous paragraph, we claim that the *ZH14* is the simplest of the five parameterizations.

6. Conclusions

In terms of overall performance for incorporation in atmospheric transport models, we suggest that parameterization accuracy and uncertainty should be considered jointly, while, based on our findings, sensitivity of the model input parameters should be treated separately for each dry deposition parameterization. The paper presents a comprehensive evaluation of the performance of five parameterizations in terms of their accuracy, model output uncertainty, and parameter sensitivity. Based on the results, it is evident that the *ZH14* parameterization is the most accurate for four of the five LUCs (grass, deciduous forest, water, and ice/snow surfaces) and second most accurate for the fifth LUC (coniferous forest). Of the five parametrizations, the uncertainty range for the *ZH14* (11-20%) has the lowest upper bound across the five LUCs for particle size ranging from 0.005-2.5 μm. In terms of the lower bound of the uncertainty range, the *ZH14* is second to the *Z01* (10-30%) parameterization. We demonstrated that the Sobol' sensitivity analysis can be successfully applied to dry deposition models to rank the input parameters by taking into account the complex interactions between them. One could argue that, if the different models exhibited greatest sensitivities to different parameters, and those parameters were more uncertain, the models exhibiting greatest sensitivity to the least certain parameters would be the most uncertain. In this way, sensitivity plays a potential role in determining which model is better. However, because our results showed that all models were most sensitive to u_*, or, at large size, *RH*, sensitivity does not end up playing a role in assigning which model is best. We also note that accurate measurement of u_* is extremely challenging (Andreas, 1992; Weber, 1999), and there exists ambiguity in its definition in boundary-layer meteorology (Weber, 1999).

The large dispersion in the parametrizations' accuracy may indicate that despite considerable efforts in developing sophisticated process-based dry deposition models, there remain major gaps in our understanding of the dry deposition process. Another possible explanation for the large dispersion may be that it is significantly caused by measurement uncertainties, which were not addressed in this paper. However, inter-variability in modeled deposition velocities is not uncommon, as pointed out by Ruijgrok et al. (1995) in an inter-comparison study of several earlier dry deposition models. We emphasize that the accuracy results presented in this paper should be discussed in terms of the locations in which the parameterization accuracy has been evaluated against measurements for the five LUCs (Table 1; Figure 1).

The results from the uncertainty analysis using the Monte Carlo simulations on the size-segregated particles should be of interest to atmospheric transport modelers as well as to the scientific community interested in quantifying the uncertainty bounds in the atmospheric deposition fluxes of pollutants to ecosystems using concentration data from monitoring stations. This is because until now, uncertainties in modeled V_d for size-segregated particles for a suite of currently-available dry deposition parameterizations has been unavailable. We stress that future work on probabilistic uncertainty analysis should focus on quantifying uncertainties for additional LUCs than those covered in this study. One of the major limitations of our uncertainty analysis approach is the assumption of uniform distribution of all imprecise model input parameters. To address this limitation, accurate information on the input parameter PDFs is needed.

With the help of field observations, and improved theoretical knowledge of dry deposition, the Sobol' parameter rankings could be used to fine-tune dry deposition models to better account for processes that are currently lacking or poorly parameterized. Future work should focus on estimating higher order (i.e., second order and total order) Sobol' indices. Such indices would be useful for model developers interested in understanding the joint influence of multiple input parameters on the modeled deposition velocities.

Based on the qualitative evaluation of relative complexity of the five parameterizations, we suggest that the model structure of the *ZH14* parameterization is the least complex. After reviewing over 100 air quality models, Kouznetsov and Sofiev (2012) reported that resistance-based approaches are extensively implemented in most of those models. Thus, in practice, it may be preferable to use a relatively simple parameterization over a complex (and potentially computationally expensive) one, if the accuracy and uncertainty of the model justify it. Based on these criteria (i.e., accuracy, uncertainty, and complexity), we propose that, of the five parameterizations we tested, the *ZH14* parameterization is currently superior for incorporation into atmospheric transport models.

7. Code availability

The R scripts used in this study are available in the supplemental material and can be found online at: https://osf.io/a6q97/. The R version 3.2.4 was used to create the scripts. A similar or higher version of R is required to run the scripts. The codes can be used, distributed, and reproduced for all non-commercial use under the terms of the Creative Commons Attribution-Noncommercial 3.0 Unported License (http://creativecommons.org/licenses/by-nc/3.0/), provided the original work is properly cited.

Note: The authors declare no competing financial interest.

8. Acknowledgements

This project was funded by the U.S. National Science Foundation's Coupled-Natural-Human System Program through Award No. 1313755.

References

Alcamo, J. and Bartnicki, J.: A framework for error analysis of a long-range transport model with emphasis on parameter uncertainty, Atmospheric Environment (1967), 21, 2121-2131, 1987.

Allen, A., Harrison, R., and Nicholson, K.: Dry deposition of fine aerosol to a short grass surface, Atmospheric Environment. Part A. General Topics, 25, 2671-2676, 1991.

Andreas, E. L.: Uncertainty in a Path-averaged Measurement of the Friction Velocity u, Journal of Applied Meteorology, 31, 1312-1321, 1992.

Beekmann, M. and Derognat, C.: Monte Carlo uncertainty analysis of a regional-scale transport chemistry model constrained by measurements from the atmospheric pollution over the Paris area (ESQUIF) campaign, Journal of Geophysical Research: Atmospheres, 108, 2003.

Bergin, M. S. and Milford, J. B.: Application of Bayesian Monte Carlo analysis to a Lagrangian photochemical air quality model, Atmospheric Environment, 34, 781-792, 2000.

Bergin, M. S., Noblet, G. S., Petrini, K., Dhieux, J. R., Milford, J. B., and Harley, R. A.: Formal uncertainty analysis of a Lagrangian photochemical air pollution model, Environmental Science & Technology, 33, 1116-1126, 1999.

Buzorius, G., Rannik, Ü., Mäkelä, J., Keronen, P., Vesala, T., and Kulmala, M.: Vertical aerosol fluxes measured by the eddy covariance method and deposition of nucleation mode particles above a Scots pine forest in southern Finland, Journal of Geophysical Research: Atmospheres, 105, 19905-19916, 2000.

Caffrey, P. F., Ondov, J. M., Zufall, M. J., and Davidson, C. I.: Determination of size-dependent dry particle deposition velocities with multiple intrinsic elemental tracers, Environmental science & technology, 32, 1615-1622, 1998.

Chen, L., Rabitz, H., Considine, D. B., Jackman, C. H., and Shorter, J. A.: Chemical reaction rate sensitivity and uncertainty in a two-dimensional middle atmospheric ozone model, Journal of Geophysical Research: Atmospheres, 102, 16201-16214, 1997.

Cherin, N., Roustan, Y., Musson-Genon, L., and Seigneur, C.: Modelling atmospheric dry deposition in urban areas using an urban canopy approach, Geoscientific Model Development, 8, 893-910, 2015.

Contini, D., Donateo, A., Belosi, F., Grasso, F., Santachiara, G., and Prodi, F.: Deposition velocity of ultrafine particles measured with the Eddy-Correlation Method over the Nansen Ice Sheet (Antarctica), Journal of Geophysical Research: Atmospheres, 115, 2010.

Derwent, R. and Hov, Ø.: Application of sensitivity and uncertainty analysis techniques to a photochemical ozone model, Journal of Geophysical Research: Atmospheres, 93, 5185-5199, 1988.

Donateo, A. and Contini, D.: Correlation of dry deposition velocity and friction velocity over different surfaces for PM2. 5 and particle number concentrations, Advances in Meteorology, 2014, 2014.

Duan, B., Fairall, C., and Thomson, D.: Eddy correlation measurements of the dry deposition of particles in wintertime, Journal of Applied Meteorology, 27, 642-652, 1988.

Efron, B. and Tibshirani, R. J.: An introduction to the bootstrap, CRC press, 1994.

Feng, J.: A size-resolved model and a four-mode parameterization of dry deposition of atmospheric aerosols, Journal of Geophysical Research: Atmospheres, 113, 2008.

Gallagher, M., Beswick, K., Duyzer, J., Westrate, H., Choularton, T., and Hummelshøj, P.: Measurements of aerosol fluxes to Speulder forest using a micrometeorological technique, Atmospheric Environment, 31, 359-373, 1997.

Gaman, A., Rannik, Ü., Aalto, P., Pohja, T., Siivola, E., Kulmala, M., and Vesala, T.: Relaxed eddy accumulation system for size-resolved aerosol particle flux measurements, Journal of Atmospheric and Oceanic Technology, 21, 933-943, 2004.

Giorgi, F.: A particle dry-deposition parameterization scheme for use in tracer transport models, Journal of Geophysical Research: Atmospheres, 91, 9794-9806, 1986.

Gould, T. and Davidson, C.: Variability and uncertainty in particle dry deposition modelling, Precipitation Scavenging and Atmosphere–Surface Exchange Processes. Hemisphere, Publ., Washington, DC, 1992. 1125-1142, 1992.

Grönholm, T., Launiainen, S., Ahlm, L., Mårtensson, E., Kulmala, M., Vesala, T., and Nilsson, E.: Aerosol particle dry deposition to canopy and forest floor measured by two-layer eddy covariance system, Journal of Geophysical Research: Atmospheres, 114, 2009.

Gronlund, A., Nilsson, D., Koponen, I. K., Virkkula, A., and Hansson, M. E.: Aerosol dry deposition measured with eddy-covariance technique at Wasa and Aboa, Dronning Maud Land, Antarctica, Annals of Glaciology, 35, 355-361, 2002.

Hanna, S. R., Chang, J. C., and Fernau, M. E.: Monte Carlo estimates of uncertainties in predictions by a photochemical grid model (UAM-IV) due to uncertainties in input variables, Atmospheric Environment, 32, 3619-3628, 1998.

Hanna, S. R., Lu, Z., Frey, H. C., Wheeler, N., Vukovich, J., Arunachalam, S., Fernau, M., and Hansen, D. A.: Uncertainties in predicted ozone concentrations due to input uncertainties for the UAM-V photochemical grid model applied to the July 1995 OTAG domain, Atmospheric Environment, 35, 891-903, 2001.

Heinonen, M.: A comparison of humidity standards at seven European national standards laboratories, Metrologia, 39, 303, 2002.

Held, A., Brooks, I., Leck, C., and Tjernstrom, M.: On the potential contribution of open lead particle emissions to the central Arctic aerosol concentration, Atmospheric Chemistry and Physics, 11, 3093-3105, 2011a.

Held, A., Orsini, D., Vaattovaara, P., Tjernström, M., and Leck, C.: Near-surface profiles of aerosol number concentration and temperature over the Arctic Ocean, Atmospheric Measurement Techniques, 4, 1603, 2011b.

Hicks, B., Baldocchi, D., Meyers, T., Hosker, R., and Matt, D.: A preliminary multiple resistance routine for deriving dry deposition velocities from measured quantities, Water, Air, & Soil Pollution, 36, 311-330, 1987.

Hicks, B. B.: On estimating dry deposition rates in complex terrain, Journal of Applied Meteorology and Climatology, 47, 1651-1658, 2008.

Hicks, B. B., Saylor, R. D., and Baker, B. D.: Dry deposition of particles to canopies—A look back and the road forward, Journal of Geophysical Research: Atmospheres, 121, 2016.

Högström, U. and Smedman, A.-S.: Accuracy of sonic anemometers: laminar wind-tunnel calibrations compared to atmospheric in situ calibrations against a reference instrument, Boundary-Layer Meteorology, 111, 33-54, 2004.

Ibrahim, M., Barrie, L., and Fanaki, F.: An experimental and theoretical investigation of the dry deposition of particles to snow, pine trees and artificial collectors, Atmospheric Environment (1967), 17, 781-788, 1983.

IPCC third assessment report, Cambridge and New York: Cambridge University Press. Volumes I (The Scientific Basis), II (Impacts, Adaptation, and Vulnerability) and III (Mitigation), 2001. 2001.

Katul, G., Grönholm, T., Launiainen, S., and Vesala, T.: Predicting the dry deposition of aerosol-sized particles using layer-resolved canopy and pipe flow analogy models: Role of turbophoresis, Journal of Geophysical Research: Atmospheres, 115, 2010.

Kouznetsov, R. and Sofiev, M.: A methodology for evaluation of vertical dispersion and dry deposition of atmospheric aerosols, Journal of Geophysical Research: Atmospheres, 117, 2012.

Lamaud, E., Brunet, Y., Labatut, A., Lopez, A., Fontan, J., and Druilhet, A.: The Landes experiment: Biosphere-atmosphere exchanges of ozone and aerosol particles above a pine forest, Journal of Geophysical Research: Atmospheres, 99, 16511-16521, 1994.

Larjavaara, M. and Muller-Landau, H. C.: Measuring tree height: a quantitative comparison of two common field methods in a moist tropical forest, Methods in Ecology and Evolution, 4, 793-801, 2013.

Lilburne, L. and Tarantola, S.: Sensitivity analysis of spatial models, International Journal of Geographical Information Science, 23, 151-168, 2009.

MacMahon, T. and Denisot, P.: Empirical atmospheric deposition-a survey, Atmospheric Environment, 13, 571-585, 1979.

Mallet, V. and Sportisse, B.: Uncertainty in a chemistry-transport model due to physical parameterizations and numerical approximations: An ensemble approach applied to ozone modeling, Journal of Geophysical Research: Atmospheres, 111, 2006.

Matsuda, K., Fujimura, Y., Hayashi, K., Takahashi, A., and Nakaya, K.: Deposition velocity of PM2. 5 sulfate in the summer above a deciduous forest in central Japan, Atmospheric Environment, 44, 4582-4587, 2010.

Möller, U. and Schumann, G.: Mechanisms of transport from the atmosphere to the Earth's surface, Journal of Geophysical Research, 75, 3013-3019, 1970.

Muyshondt, A., Anand, N., and McFarland, A. R.: Turbulent deposition of aerosol particles in large transport tubes, Aerosol Science and Technology, 24, 107-116, 1996.

Nemitz, E., Gallagher, M. W., Duyzer, J. H., and Fowler, D.: Micrometeorological measurements of particle deposition velocities to moorland vegetation, Quarterly Journal of the Royal Meteorological Society, 128, 2281-2300, 2002.

Neumann, H. and Den Hartog, G.: Eddy correlation measurements of atmospheric fluxes of ozone, sulphur, and particulates during the Champaign intercomparison study, Journal of Geophysical Research: Atmospheres, 90, 2097-2110, 1985.

Nilsson, E.D. and Rannik, Ü.: Turbulent aerosol fluxes over the Arctic Ocean 1. Dry deposition over sea and pack ice, Journal of Geophysical Research, 106, 32,125-132,137, 2001.

Noll, K. E., Jackson, M. M., and Oskouie, A. K.: Development of an atmospheric particle dry deposition model, Aerosol Science & Technology, 35, 627-636, 2001.

Nossent, J., Elsen, P., and Bauwens, W.: Sobol'sensitivity analysis of a complex environmental model, Environmental Modelling & Software, 26, 1515-1525, 2011.

Oskouie, A. K., Noll, K. E., and Wang, H.-C.: Minimizing the effect of density in determination of particle aerodynamic diameter using a time of flight instrument, Journal of aerosol science, 34, 501-506, 2003.

Pappenberger, F., Beven, K. J., Ratto, M., and Matgen, P.: Multi-method global sensitivity analysis of flood inundation models, Advances in water resources, 31, 1-14, 2008.

Petroff, A., Mailliat, A., Amielh, M., and Anselmet, F.: Aerosol dry deposition on vegetative canopies. Part I: review of present knowledge, Atmospheric Environment, 42, 3625-3653, 2008a.

Petroff, A., Mailliat, A., Amielh, M., and Anselmet, F.: Aerosol dry deposition on vegetative canopies. Part II: A new modelling approach and applications, Atmospheric Environment, 42(16), 3654-3683, 2008b.

Petroff, A., Zhang, L., Pryor, S.C. and Belot, Y.: An extended dry deposition model for aerosols onto broadleaf canopies, Journal of Aerosol Science, 40(3), 218-240, 2009.

Petroff, A. and Zhang, L.: Development and validation of a size-resolved particle dry deposition scheme for application in aerosol transport models, Geoscientific Model Development, 3, 753-769, 2010.

Pryor, S.: Size-resolved particle deposition velocities of sub-100nm diameter particles over a forest, Atmospheric Environment, 40, 6192-6200, 2006.

Pryor, S., Barthelmie, R., and Hornsby, K.: Size-resolved particle fluxes and vertical gradients over and in a sparse pine forest, Aerosol Science and Technology, 47, 1248-1257, 2013.

Pryor, S., Gallagher, M., Sievering, H., Larsen, S. E., Barthelmie, R. J., Birsan, F., Nemitz, E., Rinne, J., Kulmala, M., and Grönholm, T.: A review of measurement and modelling results of particle atmosphere–surface exchange, Tellus B, 60, 42-75, 2008.

Pryor, S., Larsen, S. E., Sørensen, L. L., Barthelmie, R. J., Grönholm, T., Kulmala, M., Launiainen, S., Rannik, Ü., and Vesala, T.: Particle fluxes over forests: Analyses of flux methods and functional dependencies, Journal of Geophysical Research: Atmospheres, 112, 2007.

Rannik, Ü., Petäjä, T., Buzorius, G., Aalto, P., Vesala, T., and Kulmala, M.: Deposition velocities of nucleation mode particles into a Scots pine forest, Environmental and Chemical Physics, 22, 97-102, 2000.

Rannik, Ü., Zhou, L., Zhou, P., Gierens, R., Mammarella, I., Sogachev, A., and Boy, M.: Aerosol dynamics within and above forest in relation to turbulent transport and dry deposition, Atmospheric Chemistry and Physics, 16, 3145-3160, 2016.

Richardson, A. D., Dail, D. B., and Hollinger, D.: Leaf area index uncertainty estimates for model–data fusion applications, Agricultural and forest meteorology, 151, 1287-1292, 2011.

Ruijgrok, W.: Uncertainty in models calculating the dry deposition of aerosols to forests, Nucleation and atmospheric aerosols. Deepak Publ., Hampton, 1992. 481-485, 1992.

Ruijgrok, W., Davidson, C. I., and Nicholson, K. W.: Dry deposition of particles: Implications and recommendations for mapping of deposition over Europe, Tellus B: Chemical and Physical Meteorology, 48, 710-710, 1996.

Ruijgrok, W., Tieben, H., and Eisinga, P.: The dry deposition of particles to a forest canopy: a comparison of model and experimental results, Atmospheric Environment, 31, 399-415, 1997.

Saltelli, A. and Annoni, P.: How to avoid a perfunctory sensitivity analysis, Environmental Modelling & Software, 25, 1508-1517, 2010.

Saltelli, A., Annoni, P., Azzini, I., Campolongo, F., Ratto, M., and Tarantola, S.: Variance based sensitivity analysis of model output. Design and estimator for the total sensitivity index, Computer Physics Communications, 181, 259-270, 2010.

Sehmel, G. and Hodgson, W.: Model for predicting dry deposition of particles and gases to environmental surfaces, Battelle Pacific Northwest Labs., Richland, WA (USA), 1978.

Sehmel, G., Sutter, S., and Simpson, C.: Particle deposition rates on a water surface as a function of particle diameter and air velocity, Battelle Pacific Northwest Labs., Richland, Wash.(USA), 1974.

Schaudt, K. and Dickinson, R.: An approach to deriving roughness length and zero-plane displacement height from satellite data, prototyped with BOREAS data, Agricultural and Forest Meteorology, 104, 143-155, 2000.

Sehmel, G. A.: Particle and gas dry deposition: a review, Atmospheric Environment (1967), 14, 983-1011, 1980.

Seinfeld, J. and Pandis, S.: Atmospheric chemistry and physics: from air pollution to climate change, 2006. 2006.

Shao, Y. and Yang, Y.: A scheme for drag partition over rough surfaces, Atmospheric Environment, 39, 7351-7361, 2005.

Shao, Y. and Yang, Y.: A theory for drag partition over rough surfaces, Journal of Geophysical Research: Earth Surface, 113, 2008.

Slinn, W.: Predictions for particle deposition to vegetative canopies, Atmospheric Environment (1967), 16, 1785-1794, 1982.

Sobol, I. M.: Sensitivity estimates for nonlinear mathematical models, Mathematical Modelling and Computational Experiments, 1, 407-414, 1993.

Stull, R. B.: An introduction to boundary layer meteorology, Springer Science & Business Media, 2012.

Su, Z., Schmugge, T., Kustas, W., and Massman, W.: An evaluation of two models for estimation of the roughness height for heat transfer between the land surface and the atmosphere, Journal of applied meteorology, 40, 1933-1951, 2001.

Tang, T., Reed, P., Wagener, T., and Van Werkhoven, K.: Comparing sensitivity analysis methods to advance lumped watershed model identification and evaluation, Hydrology and Earth System Sciences Discussions, 3, 3333-3395, 2006.

Tatang, M. A., Pan, W., Prinn, R. G., and McRae, G. J.: An efficient method for parametric uncertainty analysis of numerical geophysical models, Journal of Geophysical Research: Atmospheres, 102, 21925-21932, 1997.

Van Aaslt, R.M.: Dry deposition of aerosol particles, Lee, D., Schneider, T., Grant, L. et Verkert, P., éditeurs, Aerosols, 933-949, 1986.

Tian, X., Li, Z., Van der Tol, C., Su, Z., Li, X., He, Q., Bao, Y., Chen, E., and Li, L.: Estimating zero-plane displacement height and aerodynamic roughness length using synthesis of LiDAR and SPOT-5 data, Remote sensing of environment, 115, 2330-2341, 2011.

Van Werkhoven, K., Wagener, T., Reed, P., and Tang, Y.: Characterization of watershed model behavior across a hydroclimatic gradient, Water Resources Research, 44, 2008.

Venkatram, A. and Pleim, J.: The electrical analogy does not apply to modeling dry deposition of particles, Atmospheric Environment, 33, 3075-3076, 1999.

Vong, R. J., Vickers, D., and Covert, D. S.: Eddy correlation measurements of aerosol deposition to short grass, Tellus B, 56, 105-117, 2004.

Weber, R. O.: Remarks on the definition and estimation of friction velocity, Boundary-Layer Meteorology, 93,197-209, 1999.

Weidinger, T., Pinto, J., and Horváth, L.: Effects of uncertainties in universal functions, roughness length, and displacement height on the calculation of surface layer fluxes, Meteorologische Zeitschrift, 9, 139-154, 2000.

Wesely, M., Cook, D., and Hart, R.: Fluxes of gases and particles above a deciduous forest in wintertime, Boundary-Layer Meteorology, 27, 237-255, 1983.

Wesely, M. and Hicks, B.: A review of the current status of knowledge on dry deposition, Atmospheric environment, 34, 2261-2282, 2000.

Wesely, M., Hicks, B., Dannevik, W., Frisella, S., and Husar, R.: An eddy-correlation measurement of particulate deposition from the atmosphere, Atmospheric Environment (1967), 11, 561-563, 1977.

Williams, R. M.: A model for the dry deposition of particles to natural water surfaces, Atmospheric Environment (1967), 16, 1933-1938, 1982.

Wiman, B. L. and Ågren, G. I.: Aerosol depletion and deposition in forests—a model analysis, Atmospheric Environment (1967), 19, 335-347, 1985.

Wyers, G. and Duyzer, J.: Micrometeorological measurement of the dry deposition flux of sulphate and nitrate aerosols to coniferous forest, Atmospheric Environment, 31, 333-343, 1997.

Yang, J.: Convergence and uncertainty analyses in Monte-Carlo based sensitivity analysis, Environmental Modelling & Software, 26, 444-457, 2011.

Yu, S., Eder, B., Dennis, R., Chu, S. H., and Schwartz, S. E.: New unbiased symmetric metrics for evaluation of air quality models, Atmospheric Science Letters, 7, 26-34, 2006.

Zhang, J. and Shao, Y.: A new parameterization of particle dry deposition over rough surfaces, Atmospheric Chemistry and Physics, 14, 12429-12440, 2014.

Zhang, L., Gong, S., Padro, J., and Barrie, L.: A size-segregated particle dry deposition scheme for an atmospheric aerosol module, Atmospheric Environment, 35, 549-560, 2001.

Zhang, L. and He, Z.: Technical Note: An empirical algorithm estimating dry deposition velocity of fine, coarse and giant particles, Atmospheric Chemistry and Physics, 14, 3729-3737, 2014.

Zhang, L. and Vet, R.: A review of current knowledge concerning size-dependent aerosol removal, China Particuology, 4, 272-282, 2006.

Zufall, M. J., Davidson, C. I., Caffrey, P. F., and Ondov, J. M.: Airborne concentrations and dry deposition fluxes of particulate species to surrogate surfaces deployed in southern Lake Michigan, Environmental science & technology, 32, 1623-1628, 1998.

Table 1. Measurement studies used to evaluate the five parameterizations.

Land use category	No.	Title	Authors	Location	Latitude	Longitude	Elevation AMSL (m)	Sampling dates	Particle size (μm)
Grass	1	Dry deposition of fine aerosol to a grass surface	Allen et al. (1991)	U.K.	51.88° N	0.94° E	28	June, 1988-June, 1989	0.48
	2	An eddy-correlation measurement of particulate deposition from the atmosphere	Wesely et al. (1977)	U.S.	38.84° N	90.06° W	225	February-March, 1976	0.075
	3	Eddy correlation measurements of atmospheric fluxes of ozone, sulphur, and particulates during the Champaign intercomparison study	Neumann and den Hartog (1985)	U.S.	40.11° N	88.27° W	225	June, 1982	0.10-2.28
	4	Micrometeorological measurements of particle deposition velocities to moorland vegetation	Nemitz et al. (2002)	U.K.	55.79° N	3.23° W	109	May-October, 1999	0.12-0.45
	5	Eddy correlation measurements of aerosol deposition to grass	Vong et al. (2004)	U.S.	44.46° N	123.11° W	81	May-June, 2000	0.52
Coniferous forest	6	The Landes experiment: Biosphere-atmosphere exchanges of ozone and aerosol particles above a pine forest	Lamaud et al. (1994)	France	44.84° N	0.58° W	58	June, 1992	0.04
	7	Micrometeorological measurement of the dry deposition flux of sulphate and nitrate aerosols to coniferous forest	Wyers and Duyzers (1996)	The Netherlands	52.27° N	5.71° E	26	April-December, 1993	0.6
	8	Atmospheric particles and their interactions with natural surfaces	Gallagher et al. (1997)	The Netherlands	52.27° N	5.71° E	26	June-July, 1993	0.1-0.50
	9	The dry deposition of particles to a forest canopy: a comparison of model and experimental results	Ruijgrok et al. (1997)	The Netherlands	52.27° N	5.71° E	26	June-July, 1993	0.35-0.60
	10	Deposition velocities of nucleation mode particles into a Scots pine forest	Rannik et al. (2000)	Finland	61.85° N	24.28° E	181	September, 2000	0.015-0.35
	11	Vertical aerosol fluxes measured by the eddy covariance method and deposition of nucleation mode particles above a Scots pine forest in southern Finland	Buzorious et al. (2000)	Finland	61.85° N	24.28° E	181	March-May, 1997	0.015
	12	Relaxed eddy accumulation system for size-resolved aerosol particle flux measurements	Gaman et al. (2004)	Finland	61.85° N	24.28° E	181	September-October, 2001	0.05
	13	Analyses of flux methods and functional dependencies	Pryor et al. (2007)	Finland	61.85° N	24.28° E	181	January-December, 2004	0.01-0.07
Deciduous forest	14	Aerosol particle dry deposition to canopy and forest floor measured by two-layer eddy covariance system	Grönholm et al. (2009)	Finland	61.85° N	24.28° E	181	March, 2003	0.01-0.05
	15	Fluxes of gases and particles above a deciduous forest in wintertime	Wesely et al. (1983)	U.S.	35.98° N	78.91° W	77	January-February, 1981	0.48
	16	Size-resolved particle deposition velocities of sub-100nm diameter particles over a forest	Pryor (2006)	Denmark	55.48° N	11.64° E	40	May-June, 2004	0.025-0.065
	17	Deposition velocity of PM2.5 sulfate in the summer above a deciduous forest in central Japan	Matsuda et al. (2012)	Japan	36.40° N	138.58° E	1380	July, 2009	2.5
Water	18	Mechanisms of transport from the atmosphere to the Earth's surface	Möller and Schumann (1970)	(Wind tunnel)	-	-	-	-	0.03-1.13
	19	Particle deposition rates on a water surface as a function of particle diameter and air velocity	Sehmel et al.(1974)	(Wind tunnel)	-	-	-	-	0.25-29
	20	Airborne concentrations and dry deposition fluxes of particulate species to surrogate surfaces deployed in southern Lake Michigan	Zufall et al. (1998)	U.S.	44.00° N	87.00° W	-	July, 1994; January, 1995	0.4-24.0
	21	Determination of size-dependent dry particle deposition velocities with multiple intrinsic elemental tracers	Caffrey et al. (1998)	U.S.	44.00° N	87.00° W	-	July, 1994	0.05-48.0
Ice/snow	22	Aerosol dry deposition measured with eddy-covariance technique at Wasa and Aboa, Dronning Maud Land, Antarctica	Gronlund et al. (2002)	Antarctica	73.00° S	13.41° W	584	January, 2000	0.02-0.2
	23	Deposition velocity of ultrafine particles measured with the Eddy-Correlation Method over the Nansen Ice Sheet (Antarctica)	Contini et al. (2010)	Antarctica	74.88° S	163.17° W	84.7	December, 2006	0.06-0.070
	24	On the potential contribution of open lead particle emissions to the central Arctic aerosol concentration	Held et al. (2011a)	Arctic Ocean	87.00° N	6.00° W	-	August-September, 2008	0.045
	25	Near-surface profiles of aerosol number concentration and temperature over the Arctic Ocean	Held et al. (2011b)	Arctic Ocean	87.00° N	6.00° W	-	August-September, 2008	0.045
	26	Correlation of dry deposition velocity and friction velocity over different surfaces for PM2.5 and particle number concentrations	Donateo and Contini (2014)	Antarctica	74.88° S	163.17° W	-	December, 2006	0.015, 0.13
	27	An experimental and theoretical investigation of the dry deposition of particles to snow, pine trees and artificial collectors	Ibrahim (1983)	Canada	51.25° N	85.32° W	450	February, 1980; March, 1981	0.7,0.8, 7.0
	28	Eddy correlation measurements of the dry deposition of particles in wintertime	Duan et al. (1987)	U.S.	40.70° N	77.96° W	177	December, 1985	0.22,0.73
	29	Turbulent aerosol fluxes over the Arctic Ocean 1. Dry deposition over sea and pack ice	Nilsson and Rannik (2001)	Arctic Ocean	88.00° N	15.00° E	-	August, 1999	0.02,0.05

Table 2. Parameter values and associated uncertainties used in Monte Carlo simulation.

Parameter	Base value (assumed)		Uncertainty	Reference*
Relative humidity, *RH* (%)	80	(all LUCs)	±5%	Heinonen (2002)
Wind speed, *U* (m/s)	4	(all LUCs)	±3%	Högström and Smedman (2004)
Friction velocity, u_* (m/s)	0.3	(all LUCs)	±10%	Andreas (1992)
Monin-Obukhov length, L_O (m)	50	(all LUCs)	±10%	Weidinger et al. (2000)
Roughness length, z_0 (m)	0.04	(Grass)	±25%	Su et al. (2001)
	1.2	(Coniferous forest)		
	1.5	(Deciduous forest)		
	0.001	(Ice/snow)		
Canopy height, *h* (m)	0.5	(Grass)	±5%	Larjavaara and Muller-Landau (2013)
	15	(Coniferous forest)		
	25	(Deciduous forest)		
Zero-plane displacement height, *d* (m)	0.3	(Grass)	±25%	Su et al. (2001)
	7	(Coniferous forest)		
	16	(Deciduous forest)		
Leaf area index (one-sided), *LAI* (m^2/m^2)	4	(Grass)	±5%	Richardson et al. (2011)
	10	(Coniferous forest)		
	10	(Deciduous forest)		

* The references are for the uncertainty values (in percentage).

Table 3. Input parameter ranges for the Sobol' sensitivity analysis.

Parameter	Range		Reference
Relative humidity, *RH* (%)	10-100	(all LUCs)	Assumed
Dry particle density, ρ (kg m^{-3})	1500-2000	(all LUCs)	Studies # 1-29
Wind speed, *U* (m/s)	1-5	(all LUCs)	Studies # 1-29
Friction velocity, u_* (m/s)	0.1-0.5	(all LUCs)	Studies # 1-29
Monin-Obukhov length, L_O (m)	10-100	(all LUCs)	Studies # 1-29
Roughness length, z_0 (m)	0.02-.0.10	(Grass)	Studies # 1-5
	0.9-3.0	(Coniferous forest)	Studies # 6-14
	0.5-1.5	(Deciduous forest)	Studies # 15-17
	0.00002-0.0066	(Ice/snow)	Studies # 22-29
Canopy height, *h* (m)	0.15-0.77	(Grass)	Studies # 1-5
	14-20	(Coniferous forest)	Studies # 6-14
	20-25	(Deciduous forest)	Studies # 15-17
Zero-plane displacement height, *d* (m)	0.10-0.49	(Grass)	Studies # 1-5
	7-12	(Coniferous forest)	Studies # 6-14
	8-16	(Deciduous forest)	Studies # 15-17
Leaf area index (one-sided), *LAI* (m^2/m^2)	1-4	(Grass)	Studies # 1-5
	0.2-10	(Coniferous forest)	Studies # 6-14
	0.2-10	(Deciduous forest)	Studies # 15-17

[1]Studies are listed in Table 1.

Table 4. Results of the normalized mean bias factors for grass (bold-faced value indicates the most accurate parameterization).

	Dry particle deposition parameterization				
Study	*Z01*	*PZ10*	*KS12*	*ZH14*	*ZS14*
Allen et al. (1991)	-17.61	15.96	-18.12	-0.55	-5.13
Wesely et al. (1977)	-2.78	-28.78	-7.56	-10.62	-102.92
Neumann and den Hartog (1985)	0.96	-0.12	-0.50	4.79	0.56
Nemitz et al. (2002)	5.15	1.12	-3.82	2.17	-0.10
Vong et al. (2004)	-4.55	-4.55	-25.71	-2.12	-4.03
Five studies	5.45	-1.80	-9.37	**-0.54**	-4.30

Table 5. Results of the normalized mean bias factors for coniferous forest (bold-faced value indicates the most accurate parameterization).

	Dry particle deposition parameterization				
Study	***Z01***	***PZ10***	***KS12***	***ZH14***	***ZS14***
Lamaud et al. (1994)	0.77	-12.75	-1.91	-2.14	-16.71
Wyers and Duyzers (1996)	-25.98	-26.98	-81.39	-13.57	-4.51
Gallagher et al. (1997)	-1.74	-6.34	-19.83	-1.90	-2.39
Ruijgrok et al. (1997)	-5.70	-0.51	-0.93	-2.58	-0.48
Rannik et al. (2000)	3.16	-2.54	0.51	-1.13	-18.75
Buzorious et al. (2000)	0.75	-6.65	-2.91	-4.53	-67.41
Gaman et al. (2004)	-0.90	-13.00	-6.12	-1.84	-17.45
Pryor et al. (2007)	0.69	-5.37	-0.26	-0.84	-12.22
Grönholm et al. (2009)	0.95	0.13	1.55	1.72	-1.90
Nine studies	-2.35	-3.93	**-1.75**	-2.31	-3.67

Table 6. Results of the normalized mean bias factors for deciduous forest (bold-faced values indicate the most accurate parameterization).

	Dry particle deposition parameterization				
Study	***Z01***	***PZ10***	***KS12***	***ZH14***	***ZS14***
Wesely et al. (1983)	-9.25	-130.30	-34.58	-5.27	-2.28
Pryor (2006)	1.55	-2.42	-2.42	-0.90	-13.62
Matsuda et al. (2012)	-5.19	-1.34	-1.91	-2.37	-0.15
Three studies	-8.11	-4.51	-4.96	**-3.75**	-10.93

Table 7. Results of the normalized mean bias factors for water surfaces (bold-faced value indicates the most accurate parameterization).

	Dry particle deposition parameterization				
Study	***Z01***	***PZ10***	***KS12***	***ZH14***	***ZS14***
Möller and Schumann (1970)	18.87	-1.65	-2.51	10.28	106.00
Sehmel et al. (1974)	0.44	0.45	-0.59	1.51	3.65
Zufall et al. (1998)	-0.144	-0.39	-0.47	-0.33	5.14
Caffrey et al. (1998)	0.75	0.35	-0.85	0.70	3.61
Four studies	0.52	-0.89	-0.64	**-0.25**	4.22

Table 8. Results of the normalized mean bias factors for ice/snow surfaces (bold-faced value indicates the most accurate parameterization).

	Dry particle deposition parameterization			
Study	***Z01***	***PZ10***	***KS12***	***ZH14***
Gronlund et al. (2002)	-1.22	-271.73	-105.92	-2.58
Contini et al. (2010)	5.68	-57.22	-24.96	0.62
Held et al. (2011a)	2.96	-38.66	-15.58	0.67
Held et al. (2011b)	2.78	-42.93	-16.71	0.52
Donateo and Contini (2014)	1.62	-35.26	-12.57	-0.32
Ibrahim (1983)	4.14	-6.72	-7.72	3.98
Duan et al. (1987)	0.22	-12.09	-15.49	0.42
Nilsson and Rannik (2001)	1.69	-37.78	-13.46	-0.74
Eight studies	1.98	-53.03	-21.80	**0.26**

Table 9. Median (50th percentile) values of the simulated dry deposition velocities (m s^{-1}) with 5th and 95th percentiles of distribution indicating the range of uncertainty.

Land use category	Particle size (μm)	*Z01*			*PZ10*			*KS12*			*ZH14*			*ZS14**		
		5th	50th	95th	5th	50th	95th	5th	50th	95th	5th	50th	95th	5th	50th	95th
Grass	0.005	1.72×10^{-2}	1.9×10^{-2}	2.1×10^{-2}	9.0×10^{-3}	9.5×10^{-3}	1.0×10^{-2}	1.7×10^{-2}	1.77×10^{-2}	1.86×10^{-2}	1.4×10^{-3}	1.5×10^{-3}	1.7×10^{-3}	4.0×10^{-4}	5.0×10^{-4}	5.0×10^{-4}
	0.05	5.2×10^{-3}	5.7×10^{-3}	6.2×10^{-3}	8.0×10^{-4}	8.0×10^{-4}	9.0×10^{-4}	9.0×10^{-4}	9.0×10^{-4}	9.0×10^{-4}	1.4×10^{-3}	1.5×10^{-3}	1.7×10^{-3}	1.0×10^{-4}	1.0×10^{-4}	1.0×10^{-4}
	0.5	9.0×10^{-4}	9.0×10^{-4}	1.1×10^{-3}	9.0×10^{-4}	9.0×10^{-4}	9.0×10^{-4}	1.0×10^{-4}	1.0×10^{-4}	1.0×10^{-4}	1.4×10^{-3}	1.5×10^{-3}	1.7×10^{-3}	7.0×10^{-4}	9.0×10^{-4}	1.0×10^{-3}
	1.0	6.15×10^{-4}	6.7×10^{-4}	7.25×10^{-4}	1.7×10^{-3}	1.8×10^{-3}	1.9×10^{-3}	1.45×10^{-4}	1.49×10^{-4}	1.55×10^{-4}	1.45×10^{-3}	1.58×10^{-3}	1.72×10^{-3}	1.47×10^{-3}	1.75×10^{-3}	2.06×10^{-3}
	1.5	5.72×10^{-4}	6.16×10^{-4}	6.59×10^{-4}	2.71×10^{-3}	2.87×10^{-3}	3.04×10^{-3}	2.59×10^{-4}	2.74×10^{-4}	2.91×10^{-4}	1.52×10^{-3}	1.66×10^{-3}	1.8×10^{-3}	2.20×10^{-3}	2.61×10^{-3}	3.06×10^{-3}
	2.0	6.16×10^{-4}	6.55×10^{-4}	6.93×10^{-4}	3.97×10^{-3}	4.23×10^{-3}	4.5×10^{-3}	4.3×10^{-4}	4.6×10^{-4}	4.94×10^{-4}	1.63×10^{-3}	1.77×10^{-3}	1.9×10^{-3}	2.91×10^{-3}	3.44×10^{-3}	4.10×10^{-3}
	2.5	7.0×10^{-4}	7.0×10^{-4}	8.0×10^{-4}	5.6×10^{-3}	6.0×10^{-3}	6.4×10^{-3}	7.0×10^{-4}	7.0×10^{-4}	8.0×10^{-4}	1.8×10^{-3}	1.9×10^{-3}	2.0×10^{-3}	3.6×10^{-3}	4.2×10^{-3}	4.9×10^{-3}
Coniferous Forest	0.005	1.62×10^{-2}	1.8×10^{-2}	1.98×10^{-2}	2.31×10^{-2}	2.46×10^{-2}	2.62×10^{-2}	2.87×10^{-2}	2.99×10^{-2}	3.14×10^{-2}	1.1×10^{-3}	1.2×10^{-3}	1.3×10^{-3}			
	0.05	4.4×10^{-3}	4.9×10^{-3}	5.3×10^{-3}	2.6×10^{-3}	2.7×10^{-3}	2.9×10^{-3}	1.4×10^{-3}	1.5×10^{-3}	1.6×10^{-3}	1.1×10^{-3}	1.2×10^{-3}	1.3×10^{-3}			
	0.5	7.0×10^{-4}	8.0×10^{-4}	8.0×10^{-4}	4.7×10^{-3}	4.9×10^{-3}	5.1×10^{-3}	2.0×10^{-4}	2.0×10^{-4}	2.0×10^{-4}	1.1×10^{-3}	1.2×10^{-3}	1.3×10^{-3}			
	1.0	4.87×10^{-4}	5.29×10^{-4}	5.71×10^{-4}	9.28×10^{-3}	9.76×10^{-3}	1.03×10^{-2}	3.24×10^{-4}	3.5×10^{-4}	3.79×10^{-4}	1.16×10^{-3}	1.27×10^{-3}	1.38×10^{-3}			
	1.5	4.7×10^{-4}	5.03×10^{-4}	5.73×10^{-4}	1.48×10^{-2}	1.57×10^{-2}	1.66×10^{-2}	6.27×10^{-4}	6.96×10^{-4}	7.7×10^{-4}	1.23×10^{-3}	1.34×10^{-3}	1.45×10^{-3}			
	2.0	5.29×10^{-4}	5.6×10^{-4}	5.92×10^{-4}	2.11×10^{-2}	2.26×10^{-2}	2.41×10^{-2}	1.07×10^{-3}	1.20×10^{-3}	1.34×10^{-3}	1.34×10^{-3}	1.45×10^{-3}	1.56×10^{-3}			
	2.5	6.0×10^{-4}	7.0×10^{-4}	7.0×10^{-4}	2.72×10^{-2}	2.93×10^{-2}	3.15×10^{-2}	1.7×10^{-3}	1.9×10^{-3}	2.1×10^{-3}	1.5×10^{-3}	1.6×10^{-3}	1.7×10^{-3}			
Deciduous Forest	0.005	1.28×10^{-2}	1.42×10^{-2}	1.58×10^{-2}	9.7×10^{-3}	1.08×10^{-2}	1.2×10^{-2}	2.87×10^{-2}	3.0×10^{-2}	3.14×10^{-2}	2.2×10^{-3}	2.2×10^{-3}	2.6×10^{-3}			
	0.05	4.10×10^{-3}	4.6×10^{-3}	5.0×10^{-3}	9.0×10^{-4}	1.0×10^{-3}	1.1×10^{-3}	1.4×10^{-3}	1.5×10^{-3}	1.6×10^{-3}	2.2×10^{-3}	2.2×10^{-3}	2.6×10^{-3}			
	0.5	7.0×10^{-4}	8.0×10^{-4}	8.0×10^{-4}	9.0×10^{-4}	1.1×10^{-3}	1.2×10^{-3}	2.0×10^{-4}	2.0×10^{-4}	2.0×10^{-4}	2.2×10^{-3}	2.2×10^{-3}	2.6×10^{-3}			
	1.0	4.84×10^{-4}	5.25×10^{-4}	5.67×10^{-4}	1.68×10^{-3}	1.96×10^{-3}	2.25×10^{-3}	9.02×10^{-5}	9.16×10^{-5}	9.35×10^{-5}	2.25×10^{-3}	2.46×10^{-3}	2.68×10^{-3}			
	1.5	4.65×10^{-4}	4.98×10^{-4}	5.31×10^{-4}	2.46×10^{-3}	2.86×10^{-3}	3.28×10^{-3}	1.66×10^{-4}	1.71×10^{-4}	1.77×10^{-4}	2.33×10^{-3}	2.54×10^{-3}	2.76×10^{-3}			
	2.0	5.2×10^{-4}	5.49×10^{-4}	5.78×10^{-4}	3.29×10^{-3}	3.81×10^{-3}	4.35×10^{-3}	2.77×10^{-4}	2.87×10^{-4}	3.0×10^{-4}	2.43×10^{-3}	2.65×10^{-3}	2.86×10^{-3}			
	2.5	6.0×10^{-4}	7.0×10^{-4}	7.0×10^{-4}	4.2×10^{-3}	4.8×10^{-3}	5.5×10^{-3}	1.7×10^{-3}	1.9×10^{-3}	2.1×10^{-3}	2.6×10^{-3}	2.6×10^{-3}	3.0×10^{-3}			
Water	0.005	8.9×10^{-3}	9.9×10^{-3}	1.1×10^{-2}	4.0×10^{-4}	4.0×10^{-4}	5.0×10^{-4}	4.66×10^{-4}	5.12×10^{-4}	5.58×10^{-4}	1.6×10^{-3}	1.8×10^{-3}	1.9×10^{-3}	1.04×10^{-2}	1.14×10^{-2}	1.24×10^{-2}
	0.05	4.0×10^{-3}	4.4×10^{-3}	4.8×10^{-3}	1.0×10^{-4}	1.0×10^{-4}	1.0×10^{-4}	5.06×10^{-5}	6.06×10^{-5}	6.06×10^{-5}	1.6×10^{-3}	1.8×10^{-3}	1.9×10^{-3}	2.3×10^{-3}	2.8×10^{-3}	3.3×10^{-3}
	0.5	9.0×10^{-4}	1.0×10^{-3}	1.1×10^{-3}	1.0×10^{-4}	1.0×10^{-4}	1.0×10^{-4}	1.49×10^{-5}	1.64×10^{-5}	1.79×10^{-5}	1.6×10^{-3}	1.8×10^{-3}	1.9×10^{-3}	2.19×10^{-2}	2.62×10^{-2}	3.06×10^{-2}
	1.0	6.82×10^{-4}	7.44×10^{-4}	8.07×10^{-4}	1.11×10^{-4}	1.13×10^{-4}	1.15×10^{-4}	5.0×10^{-5}	5.5×10^{-5}	5.99×10^{-5}	1.66×10^{-3}	1.82×10^{-3}	1.98×10^{-3}	4.32×10^{-2}	5.08×10^{-2}	5.87×10^{-2}
	1.5	6.39×10^{-4}	6.92×10^{-4}	7.47×10^{-4}	1.85×10^{-4}	1.89×10^{-4}	1.94×10^{-4}	1.08×10^{-4}	1.19×10^{-4}	1.3×10^{-4}	1.73×10^{-3}	1.9×10^{-3}	2.06×10^{-3}	6.26×10^{-2}	7.29×10^{-2}	8.31×10^{-2}
	2.0	6.88×10^{-4}	7.42×10^{-4}	8.0×10^{-4}	2.87×10^{-4}	2.95×10^{-4}	3.06×10^{-4}	1.90×10^{-4}	2.09×10^{-4}	2.27×10^{-4}	1.84×10^{-3}	2.0×10^{-3}	2.17×10^{-3}	8.02×10^{-2}	9.25×10^{-2}	1.04×10^{-1}
	2.5	8.0×10^{-4}	9.0×10^{-4}	9.0×10^{-4}	4.0×10^{-4}	4.0×10^{-4}	5.0×10^{-5}	2.96×10^{-4}	3.25×10^{-4}	3.55×10^{-4}	2.0×10^{-3}	2.1×10^{-3}	2.3×10^{-3}	9.63×10^{-2}	1.1×10^{-1}	1.23×10^{-1}
Ice/snow	0.005	1.15×10^{-2}	1.26×10^{-2}	1.38×10^{-2}	4.0×10^{-4}	4.0×10^{-4}	4.0×10^{-4}	2.8×10^{-2}	2.93×10^{-2}	3.07×10^{-2}	1.1×10^{-3}	1.2×10^{-3}	1.3×10^{-2}			
	0.05	3.4×10^{-3}	3.7×10^{-3}	4.0×10^{-3}	2.0×10^{-5}	2.0×10^{-5}	2.0×10^{-5}	1.4×10^{-3}	1.5×10^{-3}	1.5×10^{-3}	1.1×10^{-3}	1.2×10^{-3}	1.3×10^{-2}			
	0.5	6.0×10^{-4}	7.0×10^{-4}	7.0×10^{-4}	2.0×10^{-5}	2.0×10^{-5}	2.0×10^{-5}	2.0×10^{-4}	2.0×10^{-4}	2.0×10^{-4}	1.1×10^{-3}	1.2×10^{-3}	1.3×10^{-2}			
	1.0	4.41×10^{-4}	4.81×10^{-4}	5.23×10^{-4}	6.71×10^{-5}	6.86×10^{-5}	7.06×10^{-5}	4.38×10^{-4}	4.85×10^{-4}	5.37×10^{-4}	1.15×10^{-3}	1.26×10^{-3}	1.37×10^{-3}			
	1.5	4.67×10^{-4}	5.14×10^{-4}	5.69×10^{-4}	1.45×10^{-4}	1.49×10^{-4}	1.55×10^{-4}	9.14×10^{-4}	1.04×10^{-3}	1.17×10^{-3}	1.24×10^{-3}	1.34×10^{-3}	1.45×10^{-3}			
	2.0	6.0×10^{-4}	6.84×10^{-4}	7.92×10^{-4}	2.54×10^{-4}	2.63×10^{-4}	2.75×10^{-4}	1.61×10^{-3}	1.84×10^{-3}	2.1×10^{-3}	1.35×10^{-3}	1.46×10^{-3}	1.57×10^{-3}			
	2.5	9.0×10^{-4}	1.0×10^{-3}	1.2×10^{-3}	4.0×10^{-4}	4.0×10^{-4}	4.0×10^{-4}	2.5×10^{-3}	2.9×10^{-3}	3.3×10^{-3}	1.5×10^{-3}	1.6×10^{-3}	1.7×10^{-3}			

*The parameterization does not categorize rough or vegetative surfaces into different LUCs. In this analysis, grass is used to represent a rough surface.

Table 10. Normalized uncertainties in modeled dry deposition velocities.

		Dry particle deposition parameterization				
Land use category	**Particle size, d_p (µm)**	***Z01***	***PZ10***	***KS12***	***ZH14***	***ZS14***
Grass	0.005	0.20	0.11	0.09	0.20	0.20
	0.05	0.18	0.13	0.00	0.20	0.00
	0.5	0.22	0.00	0.00	0.20	0.33
	1.0	0.16	0.11	0.07	0.17	0.34
	1.5	0.14	0.11	0.12	0.17	0.33
	2.0	0.12	0.12	0.14	0.16	0.32
	2.5	0.14	0.13	0.14	0.11	0.31
Coniferous forest	0.005	0.20	0.13	0.09	0.17	
	0.05	0.18	0.11	0.13	0.17	
	0.5	0.13	0.08	0.00	0.17	
	1.0	0.16	0.10	0.16	0.17	
	1.5	0.13	0.11	0.20	0.16	
	2.0	0.11	0.13	0.22	0.15	
	2.5	0.14	0.15	0.21	0.13	
Deciduous forest	0.005	0.21	0.21	0.09	0.18	
	0.05	0.20	0.20	0.13	0.18	
	0.5	0.13	0.27	0.00	0.18	
	1.0	0.16	0.29	0.04	0.18	
	1.5	0.13	0.28	0.06	0.17	
	2.0	0.10	0.28	0.08	0.16	
	2.5	0.14	0.27	0.21	0.15	
Water	0.005	0.21	0.25	0.18	0.17	0.18
	0.05	0.18	0.00	0.18	0.17	0.36
	0.5	0.20	0.00	0.18	0.17	0.33
	1.0	0.17	0.03	0.18	0.18	0.31
	1.5	0.15	0.05	0.18	0.17	0.28
	2.0	0.15	0.07	0.18	0.16	0.26
	2.5	0.11	0.25	0.18	0.14	0.24
Ice/snow	0.005	0.18	0.00	0.09	0.17	
	0.05	0.16	0.00	0.07	0.17	
	0.5	0.14	0.00	0.00	0.17	
	1.0	0.17	0.05	0.20	0.17	
	1.5	0.20	0.07	0.25	0.16	
	2.0	0.28	0.08	0.27	0.15	
	2.5	0.30	0.00	0.28	0.13	

Note: a normalized uncertainty value of zero indicates that the 95th and 5th percentile V_d are of equal magnitude.

Table 11. Ranking of first order Sobol' sensitivity indices for the five dry particle deposition parameterizations.

Land use category	d_P (μm)	*Z01*	*PZ10*	*KS12*	*ZH14*	*ZS14*
Grass	0.001	u_*, z_0, L_O, (RH, ρ_P)	u_*, LAI, z_0, U, L_O, (h, d, RH, ρ_P)	u_*, (RH, ρ_P, LAI)	u_*, (z_0, L_O, RH, ρ_P)	U, u_*, (RH, ρ_P)
	0.01	u_*, z_0, L_O, (RH, ρ_P)	LAI, U, u_*, (L_O, h), (z_0, d, RH, ρ_P)	u_*, (RH, ρ_P, LAI)	u_*, ($z0$, L_O, RH, ρP)	U, u_*, (RH, ρ_P)
	0.1	u_*, (z_0, L_O, RH, ρ_P)	LAI, U, d, (u_*, L_O, h, z_0, RH, ρ_P)	u_*, (RH, ρ_P, LAI)	u_*, (z_0, L_O, RH, ρ_P)	u_*, U, (RH, ρ_P)
	1.0	u_*, ρ_P , RH, (z_0, L_O)	U, LAI, RH, u_*, L_O, (h, z_0, d, ρ_P)	RH, u_*, ρ_P, LAI	u_*, (z_0, L_O, RH, ρ_P)	u_*, U, RH, ρ_P
	10	RH, u_*, ρ_P, (z_0, L_O)	RH, u_*, U, LAI, (ρ_P, z_0), L_O, (h, d)	RH, u_*, LAI, ρ_P	RH, ρ_P , (u_*, L_O, z_0)	u_*, U, RH, ρ_P
Coniferous Forest	0.001	u_*, L_O, z_0, (RH, ρ_P)	u_*, L_O, z_0, LAI, h, (d, U, RH, ρ_P)	u_*, (RH, ρ_P, LAI)	u_*, L_O, (z_0, RH, ρ_P)	
	0.01	u_*, L_O, z_0, (RH, ρ_P)	L_O, LAI, u_*, U, z_0, h, (d, RH, ρ_P)	u_*, (RH, ρ_P, LAI)	u_*, L_O, (z_0, RH, ρ_P)	
	0.1	u_*, L_O, (z_0, RH, ρ_P)	L_O, LAI, U, u_*, (d, z_0, h, RH, ρ_P)	u_*, (RH, ρ_P, LAI)	u_*, (L_O, z_0, RH, ρ_P)	
	1.0	u_*, ρ_P , RH, (L_O,z_0)	L_O, U, LAI, u_*, RH, (ρ_P, d, z_0, h)	u_*, RH, ρ_P, LAI	u_*, L_O, (z_0, RH, ρ_P)	
	10	RH, u_*, ρ_P, L_O, z_0	u_*, L_O, RH, z_0, (ρ_P, U), (LAI, d, h)	RH, u_*, LAI, ρ_P	RH, u_*, L_O, z_0, ρ_P	
Deciduous Forest	0.001	u_*, z_0, L_O, (RH, ρ_P)	L_O, u_*, LAI, z_0, U, (h, d, RH, ρ_P)	u_*, (RH, ρ_P, LAI)	u_*, L_O, (z_0, RH, ρ_P)	
	0.01	u_*, z_0, L_O, (RH, ρ_P)	L_O, LAI, u_*, U, (z_0, d), (h, RH, ρ_P)	u_*, (RH, ρ_P, LAI)	u_*, L_O, (z_0, RH, ρ_P)	
	0.1	u_*, z_0, (L_O, RH, ρ_P)	L_O, LAI, U, u_*, d, (z_0, h, RH, ρ_P)	u_*, (RH, ρ_P, LAI)	u_*, L_O, (z_0, RH, ρ_P)	
	1.0	u_*, ρ_P, (L_O, z_0, RH)	L_O, LAI, U, u_*, RH, (z_0, d), (h, ρ_P)	RH, ρ_P, u_*, LAI	u_*, L_O, (z_0, RH, ρ_P)	
	10	RH, u_*, ρ_P, z_0, L_O	L_O, RH, u_*, LAI, ρ_P, U z_0, (d, h)	RH, ρ_P, u_*, LAI	RH, u_*, LAI, L_O, ρ_P, z_0	
Water	0.001	u_*, (L_O, RH, ρ_P)	u_*, (L_O, RH, ρ_P)	u_*, L_O, (ρ_P, RH)	u_*, (L_O, RH, ρ_P)	
	0.01	u_*, (L_O, RH, ρ_P)	u_*, (L_O, RH, ρ_P)	u_*, L_O, (ρ_P, RH)	u_*, (L_O, RH, ρ_P)	
	0.1	u_*, (L_O, RH, ρ_P)	u_*, ρ_P, (L_O, RH)	u_*, L_O, (ρ_P, RH)	u_*, (L_O, RH, ρ_P)	
	1.0	u_*, ρ_P , (RH, L_O)	RH, ρ_P , (u_*, L_O)	ρ_P, u_*, (RH, L)	u_*, (L_O, RH, ρ_P)	
	10	u_*, RH, (ρ_P, L_O)	RH, ρ_P , (u_*, L_O)	ρ_P, u_*, L_O, RH	u_*, RH, (L_O, ρ_P)	
Ice/snow	0.001	u_*, L_O, (z_0, RH, ρ_P)	u_*, (L_O, z_0, RH, ρ_P)	u_*, RH, ρ_P	u_*, (L_O, z_0, RH, ρ_P)	
	0.01	u_*, z_0, L_O, (RH, ρ_P)	u_*, (L_O, z_0, RH, ρ_P)	u_*, RH, ρ_P	u_*, (L_O, z_0, RH, ρ_P)	
	0.1	u_*, (L_O, z_0, RH, ρ_P)	u_*, (L_O, z_0, RH, ρ_P)	u_*, RH, ρ_P	u_*, (L_O, z_0, RH, ρ_P)	
	1.0	u_*, (L_O, z_0, RH, ρ_P)	RH, ρ_P, (z_0, L_O, z_0)	u_*, RH, ρ_P	u_*, (L_O, z_0, RH, ρ_P)	
	10	u_*, RH, (ρ_P, L_O, z_0)	RH, ρ_P, (z_0, L_O, z_0)	RH, u_*, ρ_P	u_*, RH, (z_0, L_O, ρ_P)	

Note: the ranking of the parameters is from most sensitive to least sensitive. Parameters within the parentheses have identical Sobol' first order indices.

Supplement of

Evaluation of five dry particle deposition parameterizations for incorporation into atmospheric transport models

Tanvir R. Khan, Judith A. Perlinger

Correspondence to: Judith A. Perlinger (jperl@mtu.edu)

Table S1. First order sensitivity index (*Si*) with bootstrap confidence intervals (*CI*) of the modeled V_d for the *Z01* parameterization.

		d_p = 0.001 µm			d_p = 0.01 µm			d_p = 0.1 µm			d_p = 1.0 µm			d_p = 10 µm		
LUC	Parameter	*Si*	*95% CI*		*Si*	*95% CI*		*Si*	*95% CI*		*Si*	*95% CI*		*Si*	*95% CI*	
Grass	*RH*	0.000	0.000	0.000	0.000	0.000	0.000	0.000	0.000	0.000	0.001	-0.001	0.003	0.673	0.620	0.721
	ρ_P	0.000	0.000	0.000	0.000	0.000	0.000	0.000	0.000	0.000	0.002	0.000	0.003	0.019	0.016	0.022
	L_O	0.009	0.006	0.012	0.002	-0.001	0.006	0.000	0.000	0.000	0.000	0.000	0.000	0.000	0.000	0.000
	z_0	0.044	0.037	0.051	0.012	0.004	0.020	0.000	-0.001	0.001	0.000	0.000	0.000	0.000	-0.001	0.001
	u_*	0.918	0.884	0.948	0.959	0.896	1.021	0.981	0.949	1.011	0.975	0.938	1.009	0.245	0.230	0.260
Coniferous forest	*RH*	0.000	0.000	0.000	0.000	0.000	0.000	0.000	0.000	0.001	0.001	0.000	0.002	0.598	0.493	0.690
	ρ_P	0.000	0.000	0.000	0.000	0.000	0.000	0.000	0.000	0.000	0.002	0.001	0.003	0.022	0.015	0.029
	L_O	0.260	0.231	0.289	0.124	0.103	0.147	0.005	0.000	0.011	0.000	0.000	0.000	0.009	0.003	0.016
	z_0	0.012	0.003	0.019	0.003	-0.002	0.008	0.000	-0.001	0.001	0.000	0.000	0.000	0.000	-0.001	0.001
	u_*	0.674	0.624	0.723	0.836	0.778	0.893	0.972	0.906	1.036	0.984	0.964	1.004	0.311	0.275	0.344
Deciduous forest	*RH*	0.000	0.000	0.000	0.000	0.000	0.000	0.000	0.000	0.000	0.000	-0.001	0.002	0.844	0.782	0.903
	ρ_P	0.000	0.000	0.000	0.000	0.000	0.000	0.000	0.000	0.000	0.002	0.000	0.003	0.019	0.016	0.022
	z_0	0.300	0.283	0.316	0.178	0.166	0.189	0.012	0.009	0.014	0.000	0.000	0.001	0.002	0.000	0.003
	L_O	0.007	0.004	0.010	0.002	0.000	0.003	0.000	0.000	0.000	0.000	0.000	0.000	0.000	0.000	0.000
	u_*	0.671	0.643	0.698	0.791	0.762	0.817	0.972	0.947	0.996	0.979	0.950	1.009	0.092	0.084	0.098
Water	*RH*	0.000	0.000	0.000	0.000	0.000	0.000	0.000	0.000	0.000	0.000	-0.001	0.000	0.393	0.369	0.416
	ρ_P	0.000	0.000	0.000	0.000	0.000	0.000	0.000	0.000	0.000	0.002	0.000	0.003	0.008	0.006	0.009
	L_O	0.000	0.000	0.000	0.000	0.000	0.000	0.000	0.000	0.000	0.000	0.000	0.000	0.000	0.000	0.000
	u_*	0.995	0.963	1.028	0.995	0.962	1.027	0.994	0.959	1.027	0.983	0.960	1.005	0.559	0.543	0.575
Ice/snow	*RH*	0.000	0.000	0.000	0.000	0.000	0.000	0.000	0.000	0.000	0.001	-0.001	0.002	0.376	0.350	0.403
	ρ_P	0.000	0.000	0.000	0.000	0.000	0.000	0.000	0.000	0.000	0.004	0.002	0.005	0.010	0.008	0.012
	L_O	0.013	0.009	0.017	0.006	0.003	0.009	0.000	0.000	0.001	0.000	0.000	0.000	0.002	0.001	0.003
	u_*	0.926	0.893	0.959	0.963	0.928	0.996	0.982	0.956	1.007	0.978	0.949	1.005	0.551	0.531	0.569
	z_0	0.051	0.043	0.059	0.026	0.020	0.032	0.002	0.001	0.003	0.000	0.000	0.000	0.010	0.007	0.012

Table S2. First order sensitivity index with bootstrap confidence intervals (*CI*) of the modeled V_d for the *PZ10* parameterization.

		d_p = 0.001 µm			d_p = 0.01 µm			d_p = 0.1 µm			d_p = 1.0 µm			d_p = 10 µm		
LUC	Parameter	*Si*	*95% CI*		*Si*	*95% CI*		*Si*	*95% CI*		*Si*	*95% CI*		*Si*	*95% CI*	
Grass	*RH*	0.000	0.000	0.000	0.000	0.000	0.000	0.000	0.000	0.000	0.014	0.010	0.018	0.347	0.320	0.372
	ρ_P	0.000	0.000	0.000	0.000	0.000	0.000	0.000	0.000	0.000	0.000	0.000	0.001	0.012	0.010	0.015
	L_O	0.009	0.006	0.012	0.001	0.000	0.003	-0.001	-0.002	0.000	0.001	0.000	0.003	0.002	0.000	0.003
	z_0	0.034	0.027	0.041	0.000	-0.001	0.001	0.000	0.000	0.000	0.000	-0.001	0.001	0.012	0.009	0.015
	u_*	0.780	0.751	0.809	0.050	0.043	0.058	0.000	-0.001	0.001	0.006	0.004	0.009	0.244	0.229	0.258
	LAI	0.103	0.091	0.115	0.693	0.664	0.722	0.553	0.536	0.572	0.379	0.360	0.397	0.040	0.035	0.045
	h	0.000	0.000	0.001	0.001	0.000	0.002	0.000	-0.001	0.001	0.000	-0.001	0.002	0.000	-0.001	0.000
	d	0.000	0.000	0.000	0.000	-0.001	0.001	0.001	0.000	0.001	0.000	-0.001	0.002	0.000	0.000	0.001
	U	0.032	0.025	0.038	0.225	0.210	0.242	0.408	0.393	0.424	0.511	0.489	0.532	0.228	0.215	0.240
Coniferous forest	*RH*	0.000	0.000	0.000	0.000	0.000	0.000	0.000	0.000	0.000	0.009	0.007	0.011	0.198	0.179	0.215
	ρ_P	0.000	0.000	0.000	0.000	0.000	0.000	0.000	0.000	0.000	0.001	0.000	0.001	0.004	0.002	0.005
	L_O	0.462	0.440	0.483	0.493	0.468	0.514	0.375	0.357	0.393	0.358	0.347	0.368	0.350	0.334	0.366
	z_0	0.011	0.007	0.015	0.004	0.001	0.006	0.000	0.000	0.001	0.001	0.000	0.001	0.006	0.004	0.009
	u_*	0.492	0.466	0.517	0.164	0.148	0.180	0.008	0.005	0.011	0.052	0.047	0.057	0.372	0.354	0.390
	LAI	0.005	0.003	0.008	0.220	0.202	0.240	0.313	0.293	0.334	0.162	0.154	0.170	0.000	-0.001	0.001
	h	0.001	0.000	0.002	0.001	0.000	0.002	0.000	-0.001	0.001	0.001	0.000	0.001	0.000	0.000	0.001
	d	0.000	0.000	0.000	-0.001	-0.002	0.000	0.000	-0.001	0.001	0.001	0.000	0.001	0.000	0.000	0.000
	U	0.001	-0.001	0.002	0.069	0.058	0.078	0.217	0.199	0.231	0.277	0.266	0.288	0.004	0.002	0.006
Deciduous forest	*RH*	0.000	0.000	0.000	0.000	0.000	0.000	0.000	0.000	0.000	0.002	0.001	0.003	0.280	0.257	0.302
	ρ_P	0.000	0.000	0.000	0.000	0.000	0.000	0.000	0.000	0.000	0.000	0.000	0.000	0.006	0.004	0.007
	L_O	0.501	0.484	0.518	0.458	0.442	0.472	0.401	0.387	0.415	0.453	0.441	0.464	0.339	0.325	0.352
	z_0	0.004	0.002	0.005	0.001	0.000	0.002	0.000	0.000	0.000	0.001	0.000	0.001	0.002	0.001	0.004
	u_*	0.390	0.372	0.407	0.111	0.102	0.119	0.011	0.008	0.014	0.081	0.075	0.087	0.237	0.225	0.250
	LAI	0.016	0.012	0.019	0.252	0.240	0.265	0.281	0.269	0.293	0.192	0.183	0.199	0.005	0.003	0.007
	h	0.000	0.000	0.001	0.000	0.000	0.000	0.000	0.000	0.000	0.000	0.000	0.000	0.000	0.000	0.001
	d	0.000	0.000	0.001	0.001	0.000	0.002	0.002	0.001	0.003	0.001	0.000	0.002	0.000	0.000	0.000
	U	0.001	0.000	0.002	0.031	0.026	0.035	0.122	0.114	0.130	0.106	0.100	0.112	0.005	0.003	0.007
Water	*RH*	0.000	0.000	0.000	0.000	0.000	0.000	-0.001	-0.002	0.000	0.695	0.620	0.770	0.956	0.877	1.025
	ρ_P	0.000	0.000	0.000	0.000	0.000	0.000	0.013	0.003	0.023	0.241	0.194	0.285	0.016	0.013	0.019
	L_O	0.000	0.000	0.000	0.000	0.000	0.000	0.000	0.000	0.000	0.000	0.000	0.000	0.000	0.000	0.000
	u_*	0.994	0.959	1.027	0.988	0.942	1.032	0.878	0.640	1.121	-0.001	-0.003	0.002	0.000	0.000	0.000
Ice/snow	*RH*	0.000	0.000	0.000	0.000	0.000	0.000	0.000	0.000	0.000	0.703	0.654	0.750	0.974	0.912	1.034
	ρ_P	0.000	0.000	0.000	0.000	0.000	0.000	0.004	0.002	0.005	0.270	0.244	0.296	0.015	0.013	0.016
	L_O	0.002	0.001	0.003	0.000	0.000	0.000	0.000	0.000	0.000	0.000	0.000	0.000	0.000	0.000	0.000
	u_*	0.962	0.931	0.993	0.969	0.938	1.000	0.956	0.913	0.998	0.000	-0.001	0.002	0.000	0.000	0.000
	z_0	0.004	0.002	0.006	0.000	0.000	0.000	0.000	0.000	0.000	0.000	0.000	0.000	0.000	0.000	0.000

Table S3. First order sensitivity index (*Si*) with bootstrap confidence intervals (*CI*) of the modeled V_d for the *KS12* parameterization.

		d_p = 0.001 µm			d_p = 0.01 µm			d_p = 0.1 µm			d_p = 1.0 µm			d_p = 10 µm		
LUC	Parameter	*Si*	*95% CI*		*Si*	*95% CI*		*Si*	*95% CI*		*Si*	*95% CI*		*Si*	*95% CI*	
Grass	*RH*	0.000	0.000	0.000	0.000	0.000	0.000	0.000	-0.002	0.003	0.777	0.731	0.822	0.816	0.709	0.916
	ρ_P	0.000	0.000	0.000	0.000	0.000	0.000	0.000	0.000	0.000	0.039	0.031	0.047	0.000	0.000	0.001
	u_*	0.904	0.832	0.976	0.904	0.832	0.976	0.902	0.829	0.974	0.122	0.106	0.138	0.009	0.005	0.012
	LAI	0.000	0.000	0.000	0.000	0.000	0.000	0.000	0.000	0.000	0.000	0.000	0.000	0.002	-0.001	0.003
Coniferous forest	*RH*	0.000	0.000	0.000	0.000	0.000	0.000	0.000	-0.001	0.000	0.139	0.126	0.153	0.783	0.709	0.849
	ρ_P	0.000	0.000	0.000	0.000	0.000	0.000	0.000	0.000	0.000	0.004	0.002	0.007	0.002	0.001	0.003
	u_*	0.911	0.823	0.995	0.911	0.823	0.995	0.943	0.879	1.005	0.829	0.798	0.860	0.032	0.029	0.035
	LAI	0.000	0.000	0.000	0.000	0.000	0.000	0.000	0.000	0.000	0.000	0.000	0.000	0.005	0.002	0.007
Deciduous forest	*RH*	0.000	0.000	0.000	0.000	0.000	0.000	0.000	-0.001	0.000	0.629	0.571	0.686	0.934	0.856	1.004
	ρ_P	0.000	0.000	0.000	0.000	0.000	0.000	0.000	0.000	0.000	0.243	0.206	0.277	0.012	0.010	0.014
	u_*	0.944	0.880	1.005	0.944	0.880	1.005	0.967	0.929	1.005	0.054	0.037	0.072	0.002	0.000	0.004
	LAI	0.000	0.000	0.000	0.000	0.000	0.000	0.000	0.000	0.000	0.000	0.000	0.000	0.000	-0.001	0.001
Ice/snow	*RH*	0.000	0.000	0.000	0.000	0.000	0.000	0.001	-0.001	0.002	0.302	0.287	0.316	0.848	0.789	0.899
	ρ_P	0.000	0.000	0.000	0.000	0.000	0.000	0.000	0.000	0.000	0.001	0.000	0.001	0.002	0.001	0.003
	u_*	0.905	0.840	0.972	0.905	0.840	0.972	0.902	0.836	0.970	0.614	0.595	0.632	0.022	0.020	0.024

Table S4. First order sensitivity index (*Si*) with bootstrap confidence intervals (*CI*) of the modeled V_d for the *ZH14* parameterization.

		d_p = 0.001 µm			d_p = 0.01 µm			d_p = 0.1 µm			d_p = 1.0 µm			d_p = 10 µm		
LUC	Parameter	*Si*	*95% CI*		*Si*	*95% CI*		*Si*	*95% CI*		*Si*	*95% CI*		*Si*	*95% CI*	
Grass	*RH*	0.000	0.000	0.000	0.000	0.000	0.000	0.000	0.000	0.000	0.001	0.000	0.002	0.940	0.847	1.014
	ρ_P	0.000	0.000	0.000	0.000	0.000	0.000	0.000	0.000	0.000	0.001	0.000	0.001	0.006	0.004	0.008
	u_*	1.002	0.973	1.033	1.002	0.973	1.033	1.002	0.973	1.033	1.000	0.967	1.032	0.000	0.000	0.000
	L	0.000	0.000	0.000	0.000	0.000	0.000	0.000	0.000	0.000	0.000	0.000	0.000	0.000	0.000	0.000
	z_0	0.000	0.000	0.000	0.000	0.000	0.000	0.000	0.000	0.000	0.000	0.000	0.001	0.000	0.000	0.000
Coniferous forest	*RH*	0.000	0.000	0.000	0.000	0.000	0.000	0.000	0.000	0.000	0.000	0.000	0.001	0.420	0.382	0.456
	ρ_P	0.000	0.000	0.000	0.000	0.000	0.000	0.000	0.000	0.000	0.000	0.000	0.000	0.006	0.004	0.007
	u_*	0.988	0.960	1.016	0.988	0.960	1.016	0.988	0.960	1.016	0.971	0.947	0.994	0.341	0.325	0.356
	L	0.002	0.001	0.003	0.002	0.000	0.003	0.002	0.000	0.003	0.004	0.002	0.005	0.141	0.131	0.150
	z_0	0.000	0.000	0.000	0.000	0.000	0.000	0.000	0.000	0.000	0.000	0.000	0.000	0.012	0.009	0.014
Deciduous forest	*RH*	0.000	0.000	0.000	0.000	0.000	0.000	0.000	0.000	0.000	0.000	0.000	0.001	0.634	0.585	0.675
	ρ_P	0.000	0.000	0.000	0.000	0.000	0.000	0.000	0.000	0.000	0.000	0.000	0.001	0.004	0.003	0.006
	u_*	0.988	0.962	1.011	0.988	0.962	1.011	0.988	0.962	1.011	0.987	0.960	1.012	0.185	0.174	0.195
	L	0.006	0.004	0.008	0.006	0.004	0.008	0.006	0.004	0.008	0.006	0.004	0.008	0.015	0.012	0.018
	z_0	0.000	0.000	0.000	0.000	0.000	0.000	0.000	0.000	0.000	0.000	0.000	0.000	0.000	0.000	0.000
	LAI													0.053	0.048	0.057
Water	*RH*	0.000	0.000	0.000	0.000	0.000	0.000	0.000	0.000	0.000	0.000	0.000	0.001	0.465	0.429	0.499
	ρ_P	0.000	0.000	0.000	0.000	0.000	0.000	0.000	0.000	0.000	0.000	0.000	0.001	0.008	0.005	0.010
	L	0.000	0.000	0.000	0.000	0.000	0.000	0.000	0.000	0.000	0.000	0.000	0.000	0.000	0.000	0.000
	u_*	0.981	0.954	1.010	0.981	0.954	1.010	0.981	0.953	1.010	0.980	0.952	1.010	0.499	0.480	0.517
Ice/snow	*RH*	0.000	0.000	0.000	0.000	0.000	0.000	0.000	0.000	0.000	0.000	0.000	0.001	0.407	0.378	0.433
	ρ_P	0.000	0.000	0.000	0.000	0.000	0.000	0.000	0.000	0.000	0.000	0.000	0.000	0.005	0.003	0.007
	L	0.000	0.000	0.000	0.000	0.000	0.000	0.000	0.000	0.000	0.000	0.000	0.000	0.004	0.002	0.005
	u_*	0.984	0.959	1.008	0.984	0.959	1.008	0.984	0.959	1.008	0.986	0.964	1.006	0.548	0.531	0.564
	z_0	0.001	0.000	0.001	0.001	0.000	0.001	0.001	0.000	0.001	0.000	0.000	0.001	0.014	0.011	0.017

Table S5. First order sensitivity index (*Si*) with bootstrap confidence intervals (*CI*) of the modeled V_d for the *ZS14* parameterization.

		d_p = 0.001 µm			d_p = 0.01 µm			d_p = 0.1 µm			d_p = 1.0 µm			d_p = 10 µm		
LUC	Parameter	*Si*	*95% CI*		*Si*	*95% CI*		*Si*	*95% CI*		*Si*	*95% CI*		*Si*	*95% CI*	
Plant	*RH*	0.000	0.000	0.000	0.000	0.000	0.000	0.000	0.000	0.000	0.006	0.004	0.008	0.071	0.060	0.085
	ρ_P	0.000	0.000	0.000	0.000	0.000	0.000	0.000	0.000	0.000	0.000	0.000	0.000	0.000	-0.001	0.002
	u_*	0.436	0.410	0.463	0.347	0.324	0.369	0.576	0.547	0.603	0.611	0.580	0.640	0.750	0.707	0.789
	U	0.464	0.430	0.498	0.607	0.568	0.643	0.306	0.282	0.329	0.275	0.252	0.297	0.145	0.127	0.163
Water	*RH*	0.000	0.000	0.000	0.000	0.000	0.000	0.000	0.000	0.000	0.003	0.001	0.004	0.001	0.000	0.003
	ρ_P	0.000	0.000	0.000	0.000	0.000	0.000	0.000	0.000	0.000	0.000	0.000	0.000	0.000	0.000	0.001
	u_*	0.991	0.958	1.023	0.966	0.935	0.997	0.989	0.963	1.014	0.988	0.961	1.015	0.989	0.956	1.020
	U	0.000	0.000	0.001	0.027	0.022	0.032	0.000	0.000	0.000	0.000	0.000	0.000	0.000	0.000	3.180

Codes for evaluation of model accuracy using Zhang et al. (2001) parameterization

```
#Accuracy Evaluation: Grass
#Dry deposition parameterization by Zhang et al. (2001)
attach(Allen_etal_1991)                          # Use separate text file to feed V1, V2,… for different studies
C1 = 0.2789
C1 = 0.2789
C2 = 3.115
C3 = 5.145*10^-11
RH = 90/100
dp_i = 0.48
dp_d = dp_i*10^-6
rd = dp_d/2
r_w = {(C1*rd^C2)/(C3*rd^C4-log10(RH))+rd^3}^(1/3)
dp = r_w*2
#Correction factor, C
k_B = 1.38*10^-23
Temp_1 = V1
Temp = 273.15+V1
P = 101325
d_air = 3.72*10^-10
lambda = (k_B*Temp)/(sqrt(2)*3.1416*P*d_air^2)
C = 1+(2*lambda/dp)*(1.257+0.4*exp(-0.55*dp/lambda))
dyn.vis = ((5*10^-8)*Temp)+4*10^-6
rho = 2000
Vg = (rho*(dp)^2*9.81*C)/(18*dyn.vis)
# Compute aerodynamic resistance Ra:
z = 2
L = V4
x = z/L
# Compute shi_H (stability function)
shi_H.1 = 2*log(0.5*{1+(1-16*x)^0.5})
shi_H.2 = -5*x
shi_H =ifelse(x <= 0, shi_H.1 , shi_H.2)
zR = 3.5
z0 = 0.01
u_star = V2                                          #Use from input text file
k_c = 0.41
Ra = (log(zR/z0)-shi_H)/(k_c*u_star)
# Compute surface resistance Rs:
e_0 = 3
R1 = 1
# Compute E_B (collection efficiency from Brownian diffusion)
kin.vis = ((9*10^-8)*Temp)+10^-5
gamma = 0.54
D = (C*k_B*Temp)/(3*3.1416*dyn.vis*dp)
Sc = (kin.vis/D)
E_B = Sc^(-gamma)
# Compute E_IM (collection efficiency from impaction)
alpha = 1.2
beta =  2
A = 2/1000
St = (Vg*u_star)/(9.81*A)
E_IM = {St/(alpha+St)}^beta
# Compute E_IN (collection efficiency from interception)
E_IN = 0.5*(dp/A)^2
Rs = 1/{(e_0*u_star)*(E_B+E_IM+E_IN)*R1}
# Compute Dry deposition velocity

#Accuracy Evaluation: Coniferous forest
#Dry deposition parameterization by Zhang et al. (2001)
attach(Rannik_etal_2000)                    # Use separate text file to feed V1, V2,… for different studies
C1 = 0.2789
C2 = 3.115
C3 = 5.145*10^-11
C4 = -1.399
RH = 90/100
dp_i = V1
dp_d = dp_i*10^-6
rd = dp_d/2
r_w = {(C1*rd^C2)/(C3*rd^C4-log10(RH))+rd^3}^(1/3)
dp = r_w*2
#Correction factor, C
k_B = 1.38*10^-23
```

```
Temp = 273.15+25
P = 101325
d_air = 3.72*10^-10
lambda = (k_B*Temp)/(sqrt(2)*3.1416*P*d_air^2)
C = 1+(2*lambda/dp)*(1.257+0.4*exp(-0.55*dp/lambda))
dyn.vis = 1.891*10^-5
rho = 1500
Vg = (rho*(dp)^2*9.81*C)/(18*dyn.vis)
# Compute aerodynamic resistance Ra:
z = 23.7
L = 200
x = z/L
shi_H2 = -5*x
zR = 26
z0 = 1.2
u_star = V2
k_c = 0.41
Ra = (log(zR/z0)-shi_H2)/(k_c*u_star)
e_0 = 3
R1 =1
kin.vis = 1.683*10^-5
gamma = 0.56
D = (C*k_B*Temp)/(3*3.1416*dyn.vis*dp)
Sc = (kin.vis/D)
E_B = Sc^(-gamma)
# Compute E_IM (collection efficiency from impaction)
alpha = 1.0
beta =  2
A = 5/1000
St = (Vg*u_star)/(9.81*A)
E_IM = {St/(alpha+St)}^beta
# Compute E_IN (collection efficiency from interception)
E_IN = 0.5*(dp/A)^2
Rs = 1/{(e_0*u_star)*(E_B+E_IM+E_IN)*R1}
# Compute Dry deposition velocity
Vd =  Vg+(1/(Ra+Rs));Vd   #unit: m/s

#Accuracy Evaluation: Deciduous forest
#Dry deposition parameterization by Zhang et al. (2001)
attach(Wesely_etal_1983)                          # Use separate text file to feed V1, V2,… for different studies
C1 = 0.2789
C2 = 3.115
C3 = 5.145*10^-11
C4 = -1.399
RH = 95/100
dp_i = 0.4
dp_d = dp_i*10^-6
rd = dp_d/2
r_w = {(C1*rd^C2)/(C3*rd^C4-log10(RH))+rd^3}^(1/3)
dp = r_w*2
#Correction factor, C
k_B = 1.38*10^-23
Temp = V1
P = 101325
d_air = 3.72*10^-10
lambda = (k_B*Temp)/(sqrt(2)*3.1416*P*d_air^2)
C = 1+(2*lambda/dp)*(1.257+0.4*exp(-0.55*dp/lambda))
dyn.vis = V2
rho = 2000
Vg = (rho*(dp)^2*9.81*C)/(18*dyn.vis)
# Compute aerodynamic resistance Ra:
z = 39
L = V6
x = z/L
shi_H2 = -5*x
zR = 56
z0 = 1.6
u_star = V4
k_c = 0.41
Ra = (log(zR/z0)-shi_H1)/(k_c*u_star)
# Compute surface resistance Rs:
e_0 = 3
R1 =1
kin.vis = V3
```

```
gamma = 0.56
D = (C*k_B*Temp)/(3*3.1416*dyn.vis*dp)
Sc = (kin.vis/D)
E_B = Sc^(-gamma)
# Compute E_IM (collection efficiency from impaction)
alpha = 0.80
beta =  2
A = 5/1000
St = (Vg*u_star)/(9.81*A)
E_IM = {St/(alpha+St)}^beta
# Compute E_IN (collection efficiency from interception)
E_IN = 0.5*(dp/A)^2
Rs = 1/{(e_0*u_star)*(E_B+E_IM+E_IN)*R1}
# Compute Dry deposition velocity
Vd =  Vg+(1/(Ra+Rs));Vd


#Accuracy Evaluation: Water
#Dry deposition parameterization by Zhang et al. (2001)
attach(Caffrey_etal_1998)
C1 = 0.2789
C2 = 3.115
C3 = 5.415*10^-11
C4 = -1.399
RH = 79/100
dp_i = 0.005
dp_d = dp_i*10^-6
rd = dp_d/2
r_w = {(C1*rd^C2)/(C3*rd^C4-log10(RH))+rd^3}^(1/3)
dp = r_w*2
#Correction factor, C
k_B = 1.38*10^-23
Temp = 273.15+22
P = 101325
d_air = 3.72*10^-10
lambda = (k_B*Temp)/(sqrt(2)*3.1416*P*d_air^2)
C = 1+(2*lambda/dp)*(1.257+0.4*exp(-0.55*dp/lambda))
dyn.vis = ((5*10^-8)*Temp)+4*10^-6
rho = 2000
Vg = (rho*(dp)^2*9.81*C)/(18*dyn.vis)
# Compute aerodynamic resistance Ra:
z = 8/100
L = 50
x = z/L
# Compute shi_H (stability function)
shi_H.1 = 2*log(0.5*{1+(1-16*x)^0.5})
shi_H.2 = -5*x
shi_H =ifelse(x <= 0, shi_H.1 , shi_H.2)
zR = 5
u_star = 13.5/100
z0_1 = 0.021*(u_star)^3.32
z0_2 = 0.00098*(u_star)^1.65
z0 = ifelse(u_star<= 0.16, z0_1, z0_2)
k_c = 0.41
Ra = (log(zR/z0)-shi_H)/(k_c*u_star)  # m/s
# Compute surface resistance Rs:
e_0 = 3
R1 = 1
kin.vis = ((9*10^-8)*Temp)+10^-5
gamma = 0.50
D = (C*k_B*Temp)/(3*3.1416*dyn.vis*dp)
Sc = (kin.vis/D)
E_B = Sc^(-gamma)
alpha = 100
beta =  2
A = 2/1000
St = (Vg*u_star^2)/(kin.vis)
E_IM = {St/(alpha+St)}^beta
Rs = 1/{(e_0*u_star)*(E_B+E_IM)*R1}
# Compute Dry deposition velocity
Vd =  Vg+(1/(Ra+Rs));Vd
```

```
#Accuracy Evaluation: Ice/snow
#Dry deposition parameterization by Zhang et al. (2001)
attach(Ibrahim_1983)
C1 = 0.2789
C2 = 3.115
C3 = 5.415*10^-11
C4 = -1.399
RH = 60/100
dp_i = c(0.22, 0.73)
dp_d = dp_i*10^-6
rd = dp_d/2
r_w = {(C1*rd^C2)/(C3*rd^C4-log10(RH))+rd^3}^(1/3)
dp = r_w*2
#Correction factor, C
k_B = 1.38*10^-23
Temp = 273.15+25
P = 101325
d_air = 3.72*10^-10
lambda = (k_B*Temp)/(sqrt(2)*3.1416*P*d_air^2)
C = 1+(2*lambda/dp)*(1.257+0.4*exp(-0.55*dp/lambda))
dyn.vis = ((5*10^-8)*Temp)+4*10^-6
rho = 1500
Vg = (rho*(dp)^2*9.81*C)/(18*dyn.vis)
# Compute aerodynamic resistance Ra:
#z =
#L =
#x = z/L
x = 0.2
# Compute shi_H (stability function)
shi_H.1 = 2*log(0.5*{1+(1-16*x)^0.5})
shi_H.2 = -5*x
shi_H =ifelse(x <= 0, shi_H.1 , shi_H.2)
zR = 5
u_star = 0.12
z0 = 0.1/100
k_c = 0.41
Ra = (log(zR/z0)-shi_H)/(k_c*u_star)
# Compute surface resistance Rs:
e_0 = 3
R1 = 1
kin.vis = ((9*10^-8)*Temp)+10^-5
gamma = 0.54
D = (C*k_B*Temp)/(3*3.1416*dyn.vis*dp)
Sc = (kin.vis/D)
E_B = Sc^(-gamma)
alpha = 50
beta =  2
A = 2/1000
St = (Vg*u_star^2)/(kin.vis)
E_IM = {St/(alpha+St)}^beta
Rs = 1/{(e_0*u_star)*(E_B+E_IM)*R1}
# Compute Dry deposition velocity
Vd =  Vg+(1/(Ra+Rs));Vd
```

Codes for evaluation of model accuracy using Petroff and Zhang (2010) parameterization

```
#Accuracy Evaluation: Grass
#Dry deposition velocity parameterization by Petroff and Zhang (2010)
attach(Allen_etal_1991)
C1 = 0.2789
C2 = 3.115
C3 = 5.145*10^-11
C4 = -1.399
RH = 90/100
dp_i = 0.48
dp_d = dp_i*10^-6
rd = dp_d/2
r_w = {(C1*rd^C2)/(C3*rd^C4-log10(RH))+rd^3}^(1/3)
dp = r_w*2
#Correction factor, C
k_B = 1.38*10^-23
Temp = 273.15+25
P = 101325
```

```
d_air = 3.7208*10^-10
lambda = (k_B*Temp)/(sqrt(2)*3.1416*P*d_air^2)
C = 1+(2*lambda/dp)*(1.257+0.4*exp(-0.55*dp/lambda))
dyn.vis = ((5*10^-8)*Temp)+4*10^-6
rho = 1500
Tau = (rho*(dp)^2*C)/(18*dyn.vis)
Ws = Tau*9.81
Vphor = 0
Vdrift = Ws+Vphor
# Compute aerodynamic resistance (Ra):
z = 2
L = 200
x = z/L
# Compute stability function (shi_H)
shi_H.1 = 2*log(0.5*{1+(1-16*x)^0.5})
shi_H.2 = -5*x
shi_H = ifelse(x <= 0, shi_H.1 , shi_H.2)
zR = 3.5
z0 = 0.01
u_star = 0.5
k_c = 0.41
Ra = (log(zR/z0)-shi_H)/(k_c*u_star)
# Compute surface resistance (Rs)
kin.vis = ((9*10^-8)*Temp)+10^-5
D = (C*k_B*Temp)/(3*3.1416*dyn.vis*dp)
Sc = (kin.vis/D)
FSc = (Sc^(1/3))/2.9
Egb = (Sc^(-2/3)/14.5)*{1/6*log(1+FSc)^2/(1-FSc+FSc^2)+1/sqrt(3)*atan((2*FSc-
1)/sqrt(3))+3.1416/6*sqrt(3)}^-1
cd = 1/6
kx = 0.216
LAI = 4
h =  0.07
d  = 0.04
phi_H.1 = (1-16*x)^(-0.5)
phi_H.2 = 1+5*x
phi_H = ifelse(x<=0, phi_H.1, phi_H.2)
phi_M.1 = (1-16*x)^(-0.25)
phi_M.2 = 1+5*x
phi_M = ifelse(x<=0, phi_M.1, phi_M.2)
lmp = (0.41*(z-d))/(phi_H*(z-d)/abs(L))
lmp_h = (0.41*(h-d))/(phi_M*(h-d)/abs(L))
alphaPZ = {(kx*LAI)/(12*k_c^2*(1-d/h)^2)}^(1/3)*phi_M^(2/3)*{(h-d)/abs(L)}
C_IT = 0.056
Tau_phplus.1 = (Tau*u_star^2)/kin.vis
Tau_phplus.2 = C_IT
Tau_phplus = ifelse(Tau_phplus.1<20,Tau_phplus.1, Tau_phplus.2)
E_t.1 = 2.5*10^-3*C_IT*(Tau_phplus)^2
E_t.2 = C_IT
E_t = ifelse(Tau_phplus.1<20, E_t.1, E_t.2)
u_starf = u_star*exp(-alphaPZ)
Tau_phplus.f1 = (Tau*u_star^2)/kin.vis
Tau_phplus.f2 = 0.14
Tau_phplusf = ifelse(Tau_phplus.f1<20,Tau_phplus.f1, Tau_phplus.f2)
E_gt1 = 2.5*10^-3*0.14*(Tau_phplusf)^2
E_gt2 = 0.14
Egt = ifelse(Tau_phplus.f1<20, E_gt1, E_gt2)
Eg = Egb + Egt
# Compute Qg (non-dimensional number)
Qg = Eg*h/lmp_h
# Compute Q
U_z = 2
U_h = U_z/(exp(alphaPZ*(z/h-1)))
#Compute E_B (Brownian diffusion)
L_obs = 0.01
C_B = 0.996
Re_h = (U_h*L_obs)/(kin.vis)
E_B = C_B*(Sc^(-2/3))*(Re_h^(-1/2))
#Compute E_IN (Interception)
C_IN = 0.162
E_IN = C_IN*(dp/L_obs)
#Compute E_IM (Impaction)
C_IM = 0.081
beta_IM = 0.47
```

```
St_h = (Tau*U_h)/L_obs
E_IM = C_IM*(St_h/(St_h+beta_IM))^2
E_T = (U_h/u_star)*(E_B+E_IN+E_IM)+E_t
Q  = LAI*E_T*h/(lmp_h)
# Compute etaPZ
etaPZ = (alphaPZ^2/4+Q)^0.5
Vds = u_star*Eg*{(1+Q/Qg-alphaPZ/2)*tanh(etaPZ)/etaPZ}/{(1+Q+alphaPZ/2)*tanh(etaPZ)/etaPZ}
Vd = Vdrift+1/(Ra+1/Vds);Vd


#Accuracy Evaluation: Coniferous forest
#Dry deposition velocity parameterization by Petroff and Zhang (2010)
attach(Rannik_etal_2000)
C1 = 0.2789
C2 = 3.115
C3 = 5.145*10^-11
C4 = -1.399
RH= 0.90
dp_i = V1
dp_d = dp_i*10^-6
rd = dp_d/2
r_w = {(C1*rd^C2)/(C3*rd^C4-log10(RH))+rd^3}^(1/3)
dp = r_w*2
#Correction factor, C
k_B = 1.38*10^-23
Temp =  273.15+25
P = 101325
d_air = 3.7208*10^-10
lambda = (k_B*Temp)/(sqrt(2)*3.1416*P*d_air^2)
C = 1+(2*lambda/dp)*(1.257+0.4*exp(-0.55*dp/lambda))
dyn.vis = 1.891*10^-5
rho = 1500
Tau = (rho*(dp)^2*C)/(18*dyn.vis)
Ws = Tau*9.81
Vphor = 0
Vdrift = Ws+Vphor
# Compute aerodynamic resistance (Ra):
z = 23.7
L = 200
x = z/L
# Compute stability function (shi_H)
shi_H.1 = 2*log(0.5*{1+(1-16*x)^0.5})
shi_H.2 = -5*x
shi_H =ifelse(x <= 0, shi_H.1 , shi_H.2)
zR = 26
z0 = 1.2
u_star = V2
k_c = 0.41
Ra = (log(zR/z0)-shi_H)/(k_c*u_star)
kin.vis = 1.683*10^-5
D = (C*k_B*Temp)/(3*3.1416*dyn.vis*dp)
Sc = (kin.vis/D)
FSc = (Sc^(1/3))/2.9
Egb = (Sc^(-2/3)/14.5)*{1/6*log(1+FSc)^2/(1-FSc+FSc^2)+1/sqrt(3)*atan((2*FSc-1)/sqrt(3))
        +3.1416/6*sqrt(3)}^-1
cd = 1/6
kx = 0.216
LAI = 6
h =  13
d  = 9.75
phi_H.1 = (1-16*x)^(-0.5)
phi_H.2 = 1+5*x
phi_H = ifelse(x<=0, phi_H.1, phi_H.2)
phi_M.1 = (1-16*x)^(-0.25)
phi_M.2 = 1+5*x
phi_M = ifelse(x<=0, phi_M.1, phi_M.2)
lmp = (0.41*(z-d))/(phi_H*(z-d)/abs(L))
lmp_h = (0.41*(h-d))/(phi_M*(h-d)/abs(L))
alphaPZ = {(kx*LAI)/(12*k_c^2*(1-d/h)^2)}^(1/3)*phi_M^(2/3)*{(h-d)/abs(L)}
C_IT = 0
Tau_phplus.1 = (Tau*u_star^2)/kin.vis
Tau_phplus.2 = C_IT
Tau_phplus = ifelse(Tau_phplus.1<20,Tau_phplus.1, Tau_phplus.2)
E_t.1 = 2.5*10^-3*C_IT*(Tau_phplus)^2
```

```
E_t.2 = C_IT
E_t = ifelse(Tau_phplus.1<20, E_t.1, E_t.2)
u_starf = u_star*exp(-alphaPZ)
Tau_phplus.f1 = (Tau*u_star^2)/kin.vis
Tau_phplus.f2 = 0.14
Tau_phplusf = ifelse(Tau_phplus.f1<20,Tau_phplus.f1, Tau_phplus.f2)
E_gt1 = 2.5*10^-3*0.14*(Tau_phplusf)^2
E_gt2 = 0.14
Egt = ifelse(Tau_phplus.f1<20, E_gt1, E_gt2)
Eg = Egb + Egt
# Compute Qg (non-dimensional number)
Qg = Eg*h/lmp_h
# Compute Q
U_z = V3
U_h = U_z/(exp(alphaPZ*(z/h-1)))
L_obs = 0.15
C_B = 0.887
Re_h = (U_h*L_obs)/(kin.vis)
E_B = C_B*(Sc^(-2/3))*(Re_h^(-1/2))
C_IN = 0.810
E_IN = C_IN*(dp/L_obs)
#Compute E_IM (Impaction)
C_IM = 0.162
beta_IM = 0.60
St_h = (Tau*U_h)/L_obs
E_IM = C_IM*(St_h/(St_h+beta_IM))^2
E_T = (U_h/u_star)*(E_B+E_IN+E_IM)+E_t
Q  = LAI*E_T*h/(lmp_h)
# Compute etaPZ
etaPZ = (alphaPZ^2/4+Q)^0.5
Vds = u_star*Eg*{(1+Q/Qg-alphaPZ/2)*tanh(etaPZ)/etaPZ}/{(1+Q+alphaPZ/2)*tanh(etaPZ)/etaPZ}
Vd = Vdrift+1/(Ra+1/Vds);Vd


#Accuracy Evaluation: Deciduous forest
#Dry deposition parameterization by Petroff and Zhang (2010)
attach(Wesely_etal_1983)
C1 = 0.2789
C2 = 3.115
C3 = 5.145*10^-11
C4 = -1.399
RH= 95/100
dp_i = 0.4
dp_d = dp_i*10^-6
rd = dp_d/2
r_w = {(C1*rd^C2)/(C3*rd^C4-log10(RH))+rd^3}^(1/3)
dp = r_w*2
k_B = 1.38*10^-23
Temp = V1
P = 101325
d_air = 3.7208*10^-10
lambda = (k_B*Temp)/(sqrt(2)*3.1416*P*d_air^2)
C = 1+(2*lambda/dp)*(1.257+0.4*exp(-0.55*dp/lambda))
dyn.vis = V2
rho = 2000
Tau = (rho*(dp)^2*C)/(18*dyn.vis)
Ws = Tau*9.81
Vphor = 0
Vdrift = Ws+Vphor
# Compute aerodynamic resistance (Ra):
z = 39
L = (1*V6)
x = z/L
# Compute stability function (shi_H)
shi_H.1 = 2*log(0.5*{1+(1-16*x)^0.5})
shi_H.2 = -5*x
shi_H =ifelse(x <= 0, shi_H.1 , shi_H.2)
zR = 56
z0 = 1.6
u_star = V4
k_c = 0.41
Ra = (log(zR/z0)-shi_H)/(k_c*u_star)
kin.vis = V3
D = (C*k_B*Temp)/(3*3.1416*dyn.vis*dp)
```

```
Sc = (kin.vis/D)
FSc = (Sc^(1/3))/2.9
Egb = (Sc^(-2/3)/14.5)*{1/6*log(1+FSc)^2/(1-FSc+FSc^2)+1/sqrt(3)*atan((2*FSc-1)/sqrt(3))
        +3.1416/6*sqrt(3)}^-1
cd = 1/6
kx = 0.216
LAI = 0.2
h =  28
d  = 21
phi_H.1 = (1-16*x)^(-0.5)
phi_H.2 = 1+5*x
phi_H = ifelse(x<=0, phi_H.1, phi_H.2)
phi_M.1 = (1-16*x)^(-0.25)
phi_M.2 = 1+5*x
phi_M = ifelse(x<=0, phi_M.1, phi_M.2)
lmp = (0.41*(z-d))/(phi_H*(z-d)/abs(L))
lmp_h = (0.41*(h-d))/(phi_M*(h-d)/abs(L))
alphaPZ = {(kx*LAI)/(12*k_c^2*(1-d/h)^2)}^(1/3)*phi_M^(2/3)*{(h-d)/abs(L)}
C_IT = 0.056
Tau_phplus.1 = (Tau*u_star^2)/kin.vis
Tau_phplus.2 = C_IT
Tau_phplus = ifelse(Tau_phplus.1<20,Tau_phplus.1, Tau_phplus.2)
E_t.1 = 2.5*10^-3*C_IT*(Tau_phplus)^2
E_t.2 = C_IT
E_t = ifelse(Tau_phplus.1<20, E_t.1, E_t.2)
u_starf = u_star*exp(-alphaPZ)
Tau_phplus.f1 = (Tau*u_star^2)/kin.vis
Tau_phplus.f2 = 0.14
Tau_phplusf = ifelse(Tau_phplus.f1<20,Tau_phplus.f1, Tau_phplus.f2)
E_gt1 = 2.5*10^-3*0.14*(Tau_phplusf)^2
E_gt2 = 0.14
Egt = ifelse(Tau_phplus.f1<20, E_gt1, E_gt2)
Eg = Egb + Egt
# Compute Qg (non-dimensional number)
Qg = Eg*h/lmp_h
# Compute Q
U_z = V5
U_h = U_z/(exp(alphaPZ*(z/h-1)))
L_obs = 0.03
C_B = 1.262
Re_h = (U_h*L_obs)/(kin.vis)
E_B = C_B*(Sc^(-2/3))*(Re_h^(-1/2))
C_IN = 0.216
E_IN = C_IN*(dp/L_obs)*(2+log(4*L_obs/dp))
C_IM = 0.130
beta_IM = 0.47
St_h = (Tau*U_h)/L_obs
E_IM = C_IM*(St_h/(St_h+beta_IM))^2
E_T = (U_h/u_star)*(E_B+E_IN+E_IM)+E_t
Q  = LAI*E_T*h/(lmp_h)
# Compute etaPZ
etaPZ = (alphaPZ^2/4+Q)^0.5
Vds = u_star*Eg*{(1+Q/Qg-alphaPZ/2)*tanh(etaPZ)/etaPZ}/{(1+Q+alphaPZ/2)*tanh(etaPZ)/etaPZ}
Vd = Vdrift+1/(Ra+1/Vds);Vd


#Accuracy Evaluation: Water
#Dry deposition parameterization by Petroff and Zhang (2010)
attach(Moller_Schumann_1970)
C1 = 0.2789
C2 = 3.115
C3 = 5.415*10^-11
C4 = -1.399
RH = 90/100
dp_i = V1
dp_d = dp_i*10^-6
rd = dp_d/2
r_w = {(C1*rd^C2)/(C3*rd^C4-log10(RH))+rd^3}^(1/3)
dp = r_w*2
k_B = 1.38*10^-23
Temp = 273.15+25
P = 101325
d_air = 3.7208*10^-10
lambda = (k_B*Temp)/(sqrt(2)*3.1416*P*d_air^2)
```

```
C = 1+(2*lambda/dp)*(1.257+0.4*exp(-0.55*dp/lambda))
dyn.vis = ((5*10^-8)*Temp)+4*10^-6
rho = 1500
Tau = (rho*(dp)^2*C)/(18*dyn.vis)
Ws = Tau*9.81
Vphor = (5*10^-3)/100
Vdrift = Ws+Vphor
# Compute aerodynamic resistance (Ra):
z = 8/100
L = 50
x = z/L
shi_H.1 = 2*log(0.5*{1+(1-16*x)^0.5})
shi_H.2 = -5*x
shi_H = ifelse(x <= 0, shi_H.1 , shi_H.2)
zR = 5
u_star = 0.4
z0_1 = 0.021*(u_star)^3.32
z0_2 = 0.00098*(u_star)^1.65
z0 = ifelse(u_star<= 0.16, z0_1, z0_2)
k_c = 0.41
Ra = (log(zR/z0)-shi_H)/(k_c*u_star)
# Compute surface resistance (Rs)
kin.vis = ((9*10^-8)*Temp)+10^-5
D = (C*k_B*Temp)/(3*3.1416*dyn.vis*dp)
Sc = (kin.vis/D)
FSc = (Sc^(1/3))/2.9
Egb = (Sc^(-2/3)/14.5)*{1/6*log(1+FSc)^2/(1-FSc+FSc^2)+1/sqrt(3)*atan((2*FSc-
1)/sqrt(3))+3.1416/6*sqrt(3)}^-1
Eg = Egb
Vd = Vdrift+1/(Ra+(1/(Eg*u_star)));Vd


#Accuracy Evaluation: Ice/snow
#Dry deposition velocity parameterization by Petroff and Zhang (2010)
attach(Ibrahim_1983)
C1 = 0.2789
C2 = 3.115
C3 = 5.415*10^-11
C4 = -1.399
RH = 60/100
dp_i = c(0.22, 0.73)
dp_d = dp_i*10^-6
rd = dp_d/2
r_w = {(C1*rd^C2)/(C3*rd^C4-log10(RH))+rd^3}^(1/3)
dp = r_w*2
#Correction factor, C
k_B = 1.38*10^-23
#Temp_1 = 25
Temp = 273.15+3
P = 101325
d_air = 3.7208*10^-10
lambda = (k_B*Temp)/(sqrt(2)*3.1416*P*d_air^2)
C = 1+(2*lambda/dp)*(1.257+0.4*exp(-0.55*dp/lambda))
dyn.vis = ((5*10^-8)*Temp)+4*10^-6
rho = 1500
Tau = (rho*(dp)^2*C)/(18*dyn.vis)
Ws = Tau*9.81
Vphor = (2*10^-4)/100
Vdrift = Ws+Vphor
# Compute aerodynamic resistance (Ra):
#z =
#L = z/L
#x = z/L
x = 0.2
# Compute stability function (shi_H)
shi_H.1 = 2*log(0.5*{1+(1-16*x)^0.5})
shi_H.2 = -5*x
shi_H = ifelse(x <= 0, shi_H.1 , shi_H.2)
zR = 10
u_star = 0.12
z0 = 0.1/100
k_c = 0.41
Ra = (log(zR/z0)-shi_H)/(k_c*u_star)  # m/s
# Compute surface resistance (Rs)
```

```
kin.vis = ((9*10^-8)*Temp)+10^-5
D = (C*k_B*Temp)/(3*3.1416*dyn.vis*dp)
Sc = (kin.vis/D)
FSc = (Sc^(1/3))/2.9
Egb = (Sc^(-2/3)/14.5)*{1/6*log(1+FSc)^2/(1-FSc+FSc^2)+1/sqrt(3)*atan((2*FSc-1)/sqrt(3))+3.1416/6*sqrt(3)}^-1
Eg = Egb
Vd = Vdrift+1/(Ra+(1/(Eg*u_star)));Vd
```

Codes for evaluation of model accuracy using Kouznetsov and Sofiev (2012) parameterization

```
#Accuracy Evaluation: Grass
#Dry deposition parameterization by Kouznetsov and Sofiev (2012)
attach(Allen_etal_1990)
C1 = 0.4809
C2 = 3.082
C3 = 3.110*10^-11
C4 = -1.428
RH = 90/100
dp_a = 0.48
dp_i = dp_a*10^-6
rd = dp_i/2
r_w = {(C1*rd^C2)/(C3*rd^C4-log10(RH))+rd^3}^(1/3)
dp = r_w*2
#Correction factor, C
k_B = 1.38*10^-23
Temp_1 = V1
Temp = 273.15+V1
P = 101325
d_air = 3.7208*10^-10
lambda = (k_B*Temp)/(sqrt(2)*3.1416*P*d_air^2)
C = 1+(2*lambda/dp)*(1.257+0.4*exp(-0.55*dp/lambda))
dyn.vis = ((5*10^-8)*Temp)+4*10^-6
rho =  2000
Tau = (rho*(dp)^2*C)/(18*dyn.vis)
V_s = Tau*9.81
u_star = V2
a  =  2*10^-3
kin.vis = ((9*10^-8)*Temp)+10^-5
D = (C*k_B*Temp)/(3*3.1416*dyn.vis*dp)
Sc = (kin.vis/D)
Re_star = (u_star*a)/kin.vis
# Compute V_diff (velocity for diffusion)
V_diff = 2*(Re_star^(-0.5))*Sc^(-2/3) #m/s
# Compute V_int (velocity for interception)
V_int = 80*u_star*((dp/a)^2)*(Re_star^(0.5))
# Compute V_imp
C_S = 0.003
C_R = 0.3
LAI = 4
CsCR = (C_S+C_R/LAI)^0.5
u.Uh = 0.3
u_star.by.U_h = min(u.Uh, CsCR)
#Compute Re_c
Re_c = ((u_star.by.U_h)^-1)^2*Re_star
# Calculate St
St = (Tau*u_star)/a
# Calculate St_e
St_e = St - Re_c^(-0.5)
eta_impSt.e1 = exp((-0.1/(St_e - 0.15 ) )-(1/sqrt(St_e -0.15)))
eta_impSt.e2 = 0
eta_impSt.e = ifelse(St_e>0.15,eta_impSt.e1,eta_impSt.e2)
V_imp = ((2*u_star.by.U_h)/u_star)*eta_impSt.e*(St-u_star.by.U_h*Re_star^-0.5)
# Dry deposition velocity
Vd = V_diff+V_int+V_imp+V_s;Vd
```

```
#Accuracy Evaluation: Coniferous forest
#Dry deposition parameterization by Kouznetsov and Sofiev (2012)
attach(Rannik_etal_2000)
C1 = 0.2789
C2 = 3.115
C3 = 5.145*10^-11
C4 = -1.399
RH = 0.90
dp_a = V1
dp_i = dp_a*10^-6
rd = dp_i/2
r_w = {(C1*rd^C2)/(C3*rd^C4-log10(RH))+rd^3}^(1/3)
dp = r_w*2
#Correction factor, C
k_B = 1.38*10^-23
Temp =  273.15+25
P = 101325
d_air = 3.7208*10^-10
lambda = (k_B*Temp)/(sqrt(2)*3.1416*P*d_air^2)
C = 1+(2*lambda/dp)*(1.257+0.4*exp(-0.55*dp/lambda))
dyn.vis = 1.891*10^-5
#dyn.vis = V2
rho = 1500
Tau = (rho*(dp)^2*C)/(18*dyn.vis)
V_s = Tau*9.81
# Need to compute Sc, Re_star
u_star = V2
a  =  0.7*10^-3
kin.vis = 1.683*10^-5
D = (C*k_B*Temp)/(3*3.1416*dyn.vis*dp)
Sc = (kin.vis/D)
Re_star = (u_star*a)/kin.vis
# Compute V_diff (velocity for diffusion)
V_diff = 2*(Re_star^(-0.5))*Sc^(-2/3)
# Compute V_int (velocity for interception)
V_int = 80*u_star*((dp/a)^2)*(Re_star^(0.5))
# Compute V_imp
C_S = 0.003
C_R = 0.3
LAI = 6
CsCR = (C_S+C_R/LAI)^0.5
u.Uh = 0.3
u_star.by.U_h = min(u.Uh, CsCR)
#Compute Re_c
Re_c = ((u_star.by.U_h)^-1)^2*Re_star
# Calculate St
St = (Tau*u_star)/a
# Calculate St_e
St_e = St - Re_c^(-0.5)
eta_impSt.e1 = exp((-0.1/(St_e - 0.15 ) )-(1/sqrt(St_e -0.15)))
eta_impSt.e2 = 0
eta_impSt.e = ifelse(St_e>0.15,eta_impSt.e1,eta_impSt.e2)
V_imp = ((2*u_star.by.U_h)/u_star)*eta_impSt.e*(St-u_star.by.U_h*Re_star^-0.5)
# Dry deposition velocity
Vd = V_diff+V_int+V_imp+V_s;Vd


#Accuracy Evaluation: Deciduous forest
#Dry deposition parameterization by Kouznetsov and Sofiev (2012)
attach(Wesely_etal_1983)
C1 = 0.2789
C2 = 3.115
C3 = 5.145*10^-11
C4 = -1.399
RH = 0.95
dp_a = 0.4
dp_i = dp_a*10^-6
rd = dp_i/2
r_w = {(C1*rd^C2)/(C3*rd^C4-log10(RH))+rd^3}^(1/3)
dp = r_w*2
#Correction factor, C
k_B = 1.38*10^-23
Temp = V1
P = 101325
```

```
d_air = 3.7208*10^-10
lambda = (k_B*Temp)/(sqrt(2)*3.1416*P*d_air^2)
C = 1+(2*lambda/dp)*(1.257+0.4*exp(-0.55*dp/lambda))
dyn.vis = V2
rho = 2000
Tau = (rho*(dp)^2*C)/(18*dyn.vis)
V_s = Tau*9.81
# Need to compute Sc, Re_star
u_star = V4
a  = 0.7*10^-3
kin.vis = 1.597*10^-5
D = (C*k_B*Temp)/(3*3.1416*dyn.vis*dp)
Sc = (kin.vis/D)
Re_star = (u_star*a)/kin.vis
# Compute V_diff (velocity for diffusion)
V_diff = 2*(Re_star^(-0.5))*Sc^(-2/3) #m/s
# Compute V_int (velocity for interception)
V_int = 80*u_star*((dp/a)^2)*(Re_star^(0.5))
# Compute V_imp
C_S = 0.003
C_R = 0.3
LAI = 0.2
CsCR = (C_S+C_R/LAI)^0.5
u.Uh = 0.3
u_star.by.U_h = min(u.Uh, CsCR)
#Compute Re_c
Re_c = ((u_star.by.U_h)^-1)^2*Re_star
# Calculate St
St = (Tau*u_star)/a
# Calculate St_e
St_e = St - Re_c^(-0.5)
eta_impSt.e1 = exp((-0.1/(St_e - 0.15 ) )-(1/sqrt(St_e -0.15)))
eta_impSt.e2 = 0
eta_impSt.e = ifelse(St_e>0.15,eta_impSt.e1,eta_impSt.e2)
V_imp = ((2*u_star.by.U_h)/u_star)*eta_impSt.e*(St-u_star.by.U_h*Re_star^-0.5)
#Dry deposition velocity
Vd = V_diff+V_int+V_imp+V_s;Vd


#Accuracy Evaluation: Ice/snow
#Dry deposition parameterization by Kouznetsov and Sofiev (2012)
attach(Ibrahim_1983)
C1 = 0.4809
C2 = 3.082
C3 = 3.110*10^-11
C4 = -1.428
RH = 0.90
dp_a = c(0.22, 0.73)
dp_i = dp_a*10^-6
rd = dp_i/2
r_w = {(C1*rd^C2)/(C3*rd^C4-log10(RH))+rd^3}^(1/3)
dp = r_w*2
#Correction factor, C
k_B = 1.38*10^-23
Temp = 273.15+3
P = 101325
d_air = 3.7208*10^-10
lambda = (k_B*Temp)/(sqrt(2)*3.1416*P*d_air^2)
C = 1+(2*lambda/dp)*(1.257+0.4*exp(-0.55*dp/lambda))
dyn.vis = ((5*10^-8)*Temp)+4*10^-6
rho =  1500
Tau = (rho*(dp)^2*C)/(18*dyn.vis)
V_s = Tau*9.81
u_star = 0.12
a  =  0.5*10^-3
kin.vis = ((9*10^-8)*Temp)+10^-5
D = (C*k_B*Temp)/(3*3.1416*dyn.vis*dp)
Sc = (kin.vis/D)
Re_star = (u_star*a)/kin.vis
# Compute V_diff (velocity for diffusion)
V_diff = 2*(Re_star^(-0.5))*Sc^(-2/3) #m/s
# Compute V_int (velocity for interception)
V_int = 80*u_star*((dp/a)^2)*(Re_star^(0.5))
#Compute V_imp
```

```
C_S = 0.003
C_R = 0.3
LAI = 0
CsCR = (C_S+C_R/LAI)^0.5
u.Uh = 0.3
u_star.by.U_h = min(u.Uh, CsCR)
#Compute Re_c
Re_c = ((u_star.by.U_h)^-1)^2*Re_star
# Calculate St
St = (Tau*u_star)/a
# Calculate St_e
St_e = St - Re_c^(-0.5)
eta_impSt.e1 = exp((-0.1/(St_e - 0.15 ) )-(1/sqrt(St_e -0.15)))
eta_impSt.e2 = 0
eta_impSt.e = ifelse(St_e>0.15,eta_impSt.e1,eta_impSt.e2)
#V_imp = ((2*u_star.by.U_h)/u_star)*eta_impSt.e*(St-u_star.by.U_h*Re_star^-0.5)
V_imp = (2*u_star.by.U_h*eta_impSt.e*(St-(u_star.by.U_h*Re_star^-0.5)))*u_star
# Dry deposition velocity
Vd = V_diff+V_int+V_imp+V_s;Vd


#Accuracy Evaluation: Water
#Dry deposition parameterization by Kouznetsov and Sofiev (2012)
C1 = 0.2789
C2 = 3.115
C3 = 5.415*10^-11
C4 = -1.399
dp_i = c(0.22, 0.73)
dp = dp_i*10^-6
rho = 1500
RH = 0.60
Temp = 25+273.15
u_star = 0.12
z0 =0.1/100
L = 40
kin.vis = ((9*10^-8)*Temp)+10^-5
dyn.vis = ((5*10^-8)*Temp)+4*10^-6
d_air = 3.7208*10^-10
k_B = 1.38*10^-23
P = 101325
lambda = (k_B*Temp)/(sqrt(2)*3.1416*P*d_air^2)
C = 1+((2*lambda/dp)*(1.257+0.4*exp(-0.55*dp/lambda)))
tau_p = (rho*(dp)^2*C)/(18*dyn.vis)
D = (C*k_B*Temp)/(3*3.1416*dyn.vis*dp)
v_s = 9.81*tau_p
taup = (tau_p*u_star^2)/(kin.vis)
Sc = (kin.vis/D)
vsplus = v_s/u_star
rplus = (dp*u_star)/(2*kin.vis)
R_s = 0
Rsplus = u_star*R_s
z_meas = 8
zpmax = (z_meas*u_star)/(kin.vis)
MOplus = (kin.vis)/(u_star*L)
#Fixed parameters
Zbuf = 3
Ztf = 18                              #turbophoretic sublayer height
taultf = 5                            #Lagrangian time in turbophoretic layer
Nutp_Ztf= (0.4*(Ztf)^3)/(Ztf^2+200)  #Dimensionless eddy viscosity of air
It_Ztf = (2.5*log10(Ztf ))-(100/Ztf^2)
It_Zbuf = (2.5*log10(Zbuf))-(100/Zbuf^2)
S = Sc^(1/3)
Zl = 20/S
fTmp = 2.5/Sc
fTmp1 = (fTmp^3/27+(fTmp*(100+5*sqrt(8*fTmp/27)+400)))^(1/3)
Zl_1 = fTmp1+((fTmp*fTmp)/(9*fTmp1))+(1/3)*fTmp                #Zl updated as zl_1
fTmp_1 = (Zl_1^2)/(Zl_1^2+200)                                 #fTmp updated as fTmp_1
fTmp_2 = 1.2*(fTmp_1)-0.8*fTmp_1^2                             #fTmp_1 updated as fTmp_2
fTmp1_1 = 1/(Sc*fTmp_2)                                        #fTmp1 updated as fTmp1_1
fTmp_3 = 1/Sc                                                  #ftmp_2 updated as fTmp_3
x_1 = Zl_1 - fTmp1_1
x_2 = Zl_1
x_3 = Zl_1+fTmp1_1
Nutp_x_1 = (0.4*x_1^3)/(x_1^2+200)
```

```
Nutp_x_2 = (0.4*x_2^3)/(x_2^2+200)
Nutp_x_3 = (0.4*x_3^3)/(x_3^2+200)
fIvd = Rsplus+(Zl_1-
fTmp1_1)*Sc+0.3333*fTmp1_1*(1/fTmp_3+((0.4*x_1^3)/(x_1^2+200)))+4/(fTmp_3+((0.4*x_2^3)/(x_2^2+200)))+1/(fTmp_3+((0
.4*x_3^3)/(x_3^2+200)))
x_4 = zpmax
x_5 = Zl_1 + fTmp1_1
It_x_4 = 2.5*log10(x_4) - 100/(x_4^2)
It_x_5 = 2.5*log10(x_5) - 100/(x_5^2)
s = 2.35*(zpmax*MOplus+abs(zpmax*MOplus))
u1 = 0.5*(abs(zpmax*MOplus)-zpmax*MOplus)
u = -4*u1/(2.65*sqrt(u1*sqrt(u1))+1)
fu_Psi = s+u
fTmp_4 = It_x_4 - It_x_5 + 2.5*fu_Psi
fIvd_1 = fIvd+0.5*(fTmp_4+abs(fTmp_4))    #fIvd updated as fIvd_1
fu_vdplus_smooth_1 = 1/fIvd_1             #mind fu_vdplus_smooth is denoted as _1
Il_input1= Zl*S/7.92
Il_input2= rplus*S/7.92
Il_1 = -0.16667*log10(Il_input1^2-Il_input1+1)+0.57735*atan((2*Il_input1-1)*0.57735)+0.3333*log10(Il_input1+1)
Il_2 = -0.16667*log10(Il_input2^2-Il_input2+1)+0.57735*atan((2*Il_input2-1)*0.57735)+0.3333*log10(Il_input2+1)
R = 7.92*S^2*(Il_1-Il_2)  #laminar resistance
R_1 = 0.5*(R+abs(R))      #R updated as R_1 #should be zero if rplus > Zl
Zl_2 = 0.5*(rplus+Zl+abs(rplus-Zl))   #Zl updated as Zl_2, not to be confused with Zl_1 as if statement is in use
It_Zbuf = 2.5*log10(Zbuf) - (100/(Zbuf^2))
It_Zl_2 = 2.5*log10(Zl_2) - (100/(Zl_2^2))
R1 = It_Zbuf - It_Zl_2
R_2 = R_1+0.5*(R1+abs(R1))                    #R_1 updated as R_2
fTmp_5 = vsplus*R_2                           #fTmp used as fTmp_5. Not updated as previous fTmp_4 is for
different condition
fTmp_6 = exp(-fTmp_5)                         #fTmp_5 updated as fTmp_6
fIvd_2  = Rsplus*fTmp_6+(1-fTmp_6)/vsplus     #fIvd denoted as fIvd_2 NOT updated previous fIvd_1 is for different
condition
fIvd_3 = Rsplus+R_2                           #fIvd_3 used; NOT updated
fIvd_23 = ifelse(abs(fTmp_5)>0.001, fIvd_2, fIvd_3 )
#Use above values for the following calculations for turbophoretic layer
V  = 0.81*taup/(Ztf-Zbuf)/(1+taup/taultf) + vsplus   #chcek for sign of vsplus
It_Ztf = 2.5*log10(Ztf) - 100/(Ztf^2)
R_3  = ((It_Ztf)-(It_Zbuf))*(1+taup/taultf)    #R_2 updated as R_3
fTmp_7 = V*R_3                                 #fTmp_6 updated as fTmp_7
fTmp_8 = exp(-fTmp_7)                          #fTmp_7 updated as fTmp_8
fIvd_4 = (fIvd_23*fTmp_8)+(1-fTmp_8)/V         #fIvd_23 updated as fIvd_4
fIvd_5 = fIvd_3+R_3                            #fIvd_5 used; NOT updated
fIvd_45 = ifelse(abs(fTmp_7)>0.001, fIvd_4, fIvd_5)
#Now calculations for the Lagrangian turbophoretic layer
Ztf2 = 2*taup
V_1 = 0.4+vsplus
R_4 =
0.1667*((1+taup/(0.5*Ztf))/(Nutp_Ztf)+4*(1+taup/(0.25*(Ztf+Ztf2)))/((0.4*(0.5*(Ztf+Ztf2))^3)/((0.5*(Ztf+Ztf2))^2+2
00))+(1+taup/(0.5*Ztf2))/((0.4*Ztf2 ^3)/(Ztf2^2+200)))*(Ztf2-Ztf)
fTmp_9 = V_1*R_4
fTmp_10 = exp(-fTmp_9)
fIvd_6 = fIvd_45*fTmp_10 + (1-fTmp_10)/V_1   #fIvd_5 or fIvd_4 (fIvd_45)
fIvd_7 = fIvd_45+R_3                         #Either fIvd_4 or fIvd_5, R_3 used not R_4 since outside if statement
fIvd_67 = ifelse(abs(fTmp_9) > 0.001, fIvd_6, fIvd_7)
Ztf2_2 = Ztf
fIvd67_Ztf2 = ifelse(Ztf2>Ztf, fIvd_67, Ztf2_2)

#Following calculations are for aerodynamic layer
It_zpmax = 2.5*log10(zpmax) - 100/(zpmax^2)
Ztf22 = ifelse(Ztf2>Ztf, Ztf2, Ztf2_2)
It_Ztf22  = 2.5*log10(Ztf22) - 100/(Ztf22^2)       #be careful which Ztf2 to be used here based on previous
condition
R_5 = It_zpmax - It_Ztf22  + 2.5*fu_Psi            #R_5 used, NOT updated from R_4
R_6 = 0.5*(R_5+abs(R_5))                           #R_5 updated as R_6
fTmp_11  = vsplus*R_6                              #fTmp_11 used, NOT updated from fTmp_10
fTmp_12 = exp(-fTmp_11)                            #fTmp_11 updated as fTmp_12
fIvd_4567 = ifelse(Ztf2>Ztf, fIvd_67,fIvd_45)
fIvd_8 = (fIvd_4567* fTmp_12)+(1-fTmp_12)/vsplus   # Caution:fIvd_45 or fIvd_67 may be used
fIvd_9 = fIvd_4567 + R_6                           #fIvd_9 used, NOT updated. Caution:fIvd_5 or fIvd_4 may be used
fIvd_10 = ifelse(abs(fTmp_11) > 0.001, fIvd_8, fIvd_9)
fu_vdplus_smooth_3 = 1/fIvd_10                      #fu_vdplus_smooth_3 used. NOT updated. fIvd_8 could be used
fu_vdplus_smooth = ifelse(Zl>Zbuf, fu_vdplus_smooth_1, fu_vdplus_smooth_3)
Vd_smooth = fu_vdplus_smooth*u_star;Vd_smooth
```

Codes for evaluation of model accuracy using Zhang and He (2014) parameterization

```
#Accuracy Evaluation: Grass (code is similar for coniferous forest)
#Dry deposition parameterization by Zhang and He (2014)
attach(Allen_etal_1991)
C1 = 0.4809
C2 = 3.082
C3 = 3.110*10^-11
C4 = -1.428
RH = 90/100
dp_a = 0.48
dp_i = dp_a*10^-6
rd = dp_i/2
r_w = {(C1*rd^C2)/(C3*rd^C4-log10(RH))+rd^3}^(1/3)
dp = r_w*2
#Correction factor, C
k_B = 1.38*10^-23
Temp_1 = V1
Temp = 273.15+V1
P = 101325
d_air = 3.7208*10^-10
lambda = (k_B*Temp)/(sqrt(2)*3.1416*P*d_air^2)
C = 1+(2*lambda/dp)*(1.257+0.4*exp(-0.55*dp/lambda))
dyn.vis = ((5*10^-8)*Temp)+4*10^-6              # kg/m*s (temp. corrected viscosity coeff. of air)
rho = 2000
Tau = (rho*(dp)^2*C)/(18*dyn.vis)
V_g = Tau*9.81
Rg = 1/V_g
u_star = V2
a1 = 4.8*10^-3
z = 2
L = V4
x = z/L
# Compute stability function (shi_H)
shi_H.1 = 2*log(0.5*{1+(1-16*x)^0.5})
shi_H.2 = -5*x
shi_H =ifelse(x <= 0, shi_H.1 , shi_H.2)
zR = 3.5
z0 = 0.01
k_c = 0.41
Ra = (log(zR/z0)-shi_H)/(k_c*u_star)
# Calculate Vds = 1/Rs
#For PM2.5
Vds_PM2.5 = (a1*u_star)
Rds_PM2.5 = (1/Vds_PM2.5)
# For PM2.5-10
#b1= -1.6*10^-1
#b2= 1.5*10^0
#b3 = 7.8*10^-1
#c1= 1.8
#c2 = -2.0*10^-1
#c3 = -5.3*10^-1
#k = c1*u_star+c2*u_star^2+c3*u_star^3
#LAI =
#LAImax =
#Vds_PM10 = (b1*u_star+b2*u_star^2+b3*u_star^3)  #*exp(k*(LAI/LAImax)-1)
#Rds_PM10 = 1/Vds_PM10
# For PM10+
#d1= -2.2
#d2= 3.9*10^1
#d3 = -6.7
#f1= 6.2
#f2 = -1.2*10^1
#f3 = 6.1
#k = f1*u_star+f2*u_star^2+f3*u_star^3
#LAI =
#LAImax =
#Vds_PM10Plus = (d1*u_star+d2*u_star^2+d3*u_star^3)*exp(k*(LAI/LAImax)-1)
#Rds_PM10Plus = (1/Vds_PM10Plus)
#Compute Vd
Vd = 1/Rg+(1/(Ra+Rds_PM2.5));Vd
```

```
#Accuracy Evaluation: Deciduous forest
#Dry deposition parameterization by Zhang and He (2014)
attach(Rannik_etal_2000)
C1 = 0.2789
C2 = 3.115
C3 = 5.145*10^-11
C4 = -1.399
RH = 90/100
dp_a = V1
dp_i = dp_a*10^-6
rd = dp_i/2
r_w = {(C1*rd^C2)/(C3*rd^C4-log10(RH))+rd^3}^(1/3)
dp = r_w*2
k_B = 1.38*10^-23
Temp = 273.15+25
P = 101325
d_air = 3.7208*10^-10
lambda = (k_B*Temp)/(sqrt(2)*3.1416*P*d_air^2)
C = 1+(2*lambda/dp)*(1.257+0.4*exp(-0.55*dp/lambda))
dyn.vis = 1.891*10^-5
rho = 1500
Tau = (rho*(dp)^2*C)/(18*dyn.vis)
V_g = Tau*9.81
Rg = 1/V_g
u_star = V2
a1 = 4.3*10^-3
z = 23.7
L = 200
x = z/L
# Compute stability function (shi_H)
shi_H.1 = 2*log(0.5*{1+(1-16*x)^0.5})
shi_H.2 = -5*x
shi_H =ifelse(x <= 0, shi_H.1 , shi_H.2)
zR = 26
z0 = 1.2
k_c = 0.41
Ra = (log(zR/z0)-shi_H)/(k_c*u_star)
# Calculate Vds = 1/Rs
#For PM2.5
Vds_PM2.5 = (a1*u_star)
Rds_PM2.5 = (1/Vds_PM2.5)
# For PM2.5-10
#b1= -1.6*10^-1
#b2= 1.5*10^0
#b3 = 7.8*10^-1
#c1= 1.8
#c2 = -2.0*10^-1
#c3 = -5.3*10^-1
k = c1*u_star+c2*u_star^2+c3*u_star^3
LAI = 12
LAImax = 12
Vds_PM10 = (b1*u_star+b2*u_star^2+b3*u_star^3)  #*exp(k*(LAI/LAImax)-1)
Rds_PM10 = 1/Vds_PM10
# For PM10+
#d1= -2.2
#d2= 3.9*10^1
#d3 = -6.7
#f1= 6.2
#f2 = -1.2*10^1
#f3 = 6.1
#k = f1*u_star+f2*u_star^2+f3*u_star^3
#LAI =
#LAImax =
#Vds_PM10Plus = (d1*u_star+d2*u_star^2+d3*u_star^3)*exp(k*(LAI/LAImax)-1)
#Rds_PM10Plus = (1/Vds_PM10Plus)
#Compute Vd
Vd = 1/Rg+(1/(Ra+Rds_PM2.5));Vd


#Accuracy Evaluation: Water
#Dry deposition parameterization by Zhang and He (2014)
attach(Caffrey_etal_1998)
C1 = 0.2789
C2 = 3.115
```

```
C3 = 5.415*10^-11
C4 = -1.399
RH = 79/100
dp_a = V1
dp_i = dp_a*10^-6
rd = dp_i/2
r_w = {(C1*rd^C2)/(C3*rd^C4-log10(RH))+rd^3}^(1/3)
dp = r_w*2
#Correction factor, C
k_B = 1.38*10^-23
Temp = 273.15+22
P = 101325
d_air = 3.7208*10^-10
lambda = (k_B*Temp)/(sqrt(2)*3.1416*P*d_air^2)
C = 1+(2*lambda/dp)*(1.257+0.4*exp(-0.55*dp/lambda))
dyn.vis = ((5*10^-8)*Temp)+4*10^-6
rho = 2000
Tau = (rho*(dp)^2*C)/(18*dyn.vis)
V_g = Tau*9.81
Rg = 1/V_g
a1 = 6.9*10^-3
z = 8/100
L = 50
x = z/L
# Compute stability function (shi_H)
shi_H.1 = 2*log(0.5*{1+(1-16*x)^0.5})
shi_H.2 = -5*x
shi_H =ifelse(x <= 0, shi_H.1 , shi_H.2)
zR = 5
u_star = 13.5/100
z0_1 = 0.021*(u_star)^3.32
z0_2 = 0.00098*(u_star)^1.65
z0 = ifelse(u_star<= 0.16, z0_1, z0_2)
k_c = 0.41
Ra = (log(zR/z0)-shi_H)/(k_c*u_star)  # m/s
# Calculate Vds = 1/Rs
#For PM2.5
Vds_PM2.5 = (a1*u_star)
Rds_PM2.5 = (1/Vds_PM2.5)
#Compute Vd
Vd = 1/Rg+(1/(Ra+Rds_PM2.5));Vd


#Accuracy Evaluation: Ice/snow
#Dry deposition parameterization by Zhang and He (2014)
#attach(Nilsson_Rannik_2001)
C1 = 0.2789
C2 = 3.115
C3 = 5.415*10^-11
C4 = -1.399
RH = 60/100
dp_a = c(0.22, 0.73)
dp_i = dp_a*10^-6
rd = dp_i/2
r_w = {(C1*rd^C2)/(C3*rd^C4-log10(RH))+rd^3}^(1/3)
dp = r_w*2
#Correction factor, C
k_B = 1.38*10^-23
Temp = 273.15+3
P = 101325
d_air = 3.7208*10^-10
lambda = (k_B*Temp)/(sqrt(2)*3.1416*P*d_air^2)
C = 1+(2*lambda/dp)*(1.257+0.4*exp(-0.55*dp/lambda))
dyn.vis = ((5*10^-8)*Temp)+4*10^-6
rho = 1500
Tau = (rho*(dp)^2*C)/(18*dyn.vis)
V_g = Tau*9.81
Rg = 1/V_g
a1 = 4.3*10^-3
#z =
#L =
#x = z/L
x = 0.2
# Compute stability function (shi_H)
```

```
shi_H.1 = 2*log(0.5*{1+(1-16*x)^0.5})
shi_H.2 = -5*x
shi_H =ifelse(x <= 0, shi_H.1 , shi_H.2)
zR = 10
u_star = 0.12
z0 = 0.1/100
k_c = 0.41
Ra = (log(zR/z0)-shi_H)/(k_c*u_star)  # m/s
# Calculate Vds = 1/Rs
#For PM2.5
Vds_PM2.5 = (a1*u_star)
Rds_PM2.5 = (1/Vds_PM2.5)
#Compute Vd
Vd = 1/Rg+(1/(Ra+Rds_PM2.5));Vd
```

Codes for evaluation of model accuracy using Zhang and Sao (2014) parameterization

```
#Accuracy Evaluation: Rough and smooth surfaces
#Dry deposition parameterization by Zhang and He (2014)
#attach(Allen_etal_1991)
C1 = 0.4809
C2 = 3.082
C3 = 3.110*10^-11
C4 = -1.428
RH_1 = 90
RH = 90/100
dp_a = 0.50
dp_i = dp_a*10^-6
rd = dp_i/2
r_w = {(C1*rd^C2)/(C3*rd^C4-log10(RH))+rd^3}^(1/3)
dp = r_w*2
#Correction factor, C
k_B = 1.38*10^-23
Temp = 273.15+25
P = 101325
d_air = 3.7208*10^-10
lambda = (k_B*Temp)/(sqrt(2)*3.1416*P*d_air^2)
C = 1+(2*lambda/dp)*(1.257+0.4*exp(-0.55*dp/lambda))
Temp = 273.15+25
dyn.vis = ((5*10^-8)*Temp)+4*10^-6
rho = 1500
Tau = (rho*(dp_i)^2*C)/(18*dyn.vis)
Tau_wet = (rho*(dp)^2*C)/(18*dyn.vis)
Wt = Tau*9.81
Vg = Wt
Vg_wet = Tau_wet*9.81
u_star = 0.5
k =  0.41
z =  1
zd = 0.20
h_c = 0.23
z0 = 0.002
B1 = 0.45
Sc_T = (1+(Vg^2/u_star^2))^0.5
Ra = (Sc_T/(k*u_star))*(log((z-zd)/(h_c-zd)))  # For rough surface
#Ra = (B1*Sc_T/k*u_star)*log(z/z0)             # For smooth surface
Rg = 1/Vg
# Calculate surface resistance (Rs)
U_h = 2
kin.vis = ((9*10^-8)*Temp)+10^-5
d_c = 0.005
D = (C*k_B*Temp)/(3*3.1416*dyn.vis*dp)
Sc = (kin.vis/D)
Re_h = (U_h*d_c)/(kin.vis)
nB = 0.5
C_B = 0.467
E_B = C_B*Sc^(-2/3)*Re_h^(nB-1)
#Compute impaction collection efficiency (E_IM)
beta_IM = 0.6
St_h = (Tau*u_star)/d_c
E_IM = (St_h/(St_h+beta_IM))^2
#Compute interception efficiency (E_IN)
Ain = 150
```

```
E_IN = Ain*u_star*(10^(-St_h))*(2*dp/d_c)
#Compute R
b = 2
R = exp(-b*sqrt(St_h))
#Compute w_dm
B2 = 3
w_dm = (u_star/U_h*h_c)       #For rough surface
#w_dm = B2*u_star             #For smooth surface
#compute Tau_c/Tau (ratio of stress)
Beta = 200
C_1 = 6
C_2 = 0.1
lambda_FAI = 0.4
n_FAI = (lambda_FAI)/(h_c*d_c)
q = (3.1416*d_c^2)/4
eta_BAI = n_FAI*q
lambda_FAIe = ((lambda_FAI)/(1-eta_BAI)^C_2)*exp((-C_1*lambda_FAI)/(1-eta_BAI)^C_2)
Tau_c_BY_Tau = (Beta*lambda_FAIe)/(1+Beta*lambda_FAIe)
#Compute Rs
E = E_B+E_IM+E_IN
Tau_wetplus = (Tau_wet*u_star^2)/kin.vis
Cd = 1/6
Rs = (R*w_dm*((E*Tau_c_BY_Tau/Cd)+(1+Tau_c_BY_Tau)*Sc^-1+10^(-3/Tau_wetplus))+Vg_wet)^-1
#Compute Vd
Vd = (Rg+((Rs-Rg)/exp(Ra/Rg)))^-1;Vd
```

Codes for Monte Carlo uncertainty evaluation for Zhang et al. (2001) parameterization

```
#Dry deposition parameterization by Zhang et al. (2001)
#Uncertainty test: Grass
set.seed(5)
C1 = 0.2789
C2 = 3.115
C3 = 5.145*10^-11
C4 = -1.399
RH = replicate(10000,runif(100,0.76,0.84))
dp_i = 2.0*10^-6
rd = dp_i/2
r_w = {(C1*rd^C2)/(C3*rd^C4-log10(RH))+rd^3}^(1/3)
dp = r_w*2
#Correction factor, C
k_B = 1.38*10^-23
Temp = (273.15+25)
P = 101325
d_air = 3.72*10^-10
lambda = (k_B*Temp)/(sqrt(2)*3.1416*P*d_air^2)
C = 1+(2*lambda/dp)*(1.257+0.4*exp(-0.55*dp/lambda))
dyn.vis = 1.8908*10^-5
rho = 1500
Vg = (rho*(dp)^2*9.81*C)/(18*dyn.vis)
# Compute aerodynamic resistance Ra:
z = 5
L = replicate(10000,runif(100,45,55))
x = z/L
# Compute shi_H (stability function)
shi_H2 = -5*x
zR = 3.5
z0 = replicate(10000,runif(100,0.03, 0.05))
u_star = replicate(10000,runif(100,0.27,0.33))
k_c = 0.41
Ra = (log(zR/z0)-shi_H2)/(k_c*u_star)
# Compute surface resistance Rs:
e_0 = 3
R1 =1
# Compute E_B (collection efficienty from Brownian diffusion)
kin.vis = 1.6834*10^-5
gamma = 0.54
D = (C*k_B*Temp)/(3*3.1416*dyn.vis*dp)
Sc = (kin.vis/D)
E_B = Sc^(-gamma)
# Compute E_IM (collection efficiency from impaction)
alpha = 1.2
beta =  2
```

```
A = 2/1000
St = (Vg*u_star)/(9.81*A)
E_IM = {St/(alpha+St)}^beta
# Compute E_IN (collection efficiency from interception)
E_IN = 0.5*(dp/A)^2
Rs = 1/{(e_0*u_star)*(E_B+E_IM+E_IN)*R1}
# Compute Dry deposition velocity
Vd <- Vg+(1/(Ra+Rs))
quantile(Vd, c(.05, 0.10, .50, 0.95))


#Dry deposition parameterization by Zhang et al. (2001)
#Uncertainty test: Coniferous forest
set.seed(5)
C1 = 0.2789
C2 = 3.115
C3 = 5.145*10^-11
C4 = -1.399
RH = replicate(10000,runif(100,0.76,0.84))
dp_i = 2.0*10^-6                #particle dia = 0.005-50 um (assumed, vary)
rd = dp_i/2
r_w = {(C1*rd^C2)/(C3*rd^C4-log10(RH))+rd^3}^(1/3)
dp = r_w*2
#Correction factor, C
k_B = 1.38*10^-23
Temp = (273.15+25)
P = 101325
d_air = 3.72*10^-10
lambda = (k_B*Temp)/(sqrt(2)*3.1416*P*d_air^2)
C = 1+(2*lambda/dp)*(1.257+0.4*exp(-0.55*dp/lambda))
dyn.vis = 1.8908*10^-5
rho = 1500
Vg = (rho*(dp)^2*9.81*C)/(18*dyn.vis)   #m/s
# Compute aerodynamic resistance Ra:
L = replicate(10000,runif(100,45,55))
x = z/L
shi_H2 = -5*x
zR = 30
z0 = replicate(10000,runif(100,0.9, 1.5))
u_star = replicate(10000,runif(100,0.27,0.33))
k_c = 0.41
Ra = (log(zR/z0)-shi_H2)/(k_c*u_star)  # m/s
# Compute surface resistance Rs:
e_0 = 3
R1 =1
# Compute E_B (collection efficiency from Brownian diffusion)
kin.vis = 1.6834*10^-5
gamma = 0.56
D = (C*k_B*Temp)/(3*3.1416*dyn.vis*dp)
Sc = (kin.vis/D)
E_B = Sc^(-gamma)
# Compute E_IM (collection efficiency from impaction)
alpha = 1.0
beta =  2
A = 2/1000
St = (Vg*u_star)/(9.81*A)
E_IM = {St/(alpha+St)}^beta
# Compute E_IN (collection efficiency from interception)
E_IN = 0.5*(dp/A)^2
Rs = 1/{(e_0*u_star)*(E_B+E_IM+E_IN)*R1}  #(m/s)
# Compute Dry deposition velocity
Vd <- Vg+(1/(Ra+Rs))
quantile(Vd, c(.05, 0.10, .50, 0.95))


#Dry deposition parameterization by Zhang et al. (2001)
#Uncertainty test: Deciduous forest
set.seed(5)
C1 = 0.2789
C2 = 3.115
C3 = 5.145*10^-11
C4 = -1.399
RH = replicate(10000,runif(100,0.76,0.84))
dp_i = 2.0*10^-6
```

```
rd = dp_i/2
r_w = {(C1*rd^C2)/(C3*rd^C4-log10(RH))+rd^3}^(1/3)
dp = r_w*2
#Correction factor, C
k_B = 1.38*10^-23
Temp = (273.15+25)
P = 101325
d_air = 3.72*10^-10
lambda = (k_B*Temp)/(sqrt(2)*3.1416*P*d_air^2)
C = 1+(2*lambda/dp)*(1.257+0.4*exp(-0.55*dp/lambda))
dyn.vis = 1.8908*10^-5
rho = 1500
Vg = (rho*(dp)^2*9.81*C)/(18*dyn.vis)
# Compute aerodynamic resistance Ra:
z = 35
L = replicate(10000,runif(100,45,55))
x = 35/L
# Compute shi_H (stability function)
shi_H2 = -5*x
zR = 50
z0 = replicate(10000,runif(100,1.125, 1.875))
u_star = replicate(10000,runif(100,0.27,0.33))
k_c = 0.41
Ra = (log(zR/z0)-shi_H2)/(k_c*u_star)
# Compute surface resistance Rs:
e_0 = 3
R1 =1
# Compute E_B (collection efficienty from Brownian diffusion)
kin.vis = 1.6834*10^-5
gamma = 0.56
D = (C*k_B*Temp)/(3*3.1416*dyn.vis*dp)
Sc = (kin.vis/D)
E_B = Sc^(-gamma)
# Compute E_IM (collection efficienty from impaction)
alpha = 0.80
beta =  2
A = 5/1000
St = (Vg*u_star)/(9.81*A)
E_IM = {St/(alpha+St)}^beta
# Compute E_IN (collection efficienty from interception)
E_IN = 0.5*(dp/A)^2
Rs = 1/{(e_0*u_star)*(E_B+E_IM+E_IN)*R1}
# Compute Dry deposition velocity
Vd <- Vg+(1/(Ra+Rs))
quantile(Vd, c(.05, 0.10, .50, 0.95))


#Dry deposition parameterization by Zhang et al. (2001)
#Uncertainty test: Water
set.seed(5)
C1 = 0.2789
C2 = 3.115
C3 = 5.415*10^-11
C4 = -1.399
RH = replicate(10000,runif(100,0.76,0.84))
dp_i = 2.0 #Parameter to vary for MCs
dp_d = dp_i*10^-6
rd = dp_d/2
r_w = {(C1*rd^C2)/(C3*rd^C4-log10(RH))+rd^3}^(1/3)
dp = r_w*2
#Correction factor, C
k_B = 1.38*10^-23
Temp = 273.15+25
P = 101325
d_air = 3.72*10^-10
lambda = (k_B*Temp)/(sqrt(2)*3.1416*P*d_air^2)
C = 1+(2*lambda/dp)*(1.257+0.4*exp(-0.55*dp/lambda))
dyn.vis = ((5*10^-8)*Temp)+4*10^-6
rho = 1500
Vg = (rho*(dp)^2*9.81*C)/(18*dyn.vis)
# Compute aerodynamic resistance Ra:
z = 8/100
L = replicate(10000,runif(100,45,55))
x = z/L
```

```
# Compute shi_H (stability function)
shi_H.1 = 2*log(0.5*{1+(1-16*x)^0.5})
shi_H.2 = -5*x
shi_H =ifelse(x <= 0, shi_H.1 , shi_H.2)
zR = 5
u_star = replicate(10000,runif(100,0.27,0.33))
z0_1 = 0.021*(u_star)^3.32
z0_2 = 0.00098*(u_star)^1.65
z0 = ifelse(u_star<= 0.16, z0_1, z0_2)
k_c = 0.41
Ra = (log(zR/z0)-shi_H)/(k_c*u_star)
# Compute surface resistance Rs:
e_0 = 3
R1 = 1
kin.vis = ((9*10^-8)*Temp)+10^-5
gamma = 0.50
D = (C*k_B*Temp)/(3*3.1416*dyn.vis*dp)
Sc = (kin.vis/D)
E_B = Sc^(-gamma)
alpha = 100
beta =  2
A = 2/1000
St = (Vg*u_star^2)/(kin.vis)
E_IM = {St/(alpha+St)}^beta
Rs = 1/{(e_0*u_star)*(E_B+E_IM)*R1}  #(m/s)
# Compute Dry deposition velocity
Vd =  Vg+(1/(Ra+Rs))
quantile(Vd, c(.05, 0.10, .50, 0.95))


#Dry deposition parameterization by Zhang et al. (2001)
#Uncertainty test: Ice/snow
set.seed(5)
C1 = 0.2789
C2 = 3.115
C3 = 5.415*10^-11
C4 = -1.399
RH = replicate(10000,runif(100,0.76,0.84))
dp_i = 2.0
dp_d = dp_i*10^-6
rd = dp_d/2
r_w = {(C1*rd^C2)/(C3*rd^C4-log10(RH))+rd^3}^(1/3)
dp = r_w*2
#Correction factor, C
k_B = 1.38*10^-23
Temp = 273.15+0
P = 101325
d_air = 3.72*10^-10
lambda = (k_B*Temp)/(sqrt(2)*3.1416*P*d_air^2)
C = 1+(2*lambda/dp)*(1.257+0.4*exp(-0.55*dp/lambda))
dyn.vis = ((5*10^-8)*Temp)+4*10^-6
rho = 1500
Vg = (rho*(dp)^2*9.81*C)/(18*dyn.vis)
# Compute aerodynamic resistance Ra:
z = 5
L = replicate(10000,runif(100,45,55))
x = z/L
# Compute shi_H (stability function)
shi_H.1 = 2*log(0.5*{1+(1-16*x)^0.5})
shi_H.2 = -5*x
shi_H =ifelse(x <= 0, shi_H.1 , shi_H.2)
zR = 10
u_star = replicate(10000,runif(100,0.27,0.33))
z0 = replicate(10000,runif(100,0.0075,0.0125))
k_c = 0.41
Ra = (log(zR/z0)-shi_H)/(k_c*u_star)
# Compute surface resistance Rs:
e_0 = 3
R1 = 1
kin.vis = ((9*10^-8)*Temp)+10^-5
gamma = 0.54
D = (C*k_B*Temp)/(3*3.1416*dyn.vis*dp)
Sc = (kin.vis/D)
E_B = Sc^(-gamma)
```

```
alpha = 50
beta =  2
A = 2/1000
St = (Vg*u_star^2)/(kin.vis)
E_IM = {St/(alpha+St)}^beta
Rs = 1/{(e_0*u_star)*(E_B+E_IM)*R1}  #(m/s)
# Compute Dry deposition velocity
Vd =  Vg+(1/(Ra+Rs))
quantile(Vd, c(.05, 0.10, .50, 0.95))
```

Codes for Monte Carlo uncertainty evaluation for Petroff and Zhang (2010) parameterization

```
#Dry deposition parameterization by Petroff and Zhang (2010)
#Uncertainty test: Grass
set.seed(5)
C1 = 0.2789
C2 = 3.115
C3 = 5.145*10^-11
C4 = -1.399
RH = replicate(10000,runif(100,0.76,0.84))
dp_a = 2.0
dp_i = dp_a*10^-6
rd = dp_i/2
r_w = {(C1*rd^C2)/(C3*rd^C4-log10(RH))+rd^3}^(1/3)
dp = r_w*2
#Correction factor, C
k_B = 1.38*10^-23
Temp = (273.15+25)
P = 101325
d_air = 3.7208*10^-10
lambda = (k_B*Temp)/(sqrt(2)*3.1416*P*d_air^2)
C = 1+(2*lambda/dp)*(1.257+0.4*exp(-0.55*dp/lambda))
dyn.vis = 1.8908*10^-5
rho = 1500
Tau = (rho*(dp)^2*C)/(18*dyn.vis)
Ws = Tau*9.81
Vphor = 0
Vdrift = Ws+Vphor
# Compute aerodynamic resistance (Ra):
z = 5
L = replicate(10000,runif(100,45,55))
x = z/L
# Compute stability function (shi_H)
shi_H.1 = 2*log(0.5*{1+(1-16*x)^0.5})
shi_H.2 = -5*x
shi_H =ifelse(x <= 0, shi_H.1 , shi_H.2)
zR = 3.5
z0 = replicate(10000,runif(100,0.03,0.05))
u_star = replicate(10000,runif(100,0.27,0.33))
k_c = 0.41
Ra = (log(zR/z0)-shi_H)/(k_c*u_star)
# Compute surface resistance (Rs)
kin.vis = 1.6834*10^-5
D = (C*k_B*Temp)/(3*3.1416*dyn.vis*dp)
Sc = (kin.vis/D)
FSc = (Sc^(1/3))/2.9
Egb = (Sc^(-2/3)/14.5)*{1/6*log(1+FSc)^2/(1-FSc+FSc^2)+1/sqrt(3)*atan((2*FSc-1)/sqrt(3))
        +3.1416/6*sqrt(3)}^-1
cd = 1/6
kx = 0.216
LAI = replicate(10000,runif(100,3.8,4.2))
h = replicate(10000,runif(100,0.475,0.525))
d = replicate(10000,runif(100,0.225,0.375))
phi_H.1 = (1-16*x)^(-0.5)
phi_H.2 = 1+5*x
phi_H = ifelse(x<=0, phi_H.1, phi_H.2)
phi_M.1 = (1-16*x)^(-0.25)
phi_M.2 = 1+5*x
phi_M = ifelse(x<=0, phi_M.1, phi_M.2)
lmp = (0.41*(z-d))/(phi_H*(z-d)/abs(L))
lmp_h = (0.41*(h-d))/(phi_M*(h-d)/abs(L))
alphaPZ = {(kx*LAI)/(12*k_c^2*(1-d/h)^2)}^(1/3)*phi_M^(2/3)*{(h-d)/abs(L)}
C_IT = 0.042
```

```
Tau_phplus.1 = (Tau*u_star^2)/kin.vis
Tau_phplus.2 = C_IT
Tau_phplus = ifelse(Tau_phplus.1<20,Tau_phplus.1, Tau_phplus.2)
E_t.1 = 2.5*10^-3*C_IT*(Tau_phplus)^2
E_t.2 = C_IT
E_t = ifelse(Tau_phplus.1<20, E_t.1, E_t.2)
u_starf = u_star*exp(-alphaPZ)
Tau_phplus.f1 = (Tau*u_star^2)/kin.vis
Tau_phplus.f2 = 0.14
Tau_phplusf = ifelse(Tau_phplus.f1<20,Tau_phplus.f1, Tau_phplus.f2)
E_gt1 = 2.5*10^-3*0.14*(Tau_phplusf)^2
E_gt2 = 0.14
Egt = ifelse(Tau_phplus.f1<20, E_gt1, E_gt2)
Eg = Egb + Egt
Qg = Eg*h/lmp_h
U_z = replicate(10000,runif(100,2.91,3.09))
U_h = U_z/(exp(alphaPZ*(z/h-1)))
L_obs = 0.005
C_B = 0.7
Re_h = (U_h*L_obs)/(kin.vis)
E_B = C_B*(Sc^(-2/3))*(Re_h^(-1/2))
C_IN = 0.7
E_IN = C_IN*(dp/L_obs)
C_IM = 0.191
beta_IM = 0.60
St_h = (Tau*U_h)/L_obs
E_IM = C_IM*(St_h/(St_h+beta_IM))^2
E_T = (U_h/u_star)*(E_B+E_IN+E_IM)+E_t
Q  = LAI*E_T*h/(lmp_h)
etaPZ = (alphaPZ^2/4+Q)^0.5
Vds = u_star*Eg*{(1+Q/Qg-alphaPZ/2)*tanh(etaPZ)/etaPZ}/{(1+Q+alphaPZ/2)*tanh(etaPZ)/etaPZ}
Vd = Vdrift+1/(Ra+1/Vds)
quantile(Vd, c(.05, 0.10, .50, 0.95))


#Dry deposition parameterization by Petroff and Zhang (2010)
#Uncertainty test: Coniferous forest
set.seed(5)
C1 = 0.2789
C2 = 3.115
C3 = 5.145*10^-11
C4 = -1.399
RH = replicate(10000,runif(100,0.76,0.84))
dp_a = 50
dp_i = dp_a*10^-6
rd = dp_i/2
r_w = {(C1*rd^C2)/(C3*rd^C4-log10(RH))+rd^3}^(1/3)
dp = r_w*2
#Correction factor, C
k_B = 1.38*10^-23
Temp = (273.15+25)
P = 101325
d_air = 3.7208*10^-10
lambda = (k_B*Temp)/(sqrt(2)*3.1416*P*d_air^2)
C = 1+(2*lambda/dp)*(1.257+0.4*exp(-0.55*dp/lambda))
dyn.vis = 1.8908*10^-5
rho = 1500
Tau = (rho*(dp)^2*C)/(18*dyn.vis)
Ws = Tau*9.81
Vphor = 0
Vdrift = Ws+Vphor
# Compute aerodynamic resistance (Ra):
z = 35
L = replicate(10000,runif(100,180,200))
x = z/L
# Compute stability function (shi_H)
shi_H.1 = 2*log(0.5*{1+(1-16*x)^0.5})
shi_H.2 = -5*x
shi_H =ifelse(x <= 0, shi_H.1 , shi_H.2)
zR = 30
z0 = replicate(10000,runif(100,0.9,1.5))
u_star = replicate(10000,runif(100,0.27,0.33))
k_c = 0.41
Ra = (log(zR/z0)-shi_H)/(k_c*u_star)
```

```
# Compute surface resistance (Rs)
kin.vis = 1.6834*10^-5
D = (C*k_B*Temp)/(3*3.1416*dyn.vis*dp)
Sc = (kin.vis/D)
FSc = (Sc^(1/3))/2.9
Egb = (Sc^(-2/3)/14.5)*{1/6*log(1+FSc)^2/(1-FSc+FSc^2)+1/sqrt(3)*atan((2*FSc-1)/sqrt(3))
       +3.1416/6*sqrt(3)}^-1
cd = 1/6
kx = 0.216
LAI = replicate(10000,runif(100,9.5,10.5))
h = replicate(10000,runif(100,14.25,15.75))
d = replicate(10000,runif(100,5.25,8.75))
phi_H.1 = (1-16*x)^(-0.5)
phi_H.2 = 1+5*x
phi_H = ifelse(x<=0, phi_H.1, phi_H.2)
phi_M.1 = (1-16*x)^(-0.25)
phi_M.2 = 1+5*x
phi_M = ifelse(x<=0, phi_M.1, phi_M.2)
lmp = (0.41*(z-d))/(phi_H*(z-d)/abs(L))
lmp_h = (0.41*(h-d))/(phi_M*(h-d)/abs(L))
alphaPZ = {(kx*LAI)/(12*k_c^2*(1-d/h)^2)}^(1/3)*phi_M^(2/3)*{(h-d)/abs(L)}
C_IT = 0
Tau_phplus.1 = (Tau*u_star^2)/kin.vis
Tau_phplus.2 = C_IT
Tau_phplus = ifelse(Tau_phplus.1<20,Tau_phplus.1, Tau_phplus.2)
E_t.1 = 2.5*10^-3*C_IT*(Tau_phplus)^2
E_t.2 = C_IT
E_t = ifelse(Tau_phplus.1<20, E_t.1, E_t.2)
u_starf = u_star*exp(-alphaPZ)
Tau_phplus.f1 = (Tau*u_star^2)/kin.vis
Tau_phplus.f2 = 0.14
Tau_phplusf = ifelse(Tau_phplus.f1<20,Tau_phplus.f1, Tau_phplus.f2)
E_gt1 = 2.5*10^-3*0.14*(Tau_phplusf)^2
E_gt2 = 0.14
Egt = ifelse(Tau_phplus.f1<20, E_gt1, E_gt2)
Eg = Egb + Egt
# Compute Qg (non-dimensional number)
Qg = Eg*h/lmp_h
# Compute Q
U_z = replicate(10000,runif(100,3.88,4.12))
U_h = U_z/(exp(alphaPZ*(z/h-1)))
#Compute E_B (Brownian diffusion)
L_obs = 0.0015
C_B = 0.887
Re_h = (U_h*L_obs)/(kin.vis)
E_B = C_B*(Sc^(-2/3))*(Re_h^(-1/2))
#Compute E_IN (Interception)
C_IN = 0.810
E_IN = C_IN*(dp/L_obs)
#Compute E_IM (Impaction)
C_IM = 0.162
beta_IM = 0.60
St_h = (Tau*U_h)/L_obs
E_IM = C_IM*(St_h/(St_h+beta_IM))^2
E_T = (U_h/u_star)*(E_B+E_IN+E_IM)+E_t
Q  = LAI*E_T*h/(lmp_h)
# Compute etaPZ
etaPZ = (alphaPZ^2/4+Q)^0.5
Vds = u_star*Eg*{(1+Q/Qg-alphaPZ/2)*tanh(etaPZ)/etaPZ}/{(1+Q+alphaPZ/2)*tanh(etaPZ)/etaPZ}
Vd = Vdrift+1/(Ra+1/Vds)
quantile(Vd, c(.05, 0.10, .50, 0.95))


#Dry deposition parameterization by Petroff and Zhang (2010)
#Uncertainty test: Deciduous forest
set.seed(5)
C1 = 0.2789
C2 = 3.115
C3 = 5.145*10^-11
C4 = -1.399
RH = replicate(10000,runif(100,0.76,0.84))
dp_a = 2.0
dp_i = dp_a*10^-6
rd = dp_i/2
```

```
r_w = {(C1*rd^C2)/(C3*rd^C4-log10(RH))+rd^3}^(1/3)
dp = r_w*2
#Correction factor, C
k_B = 1.38*10^-23
Temp = (273.15+25)
P = 101325
d_air = 3.7208*10^-10
lambda = (k_B*Temp)/(sqrt(2)*3.1416*P*d_air^2)
C = 1+(2*lambda/dp)*(1.257+0.4*exp(-0.55*dp/lambda))
dyn.vis = 1.8908*10^-5
rho = 1500
Tau = (rho*(dp)^2*C)/(18*dyn.vis)
Ws = Tau*9.81
Vphor = 0
Vdrift = Ws+Vphor
# Compute aerodynamic resistance (Ra):
z = 35
L = replicate(10000,runif(100,45,55))
x = z/L
# Compute stability function (shi_H)
shi_H.1 = 2*log(0.5*{1+(1-16*x)^0.5})
shi_H.2 = -5*x
shi_H =ifelse(x <= 0, shi_H.1 , shi_H.2)
zR = 50
z0 = replicate(10000,runif(100,1.125, 1.875))
u_star = replicate(10000,runif(100,0.54,0.66))
k_c = 0.41
Ra = (log(zR/z0)-shi_H)/(k_c*u_star)
# Compute surface resistance (Rs)
kin.vis = 1.6834*10^-5
D = (C*k_B*Temp)/(3*3.1416*dyn.vis*dp)
Sc = (kin.vis/D)
FSc = (Sc^(1/3))/2.9
Egb = (Sc^(-2/3)/14.5)*{1/6*log(1+FSc)^2/(1-FSc+FSc^2)+1/sqrt(3)*atan((2*FSc-1)/sqrt(3))
        +3.1416/6*sqrt(3)}^-1
cd = 1/6
kx = 0.216
LAI = replicate(10000,runif(100,9.5,10.5))
h = replicate(10000,runif(100,23.75,26.25))
d = replicate(10000,runif(100,12,20))
phi_H.1 = (1-16*x)^(-0.5)
phi_H.2 = 1+5*x
phi_H = ifelse(x<=0, phi_H.1, phi_H.2)
phi_M.1 = (1-16*x)^(-0.25)
phi_M.2 = 1+5*x
phi_M = ifelse(x<=0, phi_M.1, phi_M.2)
lmp = (0.41*(z-d))/(phi_H*(z-d)/abs(L))
lmp_h = (0.41*(h-d))/(phi_M*(h-d)/abs(L))
alphaPZ = {(kx*LAI)/(12*k_c^2*(1-d/h)^2)}^(1/3)*phi_M^(2/3)*{(h-d)/abs(L)}
C_IT = 0.056
Tau_phplus.1 = (Tau*u_star^2)/kin.vis
Tau_phplus.2 = C_IT
Tau_phplus = ifelse(Tau_phplus.1<20,Tau_phplus.1, Tau_phplus.2)
E_t.1 = 2.5*10^-3*C_IT*(Tau_phplus)^2
E_t.2 = C_IT
E_t = ifelse(Tau_phplus.1<20, E_t.1, E_t.2)
u_starf = u_star*exp(-alphaPZ)
Tau_phplus.f1 = (Tau*u_star^2)/kin.vis
Tau_phplus.f2 = 0.14
Tau_phplusf = ifelse(Tau_phplus.f1<20,Tau_phplus.f1, Tau_phplus.f2)
E_gt1 = 2.5*10^-3*0.14*(Tau_phplusf)^2
E_gt2 = 0.14
Egt = ifelse(Tau_phplus.f1<20, E_gt1, E_gt2)
Eg = Egb + Egt
# Compute Qg (non-dimensional number)
Qg = Eg*h/lmp_h
U_z = replicate(10000,runif(100,3.88,4.12))
U_h = U_z/(exp(alphaPZ*(z/h-1)))
#Compute E_B (Brownian diffusion)
L_obs = 0.03
C_B = 1.262
Re_h = (U_h*L_obs)/(kin.vis)
E_B = C_B*(Sc^(-2/3))*(Re_h^(-1/2))
#Compute E_IN (Interception)
```

```
C_IN = 0.216
E_IN = C_IN*(dp/L_obs)*(2+log(4*L_obs/dp))
#Compute E_IM (Impaction)
C_IM = 0.130
beta_IM = 0.47
St_h = (Tau*U_h)/L_obs
E_IM = C_IM*(St_h/(St_h+beta_IM))^2
E_T = (U_h/u_star)*(E_B+E_IN+E_IM)+E_t
Q  = LAI*E_T*h/(lmp_h)
# Compute etaPZ
etaPZ = (alphaPZ^2/4+Q)^0.5
Vds = u_star*Eg*{(1+Q/Qg-alphaPZ/2)*tanh(etaPZ)/etaPZ}/{(1+Q+alphaPZ/2)*tanh(etaPZ)/etaPZ}
Vd = Vdrift+1/(Ra+1/Vds)
quantile(Vd, c(.05, 0.10, .50, 0.95))


#Dry deposition parameterization by Petroff and Zhang (2010)
#Uncertainty test: Water
set.seed(5)
C1 = 0.2789
C2 = 3.115
C3 = 5.415*10^-11
C4 = -1.399
RH = replicate(10000,runif(100,0.76,0.84))
dp_i = 2.0
dp_d = dp_i*10^-6
rd = dp_d/2
r_w = {(C1*rd^C2)/(C3*rd^C4-log10(RH))+rd^3}^(1/3)
dp = r_w*2
k_B = 1.38*10^-23
Temp = 273.15+25
P = 101325
d_air = 3.7208*10^-10
lambda = (k_B*Temp)/(sqrt(2)*3.1416*P*d_air^2)
C = 1+(2*lambda/dp)*(1.257+0.4*exp(-0.55*dp/lambda))
dyn.vis = ((5*10^-8)*Temp)+4*10^-6
rho = 1500
Tau = (rho*(dp)^2*C)/(18*dyn.vis)
Ws = Tau*9.81
Vphor = (5*10^-3)/100
Vdrift = Ws+Vphor
# Compute aerodynamic resistance (Ra):
z = 8/100
L = replicate(10000,runif(100,45,55))
x = z/L
# Compute stability function (shi_H)
shi_H.1 = 2*log(0.5*{1+(1-16*x)^0.5})
shi_H.2 = -5*x
shi_H = ifelse(x <= 0, shi_H.1 , shi_H.2)
zR = 5
u_star = replicate(10000,runif(100,0.27,0.33))
z0_1 = 0.021*(u_star)^3.32
z0_2 = 0.00098*(u_star)^1.65
z0 = ifelse(u_star<= 0.16, z0_1, z0_2)
k_c = 0.41
Ra = (log(zR/z0)-shi_H)/(k_c*u_star)
# Compute surface resistance (Rs)
kin.vis = ((9*10^-8)*Temp)+10^-5
D = (C*k_B*Temp)/(3*3.1416*dyn.vis*dp)
Sc = (kin.vis/D)
FSc = (Sc^(1/3))/2.9
Egb = (Sc^(-2/3)/14.5)*{1/6*log(1+FSc)^2/(1-FSc+FSc^2)+1/sqrt(3)*atan((2*FSc-
1)/sqrt(3))+3.1416/6*sqrt(3)}^-1
Eg = Egb
Vd = Vdrift+1/(Ra+(1/(Eg*u_star)))
quantile(Vd, c(.05, 0.10, .50, 0.95))


#Dry deposition parameterization by Petroff and Zhang (2010)
#Uncertainty test: Ice/snow
set.seed(5)
C1 = 0.2789
C2 = 3.115
C3 = 5.415*10^-11
```

```
C4 = -1.399
RH = replicate(10000,runif(100,0.76,0.84))
dp_i = 2.0
dp_d = dp_i*10^-6
rd = dp_d/2
r_w = {(C1*rd^C2)/(C3*rd^C4-log10(RH))+rd^3}^(1/3)
dp = r_w*2
#Correction factor, C
k_B = 1.38*10^-23
Temp = 273.15+0
P = 101325
d_air = 3.7208*10^-10
lambda = (k_B*Temp)/(sqrt(2)*3.1416*P*d_air^2)
C = 1+(2*lambda/dp)*(1.257+0.4*exp(-0.55*dp/lambda))
dyn.vis = ((5*10^-8)*Temp)+4*10^-6
rho = 1500
Tau = (rho*(dp)^2*C)/(18*dyn.vis)
Ws = Tau*9.81
Vphor = (2*10^-4)/100
Vdrift = Ws+Vphor
# Compute aerodynamic resistance (Ra)
z = 5
L = replicate(10000,runif(100,45,55))
x = z/L
# Compute stability function (shi_H)
shi_H.1 = 2*log(0.5*{1+(1-16*x)^0.5})
shi_H.2 = -5*x
shi_H = ifelse(x <= 0, shi_H.1 , shi_H.2)
zR = 10
u_star = replicate(10000,runif(100,0.27,0.33))
z0 = replicate(10000,runif(100,0.0075,0.0125))
k_c = 0.41
Ra = (log(zR/z0)-shi_H)/(k_c*u_star)
# Compute surface resistance (Rs)
kin.vis = ((9*10^-8)*Temp)+10^-5
D = (C*k_B*Temp)/(3*3.1416*dyn.vis*dp)
Sc = (kin.vis/D)
FSc = (Sc^(1/3))/2.9
Egb = (Sc^(-2/3)/14.5)*{1/6*log(1+FSc)^2/(1-FSc+FSc^2)+1/sqrt(3)*atan((2*FSc-1)/sqrt(3))+3.1416/6*sqrt(3)}^-1
Eg = Egb
Vd = Vdrift+1/(Ra+(1/(Eg*u_star)))
quantile(Vd, c(.05, 0.10, .50, 0.95))
```

Codes for Monte Carlo uncertainty evaluation for Kouznetsov and Sofiev (2012) parameterization

```
#Dry deposition parameterization by Kouznetsov and Sofiev (2012)
#Uncertainty test: Grass
set.seed(5)
C1 = 0.2789
C2 = 3.115
C3 = 5.145*10^-11
C4 = -1.399
RH = replicate(10000,runif(100,0.76,0.84))
dp_a =2.0
dp_i = dp_a*10^-6
rd = dp_i/2
r_w = {(C1*rd^C2)/(C3*rd^C4-log10(RH))+rd^3}^(1/3)
dp = r_w*2
#Correction factor, C
k_B = 1.38*10^-23
Temp = (273.15+25)
P = 101325
d_air = 3.7208*10^-10
lambda = (k_B*Temp)/(sqrt(2)*3.1416*P*d_air^2)
C = 1+(2*lambda/dp)*(1.257+0.4*exp(-0.55*dp/lambda))
dyn.vis = 1.89*10^-5
rho = 1500
Tau = (rho*(dp)^2*C)/(18*dyn.vis)
V_s = Tau*9.81
u_star = replicate(10000,runif(100,0.27,0.33))
a  = 2*10^-3
kin.vis = 1.68*10^-5
D = (C*k_B*Temp)/(3*3.1416*dyn.vis*dp)
```

```
Sc = (kin.vis/D)
Re_star = (u_star*a)/kin.vis
# Compute V_diff (velocity for diffusion)
V_diff = 2*(Re_star^(-0.5))*Sc^(-2/3)
# Compute V_int (velocity for interception)
V_int = 80*u_star*((dp/a)^2)*(Re_star^(0.5))
# Compute V_imp
C_S = 0.003
C_R = 0.3
LAI = replicate(10000,runif(100,3.8,4.2))
CsCR = (C_S+C_R/LAI)^0.5
u.Uh = 0.3
u_star.by.U_h = min(u.Uh, CsCR)
#Compute Re_c
Re_c = ((u_star.by.U_h)^-1)^2*Re_star
# Calculate St
St = (Tau*u_star)/a
# Calculate St_e
St_e = St - Re_c^(-0.5)
eta_impSt.e1 = exp((-0.1/(St_e - 0.15 ) )-(1/sqrt(St_e -0.15)))
eta_impSt.e2 = 0
eta_impSt.e = ifelse(St_e>0.15,eta_impSt.e1,eta_impSt.e2)
V_imp = ((2*u_star.by.U_h)/u_star)*eta_impSt.e*(St-u_star.by.U_h*Re_star^-0.5)
# Dry deposition velocity
Vd = V_diff+V_int+V_imp+V_s
quantile(Vd, c(.05, 0.10, .50, 0.95))


#Dry deposition parameterization by Kouznetsov and Sofiev (2012)
#Uncertainty test: Coniferous forest
set.seed(5)
C1 = 0.2789
C2 = 3.115
C3 = 5.145*10^-11
C4 = -1.399
RH = replicate(10000,runif(100,0.76,0.84))
dp_a = 2.0
dp_i = dp_a*10^-6
rd = dp_i/2
r_w = {(C1*rd^C2)/(C3*rd^C4-log10(RH))+rd^3}^(1/3)
dp = r_w*2
#Correction factor, C
k_B = 1.38*10^-23
Temp =  273.15+25
P = 101325
d_air = 3.7208*10^-10
lambda = (k_B*Temp)/(sqrt(2)*3.1416*P*d_air^2)
C = 1+(2*lambda/dp)*(1.257+0.4*exp(-0.55*dp/lambda))
dyn.vis = 1.891*10^-5
rho = 1500
Tau = (rho*(dp)^2*C)/(18*dyn.vis)
V_s = Tau*9.81
u_star = replicate(10000,runif(100,0.27,0.33))
a  =  0.7*10^-3
kin.vis = 1.683*10^-5
D = (C*k_B*Temp)/(3*3.1416*dyn.vis*dp)
Sc = (kin.vis/D)
Re_star = (u_star*a)/kin.vis
# Compute V_diff (velocity for diffusion)
V_diff = 2*(Re_star^(-0.5))*Sc^(-2/3)
# Compute V_int (velocity for interception)
V_int = 80*u_star*((dp/a)^2)*(Re_star^(0.5))
# Compute V_imp
C_S = 0.003
C_R = 0.3
LAI = replicate(10000,runif(100,5.7,6.3))
CsCR = (C_S+C_R/LAI)^0.5
u.Uh = 0.3
u_star.by.U_h = min(u.Uh, CsCR)
#Compute Re_c
Re_c = ((u_star.by.U_h)^-1)^2*Re_star
# Calculate St
St = (Tau*u_star)/a
# Calculate St_e
```

```
St_e = St - Re_c^(-0.5)
eta_impSt.e1 = exp((-0.1/(St_e - 0.15 ) )-(1/sqrt(St_e -0.15)))
eta_impSt.e2 = 0
eta_impSt.e = ifelse(St_e>0.15,eta_impSt.e1,eta_impSt.e2)
V_imp = ((2*u_star.by.U_h)/u_star)*eta_impSt.e*(St-u_star.by.U_h*Re_star^-0.5)
# Dry deposition velocity
Vd = V_diff+V_int+V_imp+V_s
quantile(Vd, c(.05, 0.10, .50, 0.95))


#Dry deposition parameterization by Kouznetsov and Sofiev (2012)
#Uncertainty test: Deciduous forest
set.seed(5)
C1 = 0.2789
C2 = 3.115
C3 = 5.145*10^-11
C4 = -1.399
RH = replicate(10000,runif(100,0.76,0.84))
dp_a = 2.0
dp_i = dp_a*10^-6
rd = dp_i/2
r_w = {(C1*rd^C2)/(C3*rd^C4-log10(RH))+rd^3}^(1/3)
dp = r_w*2
#Correction factor, C
k_B = 1.38*10^-23
Temp = (273.15+25)
P = 101325
d_air = 3.7208*10^-10
lambda = (k_B*Temp)/(sqrt(2)*3.1416*P*d_air^2)
C = 1+(2*lambda/dp)*(1.257+0.4*exp(-0.55*dp/lambda))
dyn.vis = 1.89*10^-5
rho = 1500
Tau = (rho*(dp)^2*C)/(18*dyn.vis)
V_s = Tau*9.81
u_star = replicate(10000,runif(100,0.27,0.33))
a  = 7*10^-3
kin.vis = 1.68*10^-5
D = (C*k_B*Temp)/(3*3.1416*dyn.vis*dp)
Sc = (kin.vis/D)
Re_star = (u_star*a)/kin.vis
# Compute V_diff (velocity for diffusion)
V_diff = 2*(Re_star^(-0.5))*Sc^(-2/3)
# Compute V_int (velocity for interception)
V_int = 80*u_star*((dp/a)^2)*(Re_star^(0.5))
# Compute V_imp
C_S = 0.003
C_R = 0.3
LAI = replicate(10000,runif(100,9.5,10.5))
CsCR = (C_S+C_R/LAI)^0.5
u.Uh = 0.3
u_star.by.U_h = min(u.Uh, CsCR)
#Compute Re_c
Re_c = ((u_star.by.U_h)^-1)^2*Re_star
# Calculate St
St = (Tau*u_star)/a
# Calculate St_e
St_e = St - Re_c^(-0.5)
eta_impSt.e1 = exp((-0.1/(St_e - 0.15 ) )-(1/sqrt(St_e -0.15)))
eta_impSt.e2 = 0
eta_impSt.e = ifelse(St_e>0.15,eta_impSt.e1,eta_impSt.e2)
V_imp = ((2*u_star.by.U_h)/u_star)*eta_impSt.e*(St-u_star.by.U_h*Re_star^-0.5)
# Dry deposition velocity
Vd = V_diff+V_int+V_imp+V_s
quantile(Vd, c(.05, 0.10, .50, 0.95))


#Dry deposition parameterization by Kouznetsov and Sofiev (2012)
#Uncertainty test: Smooth surface (water)
set.seed(5)
C1 = 0.2789
C2 = 3.115
C3 = 5.415*10^-11
C4 = -1.399
dp_i = 0.5
```

```
dp = dp_i*10^-6
rho = 1500
RH = replicate(10000,runif(100,0.76,0.84))
Temp = 25+273.15
u_star = replicate(10000,runif(100,0.27,0.33))
z0_1 = 0.021*(u_star)^3.32
z0_2 = 0.00098*(u_star)^1.65
z0 = ifelse(u_star<= 0.16, z0_1, z0_2)
L = replicate(10000,runif(100,45,55))
kin.vis = ((9*10^-8)*Temp)+10^-5
dyn.vis = ((5*10^-8)*Temp)+4*10^-6
d_air = 3.7208*10^-10
k_B = 1.38*10^-23
P = 101325
lambda = (k_B*Temp)/(sqrt(2)*3.1416*P*d_air^2)
C = 1+((2*lambda/dp)*(1.257+0.4*exp(-0.55*dp/lambda)))
tau_p = (rho*(dp)^2*C)/(18*dyn.vis)
D = (C*k_B*Temp)/(3*3.1416*dyn.vis*dp)
v_s = 9.81*tau_p
taup = (tau_p*u_star^2)/(kin.vis)
Sc = (kin.vis/D)
vsplus = v_s/u_star
rplus = (dp*u_star)/(2*kin.vis)
R_s = 0
Rsplus = u_star*R_s
z_meas = 8/100
zpmax = (z_meas*u_star)/(kin.vis)
MOplus = (kin.vis)/(u_star*L)
#Fixed parameters
Zbuf = 3
Ztf = 18                              #turbophoretic sublayer height
taultf = 5                            #Lagrangian time in turbophoretic layer
Nutp_Ztf= (0.4*(Ztf)^3)/(Ztf^2+200)  #Dimensionless eddy viscosity of air
It_Ztf = (2.5*log10(Ztf ))-(100/Ztf^2)
It_Zbuf = (2.5*log10(Zbuf))-(100/Zbuf^2)
S = Sc^(1/3)
Zl = 20/S
fTmp = 2.5/Sc
fTmp1 = (fTmp^3/27+(fTmp*(100+5*sqrt(8*fTmp/27)+400)))^(1/3)
Zl_1 = fTmp1+((fTmp*fTmp)/(9*fTmp1))+(1/3)*fTmp
fTmp_1 = (Zl_1^2)/(Zl_1^2+200)
fTmp_2 = 1.2*(fTmp_1)-0.8*fTmp_1^2
fTmp1_1 = 1/(Sc*fTmp_2)
fTmp_3 = 1/Sc
x_1 = Zl_1 - fTmp1_1
x_2 = Zl_1
x_3 = Zl_1+fTmp1_1
Nutp_x_1 = (0.4*x_1^3)/(x_1^2+200)
Nutp_x_2 = (0.4*x_2^3)/(x_2^2+200)
Nutp_x_3 = (0.4*x_3^3)/(x_3^2+200)
fIvd = Rsplus+(Zl_1-
fTmp1_1)*Sc+0.3333*fTmp1_1*(1/fTmp_3+((0.4*x_1^3)/(x_1^2+200)))+4/(fTmp_3+((0.4*x_2^3)/(x_2^2+200)))+1/(fTmp_3+(
(0.4*x_3^3)/(x_3^2+200)))
x_4 = zpmax
x_5 = Zl_1 + fTmp1_1
It_x_4 = 2.5*log10(x_4) - 100/(x_4^2)
It_x_5 = 2.5*log10(x_5) - 100/(x_5^2)
#Now calculate fu_Psi(zpmax*MOplus)
s = 2.35*(zpmax*MOplus+abs(zpmax*MOplus))
u1 = 0.5*(abs(zpmax*MOplus)-zpmax*MOplus)
u = -4*u1/(2.65*sqrt(u1*sqrt(u1))+1)
fu_Psi = s+u
fTmp_4 = It_x_4 - It_x_5 + 2.5*fu_Psi
fIvd_1 = fIvd+0.5*(fTmp_4+abs(fTmp_4))
fu_vdplus_smooth_1 = 1/fIvd_1
Il_input1= Zl*S/7.92
Il_input2= rplus*S/7.92
Il_1 = -0.16667*log10(Il_input1^2-Il_input1+1)+0.57735*atan((2*Il_input1-1)*0.57735)+0.3333*log10(Il_input1+1)
Il_2 = -0.16667*log10(Il_input2^2-Il_input2+1)+0.57735*atan((2*Il_input2-1)*0.57735)+0.3333*log10(Il_input2+1)
R = 7.92*S^2*(Il_1-Il_2)
R_1 = 0.5*(R+abs(R))
Zl_2 = 0.5*(rplus+Zl+abs(rplus-Zl))
It_Zbuf = 2.5*log10(Zbuf) - (100/(Zbuf^2))
It_Zl_2 = 2.5*log10(Zl_2) - (100/(Zl_2^2))
```

```
R1 = It_Zbuf - It_Zl_2
R_2 = R_1+0.5*(R1+abs(R1))
fTmp_5 = vsplus*R_2
fTmp_6 = exp(-fTmp_5)
fIvd_2  = Rsplus*fTmp_6+(1-fTmp_6)/vsplus
fIvd_3 = Rsplus+R_2
fIvd_23 = ifelse(abs(fTmp_5)>0.001, fIvd_2, fIvd_3 )
V  = 0.81*taup/(Ztf-Zbuf)/(1+taup/taultf) + vsplus   #chcek for sign of vsplus
It_Ztf = 2.5*log10(Ztf) - 100/(Ztf^2)
R_3  = ((It_Ztf)-(It_Zbuf))*(1+taup/taultf)
fTmp_7 = V*R_3
fTmp_8 = exp(-fTmp_7)
fIvd_4 = (fIvd_23*fTmp_8)+(1-fTmp_8)/V
fIvd_5 = fIvd_3+R_3
fIvd_45 = ifelse(abs(fTmp_7)>0.001, fIvd_4, fIvd_5)
#Now calculations for the Lagrangian turbophoretic layer
Ztf2 = 2*taup
V_1 = 0.4+vsplus
R_4 =
0.1667*((1+taup/(0.5*Ztf))/(Nutp_Ztf)+4*(1+taup/(0.25*(Ztf+Ztf2)))/((0.4*(0.5*(Ztf+Ztf2))^3)/((0.5*(Ztf+Ztf2))^2
+200))+(1+taup/(0.5*Ztf2))/((0.4*Ztf2 ^3)/(Ztf2^2+200)))*(Ztf2-Ztf)
fTmp_9 = V_1*R_4
fTmp_10 = exp(-fTmp_9)
fIvd_6 = fIvd_45*fTmp_10 + (1-fTmp_10)/V_1
fIvd_7 = fIvd_45+R_3
fIvd_67 = ifelse(abs(fTmp_9) > 0.001, fIvd_6, fIvd_7)
Ztf2_2 = Ztf
fIvd67_Ztf2 = ifelse(Ztf2>Ztf, fIvd_67, Ztf2_2)
#Following calculations are for aerodynamic layer
It_zpmax = 2.5*log10(zpmax) - 100/(zpmax^2)
Ztf22 = ifelse(Ztf2>Ztf, Ztf2, Ztf2_2)
It_Ztf22  = 2.5*log10(Ztf22) - 100/(Ztf22^2)
R_5 = It_zpmax - It_Ztf22  + 2.5*fu_Psi
R_6 = 0.5*(R_5+abs(R_5))
fTmp_11  = vsplus*R_6
fTmp_12 = exp(-fTmp_11)
fIvd_4567 = ifelse(Ztf2>Ztf, fIvd_67,fIvd_45)
fIvd_8 = (fIvd_4567* fTmp_12)+(1-fTmp_12)/vsplus
fIvd_9 = fIvd_4567 + R_6
fIvd_10 = ifelse(abs(fTmp_11) > 0.001, fIvd_8, fIvd_9)
fu_vdplus_smooth_3 = 1/fIvd_10
fu_vdplus_smooth = ifelse(Zl>Zbuf, fu_vdplus_smooth_1, fu_vdplus_smooth_3)
Vd_smooth = fu_vdplus_smooth*u_star
quantile(Vd_smooth, c(.05, 0.10, .50, 0.95))


#Dry deposition parameterization by Kouznetsov and Sofiev (2012)
#Uncertainty test: Ice/snow
set.seed(5)
C1 = 0.2789
C2 = 3.115
C3 = 5.415*10^-11
C4 = -1.399
RH = replicate(10000,runif(100,0.76,0.84))
dp_a = 2.0
dp_i = dp_a*10^-6
rd = dp_i/2
r_w = {(C1*rd^C2)/(C3*rd^C4-log10(RH))+rd^3}^(1/3)
dp = r_w*2
#Correction factor, C
k_B = 1.38*10^-23
Temp = 273.15+0
P = 101325
d_air = 3.7208*10^-10
lambda = (k_B*Temp)/(sqrt(2)*3.1416*P*d_air^2)
C = 1+(2*lambda/dp)*(1.257+0.4*exp(-0.55*dp/lambda))
dyn.vis = ((5*10^-8)*Temp)+4*10^-6
rho =  1500
Tau = (rho*(dp)^2*C)/(18*dyn.vis)
V_s = Tau*9.81
# Need to compute Sc, Re_star
u_star = replicate(10000,runif(100,0.27,0.33))
#u_star = replicate(10000,runif(100,0.27,0.33))
a  =  0.5*10^-3
```

```
kin.vis = ((9*10^-8)*Temp)+10^-5
D = (C*k_B*Temp)/(3*3.1416*dyn.vis*dp)
Sc = (kin.vis/D)
Re_star = (u_star*a)/kin.vis
# Compute V_diff (velocity for diffusion)
V_diff = 2*(Re_star^(-0.5))*Sc^(-2/3)
# Compute V_int (velocity for interception)
V_int = 80*u_star*((dp/a)^2)*(Re_star^(0.5))
# Compute V_imp
C_S = 0.003
C_R = 0.3
LAI = 0
CsCR = (C_S+C_R/LAI)^0.5
u.Uh = 0.3
u_star.by.U_h = min(u.Uh, CsCR)
#Compute Re_c
Re_c = ((u_star.by.U_h)^-1)^2*Re_star
# Calculate St
St = (Tau*u_star)/a
# Calculate St_e
St_e = St - Re_c^(-0.5)
eta_impSt.e1 = exp((-0.1/(St_e - 0.15 ) )-(1/sqrt(St_e -0.15)))
eta_impSt.e2 = 0
eta_impSt.e = ifelse(St_e>0.15,eta_impSt.e1,eta_impSt.e2)
V_imp = (2*u_star.by.U_h*eta_impSt.e*(St-(u_star.by.U_h*Re_star^-0.5)))*u_star
# Dry deposition velocity
Vd = V_diff+V_int+V_imp+V_s
quantile(Vd, c(.05, 0.10, .50, 0.95))
```

Codes for Monte Carlo uncertainty evaluation for Zhang and He (2014) parameterization

```
#Dry deposition parameterization by Zhang and He (2014)
#Uncertainty test: Grass
set.seed(5)
C1 = 0.2789
C2 = 3.115
C3 = 5.145*10^-11
C4 = -1.399
RH = replicate(10000,runif(100,0.76,0.84))
dp_a = 2.0
dp_i = dp_a*10^-6
rd = dp_i/2
r_w = {(C1*rd^C2)/(C3*rd^C4-log10(RH))+rd^3}^(1/3)
dp = r_w*2
#Correction factor, C
k_B = 1.38*10^-23
Temp = (273.15+25)
P = 101325
d_air = 3.7208*10^-10
lambda = (k_B*Temp)/(sqrt(2)*3.1416*P*d_air^2)
C = 1+(2*lambda/dp)*(1.257+0.4*exp(-0.55*dp/lambda))
dyn.vis = 1.89*10^-5
rho = 1500
Tau = (rho*(dp)^2*C)/(18*dyn.vis)
V_g = Tau*9.81
Rg = 1/V_g
u_star = replicate(10000,runif(100,0.27,0.33))
a1 = 5.4*10^-3
z = 5
L = replicate(10000,runif(100,45,55))
x = z/L
# Compute stability function (shi_H)
shi_H.1 = 2*log(0.5*{1+(1-16*x)^0.5})
shi_H.2 = -5*x
shi_H =ifelse(x <= 0, shi_H.1 , shi_H.2)
zR = 3.5
z0 = replicate(10000,runif(100,0.03,0.05))
k_c = 0.41
Ra = (log(zR/z0)-shi_H)/(k_c*u_star)
# Calculate Vds = 1/Rs
# For PM2.5
Vds_PM2.5 = (a1*u_star)
Rds_PM2.5 = (1/Vds_PM2.5)
```

```
#For PM2.5-10
#b1=
#b2=
#b3 =
#c1=
#c2 =
#c3 =
#k = c1*u_star+c2*u_star^2+c3*u_star^3
#LAI = replicate(10000,runif(100,3.8,4.2))
#LAImax =
#Vds_PM10 = (b1*u_star+b2*u_star^2+b3*u_star^3)*exp(k*(LAI/LAImax)-1)
#Vds_PM10 = (b1*u_star+b2*u_star^2+b3*u_star^3)
#Rds_PM10 = 1/Vds_PM10
# For PM10+
#d1=
#d2=
#d3 =
#f1=
#f2 =
#f3 =
#k = f1*u_star+f2*u_star^2+f3*u_star^3
#LAI =
#LAImax =
#Vds_10plus = (d1*u_star+d2*u_star^2+d3*u_star^3)*exp(k*(LAI/LAImax)-1)
#Vds_10plus = (d1*u_star+d2*u_star^2+d3*u_star^3)
#Rds_PM2.5 = (1/Vds_PM2.5)
#Compute Vd
Vd = 1/Rg+(1/(Ra+Rds_PM2.5))
quantile(Vd, c(.05, 0.10, .50, 0.95))


#Dry deposition parameterization by Zhang and He (2014)
#Uncertainty test: Coniferous forest
set.seed(5)
C1 = 0.2789
C2 = 3.115
C3 = 5.145*10^-11
C4 = -1.399
RH = replicate(10000,runif(100,0.76,0.84))
dp_a = 2.0
dp_i = dp_a*10^-6
rd = dp_i/2
r_w = {(C1*rd^C2)/(C3*rd^C4-log10(RH))+rd^3}^(1/3)
dp = r_w*2
#Correction factor, C
k_B = 1.38*10^-23
Temp = (273.15+25)
P = 101325
d_air = 3.7208*10^-10
lambda = (k_B*Temp)/(sqrt(2)*3.1416*P*d_air^2)
C = 1+(2*lambda/dp)*(1.257+0.4*exp(-0.55*dp/lambda))
dyn.vis = 1.89*10^-5
rho = 1500
Tau = (rho*(dp)^2*C)/(18*dyn.vis)
V_g = Tau*9.81
Rg = 1/V_g
u_star = replicate(10000,runif(100,0.27,0.33))
a1 = 4.3*10^-3
z = 35
L = replicate(10000,runif(100,45,55))
x = z/L
# Compute stability function (shi_H)
shi_H.1 = 2*log(0.5*{1+(1-16*x)^0.5})
shi_H.2 = -5*x
shi_H =ifelse(x <= 0, shi_H.1 , shi_H.2)
zR = 30
z0 = replicate(10000,runif(100,0.9,1.5))
k_c = 0.41
Ra = (log(zR/z0)-shi_H)/(k_c*u_star)
# Calculate Vds = 1/Rs
# For PM2.5
Vds_PM2.5 = (a1*u_star)
Rds_PM2.5 = (1/Vds_PM2.5)
#For PM2.5-10
```

```
#b1=
#b2=
#b3 =
#c1=
#c2 =
#c3 =
#k = c1*u_star+c2*u_star^2+c3*u_star^3
#LAI =
#LAImax =
#Vds_PM10 =
(b1*u_star+b2*u_star^2+b3*u_star^3)*exp(k*(LAI/LAImax)-
1)
#Vds_PM10 = (b1*u_star+b2*u_star^2+b3*u_star^3)
#Rds_PM10 = 1/Vds_PM10
# For PM10+
#d1=
#d2=
#d3 =
#f1=
#f2 =
#f3 =
#k = f1*u_star+f2*u_star^2+f3*u_star^3
#LAI =
#LAImax =
#Vds_10plus =
(d1*u_star+d2*u_star^2+d3*u_star^3)*exp(k*(LAI/LAImax)-
1)
#Vds_10plus = (d1*u_star+d2*u_star^2+d3*u_star^3)
Rds_PM10plus = (1/Vds_PM2.5)
#Compute Vd
Vd = 1/Rg+(1/(Ra+Rds_PM2.5))
quantile(Vd, c(.05, 0.10, .50, 0.95))


#Dry deposition parameterization by Zhang and He (2014)
#Uncertainty test: Deciduous forest
set.seed(5)
C1 = 0.2789
C2 = 3.115
C3 = 5.145*10^-11
C4 = -1.399
RH = replicate(10000,runif(100,0.76,0.84))
dp_a = 2.0
dp_i = dp_a*10^-6
rd = dp_i/2
r_w = {(C1*rd^C2)/(C3*rd^C4-log10(RH))+rd^3}^(1/3)
dp = r_w*2
#Correction factor, C
k_B = 1.38*10^-23
Temp = (273.15+25)
P = 101325
d_air = 3.7208*10^-10
lambda = (k_B*Temp)/(sqrt(2)*3.1416*P*d_air^2)
C = 1+(2*lambda/dp)*(1.257+0.4*exp(-0.55*dp/lambda))
dyn.vis = 1.89*10^-5
rho = 1500
Tau = (rho*(dp)^2*C)/(18*dyn.vis)
V_g = Tau*9.81 # m/s
Rg = 1/V_g
u_star = replicate(10000,runif(100,0.54,0.66))
a1 = 4.3*10^-3
z = 35
L = replicate(10000,runif(100,45,55))
x = z/L
# Compute stability function (shi_H)
shi_H.1 = 2*log(0.5*{1+(1-16*x)^0.5})
shi_H.2 = -5*x
shi_H =ifelse(x <= 0, shi_H.1 , shi_H.2)
zR = 50
z0 = replicate(10000,runif(100,1.125, 1.875))
k_c = 0.41
Ra = (log(zR/z0)-shi_H)/(k_c*u_star)
#Calculate Vds = 1/Rs
# For PM2.5
```

```
Vds_PM2.5 = (a1*u_star)
Rds_PM2.5 = (1/Vds_PM2.5)
# For PM2.5-10
#b1=
#b2=
#b3 =
#c1=
#c2 =
#c3 =
#k = c1*u_star+c2*u_star^2+c3*u_star^3
#LAI =
#LAImax =
#Vds_PM10 =
(b1*u_star+b2*u_star^2+b3*u_star^3)*exp(k*(LAI/LAImax)-
1)
#Rds_PM10 = 1/Vds_PM10
# For PM10+
#d1= -2.2
#d2= 3.9*10^1
#d3 = -6.7
#f1= 6.2
#f2 = -1.2*10^1
#f3 = 6.1
#k = f1*u_star+f2*u_star^2+f3*u_star^3
#LAI =
#LAImax =
#Vds_10plus =
(d1*u_star+d2*u_star^2+d3*u_star^3)*exp(k*(LAI/LAImax)-
1)
#Rds_10plus = (1/Vds_10plus)
#Compute Vd
Vd = 1/Rg+(1/(Ra+Rds_PM2.5))
quantile(Vd, c(.05, 0.10, .50, 0.95))


#Dry deposition parameterization by Zhang and He (2014)
#Uncertainty test: Water
set.seed(5)
C1 = 0.2789
C2 = 3.115
C3 = 5.415*10^-11
C4 = -1.399
RH = replicate(10000,runif(100,0.76,0.84))
dp_a =2.0
dp_i = dp_a*10^-6
rd = dp_i/2
r_w = {(C1*rd^C2)/(C3*rd^C4-log10(RH))+rd^3}^(1/3)
dp = r_w*2
#Correction factor, C
k_B = 1.38*10^-23
Temp = 273.15+25
P = 101325
d_air = 3.7208*10^-10
lambda = (k_B*Temp)/(sqrt(2)*3.1416*P*d_air^2)
C = 1+(2*lambda/dp)*(1.257+0.4*exp(-0.55*dp/lambda))
dyn.vis = ((5*10^-8)*Temp)+4*10^-6
rho = 1500
Tau = (rho*(dp)^2*C)/(18*dyn.vis)
V_g = Tau*9.81
Rg = 1/V_g
a1 = 6.9*10^-3
z = 8/100
L = replicate(10000,runif(100,45,55))
x = z/L
# Compute stability function (shi_H)
shi_H.1 = 2*log(0.5*{1+(1-16*x)^0.5})
shi_H.2 = -5*x
shi_H =ifelse(x <= 0, shi_H.1 , shi_H.2)
zR = 5
u_star = replicate(10000,runif(100,0.27,0.33))
z0_1 = 0.021*(u_star)^3.32
z0_2 = 0.00098*(u_star)^1.65
z0 = ifelse(u_star<= 0.16, z0_1, z0_2)
k_c = 0.41
```

```
Ra = (log(zR/z0)-shi_H)/(k_c*u_star)
# Calculate Vds = 1/Rs
#For PM2.5
Vds_PM2.5 = (a1*u_star)
Rds_PM2.5 = (1/Vds_PM2.5)
# For PM2.5-10
#b1= 2.6*10^-1
#b2= -1.3*10^0
#b3 = 3.0*10^0
#c1= 1.8
#c2 = -2.0*10^-1
#c3 = -5.3*10^-1
#k = c1*u_star+c2*u_star^2+c3*u_star^3
#LAI =
#LAImax =
#Vds_PM10 =
(b1*u_star+b2*u_star^2+b3*u_star^3)*exp(k*(LAI/LAImax)-
1)
#Rds_PM10 = 1/Vds_PM10
#For PM10+
#d1= -
#d2=
#d3 =
#f1=
#f2 =
#f3 =
#k = f1*u_star+f2*u_star^2+f3*u_star^3
#LAI =
#LAImax =
#Vds_PM10Plus =
(d1*u_star+d2*u_star^2+d3*u_star^3)*exp(k*(LAI/LAImax)-
1)
#Rds_PM10Plus = (1/Vds_PM10Plus)
#Compute Vd
Vd = 1/Rg+(1/(Ra+Rds_PM2.5))
quantile(Vd, c(.05, 0.10, .50, 0.95))


#Dry deposition parameterization by Zhang and He (2014)
#Uncertainty test: Ice/Water
set.seed(5)
C1 = 0.2789
C2 = 3.115
C3 = 5.415*10^-11
C4 = -1.399
RH = replicate(10000,runif(100,0.76,0.84))
dp_a = 2.0
dp_i = dp_a*10^-6
rd = dp_i/2
r_w = {(C1*rd^C2)/(C3*rd^C4-log10(RH))+rd^3}^(1/3)
dp = r_w*2
#Correction factor, C
k_B = 1.38*10^-23
Temp = 273.15+0
P = 101325
d_air = 3.7208*10^-10
lambda = (k_B*Temp)/(sqrt(2)*3.1416*P*d_air^2)
C = 1+(2*lambda/dp)*(1.257+0.4*exp(-0.55*dp/lambda))
dyn.vis = ((5*10^-8)*Temp)+4*10^-6
rho = 1500
Tau = (rho*(dp)^2*C)/(18*dyn.vis)
V_g = Tau*9.81
Rg = 1/V_g
a1 = 4.3*10^-3
z = 5
L = replicate(10000,runif(100,45,55))
x = z/L
# Compute stability function (shi_H)
shi_H.1 = 2*log(0.5*{1+(1-16*x)^0.5})
shi_H.2 = -5*x
shi_H =ifelse(x <= 0, shi_H.1 , shi_H.2)
zR = 10
u_star = replicate(10000,runif(100,0.27,0.33))
z0 = replicate(10000,runif(100,0.0075,0.0125))
```

```
k_c = 0.41
Ra = (log(zR/z0)-shi_H)/(k_c*u_star)
# Calculate Vds = 1/Rs#For PM2.5
Vds_PM2.5 = (a1*u_star)
Rds_PM2.5 = (1/Vds_PM2.5)
# For PM2.5-10
#b1=
#b2=
#b3 =
#c1=
#c2 =
#c3 =
#k = c1*u_star+c2*u_star^2+c3*u_star^3
#LAI =
# LAImax =
#Vds_PM10 = (b1*u_star+b2*u_star^2+b3*u_star^3)*exp(k*(LAI/LAImax)-1)
#Rds_PM10 = 1/Vds_PM10
# For PM10+
#d1=
#d2=
#d3 =
#f1=
#f2 =
#f3 =
#k = f1*u_star+f2*u_star^2+f3*u_star^3
#LAI =
#LAImax =
#Vds_PM10Plus = (d1*u_star+d2*u_star^2+d3*u_star^3)*exp(k*(LAI/LAImax)-1)
#Rds_PM10Plus = (1/Vds_PM10Plus)
#Compute Vd
Vd = 1/Rg+(1/(Ra+Rds_PM2.5))
quantile(Vd, c(.05, 0.10, .50, 0.95))
```

Codes for Monte Carlo uncertainty evaluation for Zhang and Sao (2014) parameterization

```
#Dry deposition parameterization by Zhang and Sao (2014)
#Uncertainty test: Plant (Grass, coniferous, and deciduous forests)
set.seed(5)
C1 = 0.2789
C2 = 3.115
C3 = 5.145*10^-11
C4 = -1.399
RH = replicate(10000,runif(100,0.76,0.84))
dp_a = 2.0
dp_i = dp_a*10^-6
rd = dp_i/2
r_w = {(C1*rd^C2)/(C3*rd^C4-log10(RH))+rd^3}^(1/3)
dp = r_w*2
#Correction factor, C
k_B = 1.38*10^-23
Temp = (273.15+15)
P = 101325
d_air = 3.7208*10^-10
lambda = (k_B*Temp)/(sqrt(2)*3.1416*P*d_air^2)
C = 1+(2*lambda/dp)*(1.257+0.4*exp(-0.55*dp/lambda))
dyn.vis = 1.841*10^-5
rho = 1500
Tau = (rho*(dp_i)^2*C)/(18*dyn.vis)
Tau_wet = (rho*(dp)^2*C)/(18*dyn.vis)
Wt = Tau*9.81
Vg = Wt
Vg_wet = Tau_wet*9.81
u_star = replicate(10000,runif(100,0.27,0.33))
k =  0.41
z =  1
zd = 0.20
h_c = 0.23
z0 = replicate(10000,runif(100,0.0015, 0.0025))
B1 = 0.45
Sc_T = (1+(Vg^2/u_star^2))^0.5
Ra = (Sc_T/(k*u_star))*(log((z-zd)/(h_c-zd)))
Rg = 1/Vg
U_h = replicate(10000,runif(100,3.88,4.12))
```

```
kin.vis = 1.593*10^-5
d_c = 0.005
D = (C*k_B*Temp)/(3*3.1416*dyn.vis*dp)
Sc = (kin.vis/D)
Re_h = (U_h*d_c)/(kin.vis)
nB = 0.5
C_B = 0.467
E_B = C_B*Sc^(-2/3)*Re_h^(nB-1)
#Compute impaction collection efficiency (E_IM)
beta_IM = 0.6
St_h = (Tau*u_star)/d_c
E_IM = (St_h/(St_h+beta_IM))^2
#Compute interception efficiency (E_IN)
Ain = 150
E_IN = Ain*u_star*(10^(-St_h))*(2*dp/d_c)
#Compute R
b = 2
R = exp(-b*sqrt(St_h))
#Compute w_dm
B2 = 3
w_dm = (u_star/U_h*h_c)       #For rough surface
#compute Tau_c/Tau (ratio of stress)
Beta = 200
C1 = 6
C2 = 0.1
lambda_FAI = 0.4
n_FAI = (lambda_FAI)/(h_c*d_c)
q = (3.1416*d_c^2)/4
eta_BAI = n_FAI*q
lambda_FAIe = ((lambda_FAI)/(1-eta_BAI)^C2)*exp((-C1*lambda_FAI)/(1-eta_BAI)^C2)
Tau_c_BY_Tau = (Beta*lambda_FAIe)/(1+Beta*lambda_FAIe)
#Compute Rs
E = E_B+E_IM+E_IN
Tau_wetplus = (Tau_wet*u_star^2)/kin.vis
Cd = 1/6
Rs = (R*w_dm*((E*Tau_c_BY_Tau/Cd)+(1+Tau_c_BY_Tau)*Sc^-1+10^(-3/Tau_wetplus))+Vg_wet)^-1
#Compute Vd
Vd = (Rg+((Rs-Rg)/exp(Ra/Rg)))^-1
quantile(Vd, c(.05, 0.10, .50, 0.95))


#Dry deposition parameterization by Zhang and Sao (2014)
#Uncertainty test: Water
set.seed(5)
C1 = 0.2789
C2 = 3.115
C3 = 5.415*10^-11
C4 = -1.399
RH = replicate(10000,runif(100,0.76,0.84))
dp_a = 2.0
dp_i = dp_a*10^-6
rd = dp_i/2
r_w = {(C1*rd^C2)/(C3*rd^C4-log10(RH))+rd^3}^(1/3)
dp = r_w*2
#Correction factor, C
k_B = 1.38*10^-23
Temp = 273.15+25
P = 101325
d_air = 3.7208*10^-10
lambda = (k_B*Temp)/(sqrt(2)*3.1416*P*d_air^2)
C = 1+(2*lambda/dp)*(1.257+0.4*exp(-0.55*dp/lambda))
dyn.vis = ((5*10^-8)*Temp)+4*10^-6
rho = 1500
Tau = (rho*(dp_i)^2*C)/(18*dyn.vis)
Tau_wet = (rho*(dp)^2*C)/(18*dyn.vis)
Wt = Tau*9.81
Vg = Wt
Vg_wet = Tau_wet*9.81
u_star = replicate(10000,runif(100,0.27,0.33))
k =  0.41
z0 = 0.3/1000
z = 8/100
U_h = replicate(10000,runif(100,4.85,5.15))
zd = 0
```

```
h_c = 30*z0
B1 = 0.45
Sc_T = (1+(Vg^2/u_star^2))^0.5
Ra = (B1*Sc_T/k*u_star)*log(z/z0)          # For smooth surface
Rg = 1/Vg
# Calculate surface resistance (Rs)
kin.vis = ((9*10^-8)*Temp)+10^-5
d_c = 0.005
D = (C*k_B*Temp)/(3*3.1416*dyn.vis*dp)
Sc = (kin.vis/D)
Re_h = (U_h*d_c)/(kin.vis)
nB = 0.5
C_B = 0.467
E_B = C_B*Sc^(-2/3)*Re_h^(nB-1)
#Compute impaction collection efficiency (E_IM)
beta_IM = 0.6
St_h = (Tau*u_star)/d_c
E_IM = (St_h/(St_h+beta_IM))^2
#Compute interception efficiency (E_IN)
Ain = 100
E_IN = Ain*u_star*(10^(-St_h))*(2*dp/d_c)
#Compute R
b = 2
R = exp(-b*sqrt(St_h))
#Compute w_dm
B2 = 3
w_dm = B2*u_star                           #For smooth surface
#compute Tau_c/Tau (ratio of stress)
Beta = 200
C_1 = 6
C_2 = 0.1
lambda_FAI = 0.538
n_FAI = (lambda_FAI)/(h_c*d_c)
q = (3.1416*d_c^2)/4
eta_BAI = n_FAI*q
lambda_FAIe = ((lambda_FAI)/(1-eta_BAI)^C_2)*exp((-C_1*lambda_FAI)/(1-eta_BAI)^C_2)
Tau_c_BY_Tau = (Beta*lambda_FAIe)/(1+Beta*lambda_FAIe)
#Compute Rs
E = E_B+E_IM+E_IN
Tau_wetplus = (Tau_wet*u_star^2)/kin.vis
Cd = 1/6
Rs = (R*w_dm*((E*Tau_c_BY_Tau/Cd)+(1+Tau_c_BY_Tau)*Sc^-1+10^(-3/Tau_wetplus))+Vg_wet)^-1
#Compute Vd
Vd = (Rg+((Rs-Rg)/exp(Ra/Rg)))^-1
quantile(Vd, c(.05, 0.10, .50, 0.95))
```

Codes for Sobol' sensitivity test for Zhang et al. (2001) parameterization

```
#Dry deposition parameterization by Zhang et al. (2001)
#Sobol sensitivity test: Grass (the code is similar for other LUCs)
#Change LUC dependent parameters for other LUCs
#Change sensitivity ranges for other LUCs
set.seed(5)
library(sensitivity)
library(boot)
C1 = 0.2789
C2 = 3.115
C3 = 5.415*10^-11
C4 = -1.399
dp_i = 10
dp_d = dp_i*10^-6
rd = dp_d/2
k_B = 1.38*10^-23
Temp = 273.15+25
P = 101325
d_air = 3.72*10^-10
lambda = (k_B*Temp)/(sqrt(2)*3.1416*P*d_air^2)
dyn.vis = ((5*10^-8)*Temp)+4*10^-6
z = 2
zR = 3.5
k_c = 0.41
e_0 = 3
R1 = 1
```

```
kin.vis = ((9*10^-8)*Temp)+10^-5
gamma = 0.54
alpha = 1.2
beta =  2
A = 2/1000
model <- function (X) ((((X[,2])*(2*{(C1*rd^C2)/(C3*rd^C4-
log10(X[,1]))+rd^3}^(1/3))^2*9.81*(1+(2*lambda/(2*{(C1*rd^C2)/(C3*rd^C4-
log10(X[,1]))+rd^3}^(1/3)))*(1.257+0.4*exp(-0.55*((2*{(C1*rd^C2)/(C3*rd^C4-
log10(X[,1]))+rd^3}^(1/3)))/lambda))))/(18*dyn.vis)))+
  (1/((((log(zR/(X[,4]))+5*z/(X[,3]))/(k_c*(X[,5])))+
        (1/{(e_0*(X[,5]))*
              ((((kin.vis/(((1+(2*lambda/(2*{(C1*rd^C2)/(C3*rd^C4-log10(X[,1]))+rd^3}^(1/3)))*(1.257+0.4*exp(-
0.55*(2*{(C1*rd^C2)/(C3*rd^C4-
log10(X[,1]))+rd^3}^(1/3))/lambda)))*k_B*Temp)/(3*3.1416*dyn.vis*(2*{(C1*rd^C2)/(C3*rd^C4-
log10(X[,1]))+rd^3}^(1/3))))))^(-gamma))+
                 ({{{{{(X[,2])*(2*{(C1*rd^C2)/(C3*rd^C4-
log10(X[,1]))+rd^3}^(1/3))^2*9.81*(1+(2*lambda/(2*{(C1*rd^C2)/(C3*rd^C4-
log10(X[,1]))+rd^3}^(1/3)))*(1.257+0.4*exp(-0.55*((2*{(C1*rd^C2)/(C3*rd^C4-
log10(X[,1]))+rd^3}^(1/3)))/lambda))))/(18*dyn.vis))*(X[,5]))/(9.81*A))/(alpha+(((((X[,2])*(2*{(C1*rd^C2)/(C3*rd^C
4-log10(X[,1]))+rd^3}^(1/3))^2*9.81*(1+(2*lambda/(2*{(C1*rd^C2)/(C3*rd^C4-
log10(X[,1]))+rd^3}^(1/3)))*(1.257+0.4*exp(-0.55*((2*{(C1*rd^C2)/(C3*rd^C4-
log10(X[,1]))+rd^3}^(1/3)))/lambda))))/(18*dyn.vis))*(X[,5]))/(9.81*A)))}^beta)+
                 (0.5*((2*{(C1*rd^C2)/(C3*rd^C4-log10(X[,1]))+rd^3}^(1/3))/A)^2))*R1})))


N <- 100000
x1 = runif(1*N,0.1,1.0)           #RH
x2 = runif(1*N,1500,2000)         #rho
x3 = runif(1*N,10,100)            #L
x4 = runif(1*N,0.02,0.10)         #z0
x5 = runif(1*N,0.1,0.5)           #u_star
x_1 = runif(1*N,0.1,1.0)          #RH
x_2 = runif(1*N,1500,2000)        #rho
x_3 = runif(1*N,10,100)           #L
x_4 = runif(1*N,0.02,0.10)        #z0
x_5 = runif(1*N,0.1,0.5)          #u_star
Y1 = matrix(c(x1,x2,x3,x4,x5), nrow=N)
X1 = data.frame(matrix(Y1,nrow=N))
Y2 = matrix(c(x_1,x_2,x_3,x_4,x_5), nrow=N)
X2 = data.frame(matrix(Y2, nrow=N))
a = sobol2007(model = model, X1 = X1, X2= X2, nboot = 2000, conf = 0.95);a
```

Codes for Sobol' sensitivity test for the Petroff and Zhang (2010) parameterization

```
#Dry deposition parameterization by Petroff and Zhang (2010)
#Sobol sensitivity test: Grass (the code is similar for other LUCs)
#Change LUC dependent parameters for other LUCs
#Change sensitivity ranges for other LUCs
set.seed(5)
library(sensitivity)
library(boot)
C1 = 0.2789
C2 = 3.115
C3 = 5.415*10^-11
C4 = -1.399
dp_i = 10
dp_d = dp_i*10^-6
rd = dp_d/2
k_B = 1.38*10^-23
Temp = 273.15+25
P = 101325
d_air = 3.7208*10^-10
lambda = (k_B*Temp)/(sqrt(2)*3.1416*P*d_air^2)
dyn.vis = ((5*10^-8)*Temp)+4*10^-6
kin.vis = ((9*10^-8)*Temp)+10^-5
Vphor = 0
z = 2
zR = 3.5
k_c = 0.41
cd = 1/6
kx = 0.216
C_IT = 0.056
L_obs = 0.01
```

```
C_B = 0.996
C_IN = 0.162
C_IM = 0.081
beta_IM = 0.47


model <- function (X) ((((((X[,2])*(2*({{(C1*rd^C2)/(C3*rd^C4-
log10(X[,1]))+rd^3}^(1/3)))^2*(1+(2*lambda/(2*({{(C1*rd^C2)/(C3*rd^C4-log10(X[,1]))+rd^3}^(1/3))))*(1.257+0.4*exp(-
0.55*(2*({{(C1*rd^C2)/(C3*rd^C4-
log10(X[,1]))+rd^3}^(1/3)))/lambda))))/(18*dyn.vis))*9.81)+Vphor)+1/(((log(zR/(X[,4]))+(5*(z/(X[,3])))))/(k_c*(X[,5
]))+1/((X[,5])*(((((kin.vis/(((1+(2*lambda/(2*({{(C1*rd^C2)/(C3*rd^C4-
log10(X[,1]))+rd^3}^(1/3))))*(1.257+0.4*exp(-0.55*(2*({{(C1*rd^C2)/(C3*rd^C4-
log10(X[,1]))+rd^3}^(1/3)))/lambda)))*k_B*Temp)/(3*3.1416*dyn.vis*(2*({{(C1*rd^C2)/(C3*rd^C4-
log10(X[,1]))+rd^3}^(1/3)))))))^(-2/3)/14.5)*{1/6*log(1+((((kin.vis/(((1+(2*lambda/(2*({{(C1*rd^C2)/(C3*rd^C4-
log10(X[,1]))+rd^3}^(1/3))))*(1.257+0.4*exp(-0.55*(2*({{(C1*rd^C2)/(C3*rd^C4-
log10(X[,1]))+rd^3}^(1/3)))/lambda)))*k_B*Temp)/(3*3.1416*dyn.vis*(2*({{(C1*rd^C2)/(C3*rd^C4-
log10(X[,1]))+rd^3}^(1/3)))))))^(1/3))/2.9))^2/(1-((((kin.vis/(((1+(2*lambda/(2*({{(C1*rd^C2)/(C3*rd^C4-
log10(X[,1]))+rd^3}^(1/3))))*(1.257+0.4*exp(-0.55*(2*({{(C1*rd^C2)/(C3*rd^C4-
log10(X[,1]))+rd^3}^(1/3)))/lambda)))*k_B*Temp)/(3*3.1416*dyn.vis*(2*({{(C1*rd^C2)/(C3*rd^C4-
log10(X[,1]))+rd^3}^(1/3)))))))^(1/3))/2.9)+((((kin.vis/(((1+(2*lambda/(2*({{(C1*rd^C2)/(C3*rd^C4-
log10(X[,1]))+rd^3}^(1/3))))*(1.257+0.4*exp(-0.55*(2*({{(C1*rd^C2)/(C3*rd^C4-
log10(X[,1]))+rd^3}^(1/3)))/lambda)))*k_B*Temp)/(3*3.1416*dyn.vis*(2*({{(C1*rd^C2)/(C3*rd^C4-
log10(X[,1]))+rd^3}^(1/3)))))))^(1/3))/2.9)^2)+1/sqrt(3)*atan((2*((((kin.vis/(((1+(2*lambda/(2*({{(C1*rd^C2)/(C3*rd
^C4-log10(X[,1]))+rd^3}^(1/3))))*(1.257+0.4*exp(-0.55*(2*({{(C1*rd^C2)/(C3*rd^C4-
log10(X[,1]))+rd^3}^(1/3)))/lambda)))*k_B*Temp)/(3*3.1416*dyn.vis*(2*({{(C1*rd^C2)/(C3*rd^C4-
log10(X[,1]))+rd^3}^(1/3)))))))^(1/3))/2.9)-1)/sqrt(3))+3.1416/6*sqrt(3)}^-1) + (2.5*10^-
3*0.14*((((((X[,2])*(2*({{(C1*rd^C2)/(C3*rd^C4-
log10(X[,1]))+rd^3}^(1/3)))^2*(1+(2*lambda/(2*({{(C1*rd^C2)/(C3*rd^C4-log10(X[,1]))+rd^3}^(1/3))))*(1.257+0.4*exp(-
0.55*(2*({{(C1*rd^C2)/(C3*rd^C4-log10(X[,1]))+rd^3}^(1/3)))/lambda))))/(18*dyn.vis))*(X[,5])^2)/kin.vis))^2)
)*{(1+((X[,6])*((((X[,9])/(exp(({{kx*(X[,6]))/(12*k_c^2*(1-
(X[,8])/(X[,7]))^2)}^(1/3)*(1+5*(z/(X[,3])))^(2/3)*{((X[,7])-(X[,8]))/((X[,3]))})*((z)/(X[,7])-
1))))/(X[,5]))*((C_B*((kin.vis/(((1+(2*lambda/(2*({{(C1*rd^C2)/(C3*rd^C4-
log10(X[,1]))+rd^3}^(1/3))))*(1.257+0.4*exp(-0.55*(2*({{(C1*rd^C2)/(C3*rd^C4-
log10(X[,1]))+rd^3}^(1/3)))/lambda)))*k_B*Temp)/(3*3.1416*dyn.vis*(2*({{(C1*rd^C2)/(C3*rd^C4-
log10(X[,1]))+rd^3}^(1/3)))))))^(-2/3))*(((((X[,9])/(exp(({{kx*(X[,6]))/(12*k_c^2*(1-
(X[,8])/(X[,7]))^2)}^(1/3)*(1+5*(z/(X[,3])))^(2/3)*{((X[,7])-(X[,8]))/((X[,3]))})*((z)/(X[,7])-
1))))*L_obs)/(kin.vis))^(-1/2)))+(C_IN*((2*({{(C1*rd^C2)/(C3*rd^C4-
log10(X[,1]))+rd^3}^(1/3)))/L_obs)*(2+log(4*L_obs/(2*({{(C1*rd^C2)/(C3*rd^C4-
log10(X[,1]))+rd^3}^(1/3)))))+(C_IM*((((((X[,2])*(2*({{(C1*rd^C2)/(C3*rd^C4-
log10(X[,1]))+rd^3}^(1/3)))^2*(1+(2*lambda/(2*({{(C1*rd^C2)/(C3*rd^C4-log10(X[,1]))+rd^3}^(1/3))))*(1.257+0.4*exp(-
0.55*(2*({{(C1*rd^C2)/(C3*rd^C4-log10(X[,1]))+rd^3}^(1/3)))/lambda))))/(18*dyn.vis)
)*((X[,9])/(exp(({{kx*(X[,6]))/(12*k_c^2*(1-(X[,8])/(X[,7]))^2)}^(1/3)*(1+5*(z/(X[,3])))^(2/3)*{((X[,7])-
(X[,8]))/((X[,3]))})*((z)/(X[,7])-1)))))/L_obs)/((((((X[,2])*(2*({{(C1*rd^C2)/(C3*rd^C4-
log10(X[,1]))+rd^3}^(1/3)))^2*(1+(2*lambda/(2*({{(C1*rd^C2)/(C3*rd^C4-log10(X[,1]))+rd^3}^(1/3))))*(1.257+0.4*exp(-
0.55*(2*({{(C1*rd^C2)/(C3*rd^C4-log10(X[,1]))+rd^3}^(1/3)))/lambda))))/(18*dyn.vis)
)*((X[,9])/(exp(({{kx*(X[,6]))/(12*k_c^2*(1-(X[,8])/(X[,7]))^2)}^(1/3)*(1+5*(z/(X[,3])))^(2/3)*{((X[,7])-
(X[,8]))/((X[,3]))})*((z)/(X[,7])-1)))))/L_obs)+(beta_IM)))^2))+(2.5*10^-
3*C_IT*(((((X[,2])*(2*({{C1*rd^C2)/(C3*rd^C4-log10(X[,1]))+rd^3}^(1/3)))^2*(1+(2*lambda/(2*({{(C1*rd^C2)/(C3*rd^C4-
log10(X[,1]))+rd^3}^(1/3))))*(1.257+0.4*exp(-0.55*(2*({{(C1*rd^C2)/(C3*rd^C4-
log10(X[,1]))+rd^3}^(1/3)))/lambda))))/(18*dyn.vis))*(X[,5])^2)/kin.vis)^2)
)*(X[,7])/((((0.41*((X[,7])-(X[,8])))/((1+5*(z/(X[,3])))*((X[,7])-
(X[,8]))/((X[,3])))))))/((((((kin.vis/(((1+(2*lambda/(2*({{(C1*rd^C2)/(C3*rd^C4-
log10(X[,1]))+rd^3}^(1/3))))*(1.257+0.4*exp(-0.55*(2*({{(C1*rd^C2)/(C3*rd^C4-
log10(X[,1]))+rd^3}^(1/3)))/lambda)))*k_B*Temp)/(3*3.1416*dyn.vis*(2*({{(C1*rd^C2)/(C3*rd^C4-
log10(X[,1]))+rd^3}^(1/3)))))))^(-2/3)/14.5)*{1/6*log(1+((((kin.vis/(((1+(2*lambda/(2*({{(C1*rd^C2)/(C3*rd^C4-
log10(X[,1]))+rd^3}^(1/3))))*(1.257+0.4*exp(-0.55*(2*({{(C1*rd^C2)/(C3*rd^C4-
log10(X[,1]))+rd^3}^(1/3)))/lambda)))*k_B*Temp)/(3*3.1416*dyn.vis*(2*({{(C1*rd^C2)/(C3*rd^C4-
log10(X[,1]))+rd^3}^(1/3)))))))^(1/3))/2.9))^2/(1-((((kin.vis/(((1+(2*lambda/(2*({{(C1*rd^C2)/(C3*rd^C4-
log10(X[,1]))+rd^3}^(1/3))))*(1.257+0.4*exp(-0.55*(2*({{(C1*rd^C2)/(C3*rd^C4-
log10(X[,1]))+rd^3}^(1/3)))/lambda)))*k_B*Temp)/(3*3.1416*dyn.vis*(2*({{(C1*rd^C2)/(C3*rd^C4-
log10(X[,1]))+rd^3}^(1/3)))))))^(1/3))/2.9)+((((kin.vis/(((1+(2*lambda/(2*({{(C1*rd^C2)/(C3*rd^C4-
log10(X[,1]))+rd^3}^(1/3))))*(1.257+0.4*exp(-0.55*(2*({{(C1*rd^C2)/(C3*rd^C4-
log10(X[,1]))+rd^3}^(1/3)))/lambda)))*k_B*Temp)/(3*3.1416*dyn.vis*(2*({{(C1*rd^C2)/(C3*rd^C4-
log10(X[,1]))+rd^3}^(1/3)))))))^(1/3))/2.9)^2)+1/sqrt(3)*atan((2*((((kin.vis/(((1+(2*lambda/(2*({{(C1*rd^C2)/(C3*rd
^C4-log10(X[,1]))+rd^3}^(1/3))))*(1.257+0.4*exp(-0.55*(2*({{(C1*rd^C2)/(C3*rd^C4-
log10(X[,1]))+rd^3}^(1/3)))/lambda)))*k_B*Temp)/(3*3.1416*dyn.vis*(2*({{(C1*rd^C2)/(C3*rd^C4-
log10(X[,1]))+rd^3}^(1/3)))))))^(1/3))/2.9)-1)/sqrt(3))+3.1416/6*sqrt(3)}^-1) + (2.5*10^-
3*0.14*((((((X[,2])*(2*({{(C1*rd^C2)/(C3*rd^C4-
log10(X[,1]))+rd^3}^(1/3)))^2*(1+(2*lambda/(2*({{(C1*rd^C2)/(C3*rd^C4-log10(X[,1]))+rd^3}^(1/3))))*(1.257+0.4*exp(-
0.55*(2*({{(C1*rd^C2)/(C3*rd^C4-
log10(X[,1]))+rd^3}^(1/3)))/lambda))))/(18*dyn.vis))*(X[,5])^2)/kin.vis))^2))*(X[,7])/((0.41*((X[,7])-
(X[,8])))/((1+5*(z/(X[,3])))*((X[,7])-(X[,8]))/((X[,3]))))
)-({(kx*(X[,6]))/(12*k_c^2*(1-(X[,8])/(X[,7]))^2)}^(1/3)*(1+5*(z/(X[,3])))^(2/3)*{((X[,7])-
(X[,8]))/((X[,3]))})/2)*tanh(((((kx*(X[,6]))/(12*k_c^2*(1-
```

```
(X[,8])/(X[,7]))^2)}^(1/3)*(1+5*(z/(X[,3])))^(2/3)*{((X[,7])-
(X[,8]))/((X[,3]))})^2/4+((X[,6])*((((X[,9])/(exp(({{kx*(X[,6]))/(12*k_c^2*(1-
(X[,8])/(X[,7]))^2)}^(1/3)*(1+5*(z/(X[,3])))^(2/3)*{((X[,7])-(X[,8]))/((X[,3]))})*((z)/(X[,7])-
1))))/(X[,5]))*((C_B*((kin.vis/(((1+(2*lambda/(2*{((C1*rd^C2)/(C3*rd^C4-
log10(X[,1]))+rd^3}^(1/3))))*(1.257+0.4*exp(-0.55*(2*({((C1*rd^C2)/(C3*rd^C4-
log10(X[,1]))+rd^3}^(1/3)))/lambda)))*k_B*Temp)/(3*3.1416*dyn.vis*(2*({((C1*rd^C2)/(C3*rd^C4-
log10(X[,1]))+rd^3}^(1/3)))))))^(-2/3))*(((((X[,9])/(exp(({{kx*(X[,6]))/(12*k_c^2*(1-
(X[,8])/(X[,7]))^2)}^(1/3)*(1+5*(z/(X[,3])))^(2/3)*{((X[,7])-(X[,8]))/((X[,3]))})*((z)/(X[,7])-
1))))*L_obs)/(kin.vis))^(-1/2)))+(C_IN*((2*({((C1*rd^C2)/(C3*rd^C4-
log10(X[,1]))+rd^3}^(1/3)))/L_obs)*(2+log(4*L_obs/(2*({((C1*rd^C2)/(C3*rd^C4-
log10(X[,1]))+rd^3}^(1/3)))))+(C_IM*((((((X[,2])*(2*({((C1*rd^C2)/(C3*rd^C4-
log10(X[,1]))+rd^3}^(1/3)))^2*(1+(2*lambda/(2*({((C1*rd^C2)/(C3*rd^C4-log10(X[,1]))+rd^3}^(1/3))))*(1.257+0.4*exp(-
0.55*(2*({((C1*rd^C2)/(C3*rd^C4-log10(X[,1]))+rd^3}^(1/3)))/lambda))))/(18*dyn.vis)
)*((X[,9])/(exp(({{kx*(X[,6]))/(12*k_c^2*(1-(X[,8])/(X[,7]))^2)}^(1/3)*(1+5*(z/(X[,3])))^(2/3)*{((X[,7])-
(X[,8]))/((X[,3]))})*((z)/(X[,7])-1)))))/L_obs)/((((((X[,2])*(2*({((C1*rd^C2)/(C3*rd^C4-
log10(X[,1]))+rd^3}^(1/3)))^2*(1+(2*lambda/(2*({((C1*rd^C2)/(C3*rd^C4-log10(X[,1]))+rd^3}^(1/3))))*(1.257+0.4*exp(-
0.55*(2*({((C1*rd^C2)/(C3*rd^C4-log10(X[,1]))+rd^3}^(1/3)))/lambda))))/(18*dyn.vis)
)*((X[,9])/(exp(({{kx*(X[,6]))/(12*k_c^2*(1-(X[,8])/(X[,7]))^2)}^(1/3)*(1+5*(z/(X[,3])))^(2/3)*{((X[,7])-
(X[,8]))/((X[,3]))})*((z)/(X[,7])-1)))))/L_obs)+(beta_IM)))^2))+(2.5*10^-
3*C_IT*(((((X[,2])*(2*({((C1*rd^C2)/(C3*rd^C4-log10(X[,1]))+rd^3}^(1/3)))^2*(1+(2*lambda/(2*({((C1*rd^C2)/(C3*rd^C4-
log10(X[,1]))+rd^3}^(1/3))))*(1.257+0.4*exp(-0.55*(2*({((C1*rd^C2)/(C3*rd^C4-
log10(X[,1]))+rd^3}^(1/3)))/lambda))))/(18*dyn.vis))*(X[,5])^2)/kin.vis)^2)
)*(X[,7])/((((0.41*((X[,7])-(X[,8])))/((1+5*(z/(X[,3])))*((X[,7])-
(X[,8]))/((X[,3])))))))^0.5))/(((((kx*(X[,6]))/(12*k_c^2*(1-
(X[,8])/(X[,7]))^2)}^(1/3)*(1+5*(z/(X[,3])))^(2/3)*{((X[,7])-
(X[,8]))/((X[,3]))})^2/4+((X[,6])*((((X[,9])/(exp(({{kx*(X[,6]))/(12*k_c^2*(1-
(X[,8])/(X[,7]))^2)}^(1/3)*(1+5*(z/(X[,3])))^(2/3)*{((X[,7])-(X[,8]))/((X[,3]))})*((z)/(X[,7])-
1))))/(X[,5]))*((C_B*((kin.vis/(((1+(2*lambda/(2*({((C1*rd^C2)/(C3*rd^C4-
log10(X[,1]))+rd^3}^(1/3))))*(1.257+0.4*exp(-0.55*(2*({((C1*rd^C2)/(C3*rd^C4-
log10(X[,1]))+rd^3}^(1/3)))/lambda)))*k_B*Temp)/(3*3.1416*dyn.vis*(2*({((C1*rd^C2)/(C3*rd^C4-
log10(X[,1]))+rd^3}^(1/3)))))))^(-2/3))*(((((X[,9])/(exp(({{kx*(X[,6]))/(12*k_c^2*(1-
(X[,8])/(X[,7]))^2)}^(1/3)*(1+5*(z/(X[,3])))^(2/3)*{((X[,7])-(X[,8]))/((X[,3]))})*((z)/(X[,7])-
1))))*L_obs)/(kin.vis))^(-1/2)))+(C_IN*((2*({((C1*rd^C2)/(C3*rd^C4-
log10(X[,1]))+rd^3}^(1/3)))/L_obs)*(2+log(4*L_obs/(2*({((C1*rd^C2)/(C3*rd^C4-
log10(X[,1]))+rd^3}^(1/3)))))+(C_IM*((((((X[,2])*(2*({((C1*rd^C2)/(C3*rd^C4-
log10(X[,1]))+rd^3}^(1/3)))^2*(1+(2*lambda/(2*({((C1*rd^C2)/(C3*rd^C4-log10(X[,1]))+rd^3}^(1/3))))*(1.257+0.4*exp(-
0.55*(2*({((C1*rd^C2)/(C3*rd^C4-log10(X[,1]))+rd^3}^(1/3)))/lambda))))/(18*dyn.vis)
)*((X[,9])/(exp(({{kx*(X[,6]))/(12*k_c^2*(1-(X[,8])/(X[,7]))^2)}^(1/3)*(1+5*(z/(X[,3])))^(2/3)*{((X[,7])-
(X[,8]))/((X[,3]))})*((z)/(X[,7])-1)))))/L_obs)/((((((X[,2])*(2*({((C1*rd^C2)/(C3*rd^C4-
log10(X[,1]))+rd^3}^(1/3)))^2*(1+(2*lambda/(2*({((C1*rd^C2)/(C3*rd^C4-log10(X[,1]))+rd^3}^(1/3))))*(1.257+0.4*exp(-
0.55*(2*({((C1*rd^C2)/(C3*rd^C4-log10(X[,1]))+rd^3}^(1/3)))/lambda))))/(18*dyn.vis)
)*((X[,9])/(exp(({{kx*(X[,6]))/(12*k_c^2*(1-(X[,8])/(X[,7]))^2)}^(1/3)*(1+5*(z/(X[,3])))^(2/3)*{((X[,7])-
(X[,8]))/((X[,3]))})*((z)/(X[,7])-1)))))/L_obs)+(beta_IM)))^2))+(2.5*10^-
3*C_IT*(((((X[,2])*(2*({((C1*rd^C2)/(C3*rd^C4-log10(X[,1]))+rd^3}^(1/3)))^2*(1+(2*lambda/(2*({((C1*rd^C2)/(C3*rd^C4-
log10(X[,1]))+rd^3}^(1/3))))*(1.257+0.4*exp(-0.55*(2*({((C1*rd^C2)/(C3*rd^C4-
log10(X[,1]))+rd^3}^(1/3)))/lambda))))/(18*dyn.vis))*(X[,5])^2)/kin.vis)^2)
)*(X[,7])/((((0.41*((X[,7])-(X[,8])))/((1+5*(z/(X[,3])))*((X[,7])-
(X[,8]))/((X[,3])))))))^0.5)}/{(1+((X[,6])*((((X[,9])/(exp(({{kx*(X[,6]))/(12*k_c^2*(1-
(X[,8])/(X[,7]))^2)}^(1/3)*(1+5*(z/(X[,3])))^(2/3)*{((X[,7])-(X[,8]))/((X[,3]))})*((z)/(X[,7])-
1))))/(X[,5]))*((C_B*((kin.vis/(((1+(2*lambda/(2*({((C1*rd^C2)/(C3*rd^C4-
log10(X[,1]))+rd^3}^(1/3))))*(1.257+0.4*exp(-0.55*(2*({((C1*rd^C2)/(C3*rd^C4-
log10(X[,1]))+rd^3}^(1/3)))/lambda)))*k_B*Temp)/(3*3.1416*dyn.vis*(2*({((C1*rd^C2)/(C3*rd^C4-
log10(X[,1]))+rd^3}^(1/3)))))))^(-2/3))*(((((X[,9])/(exp(({{kx*(X[,6]))/(12*k_c^2*(1-
(X[,8])/(X[,7]))^2)}^(1/3)*(1+5*(z/(X[,3])))^(2/3)*{((X[,7])-(X[,8]))/((X[,3]))})*((z)/(X[,7])-
1))))*L_obs)/(kin.vis))^(-1/2)))+(C_IN*((2*({((C1*rd^C2)/(C3*rd^C4-
log10(X[,1]))+rd^3}^(1/3)))/L_obs)*(2+log(4*L_obs/(2*({((C1*rd^C2)/(C3*rd^C4-
log10(X[,1]))+rd^3}^(1/3)))))+(C_IM*((((((X[,2])*(2*({((C1*rd^C2)/(C3*rd^C4-
log10(X[,1]))+rd^3}^(1/3)))^2*(1+(2*lambda/(2*({((C1*rd^C2)/(C3*rd^C4-log10(X[,1]))+rd^3}^(1/3))))*(1.257+0.4*exp(-
0.55*(2*({((C1*rd^C2)/(C3*rd^C4-log10(X[,1]))+rd^3}^(1/3)))/lambda))))/(18*dyn.vis)
)*((X[,9])/(exp(({{kx*(X[,6]))/(12*k_c^2*(1-(X[,8])/(X[,7]))^2)}^(1/3)*(1+5*(z/(X[,3])))^(2/3)*{((X[,7])-
(X[,8]))/((X[,3]))})*((z)/(X[,7])-1)))))/L_obs)/((((((X[,2])*(2*({((C1*rd^C2)/(C3*rd^C4-
log10(X[,1]))+rd^3}^(1/3)))^2*(1+(2*lambda/(2*({((C1*rd^C2)/(C3*rd^C4-log10(X[,1]))+rd^3}^(1/3))))*(1.257+0.4*exp(-
0.55*(2*({((C1*rd^C2)/(C3*rd^C4-log10(X[,1]))+rd^3}^(1/3)))/lambda))))/(18*dyn.vis)
)*((X[,9])/(exp(({{kx*(X[,6]))/(12*k_c^2*(1-(X[,8])/(X[,7]))^2)}^(1/3)*(1+5*(z/(X[,3])))^(2/3)*{((X[,7])-
(X[,8]))/((X[,3]))})*((z)/(X[,7])-1)))))/L_obs)+(beta_IM)))^2))+(2.5*10^-
3*C_IT*(((((X[,2])*(2*({((C1*rd^C2)/(C3*rd^C4-log10(X[,1]))+rd^3}^(1/3)))^2*(1+(2*lambda/(2*({((C1*rd^C2)/(C3*rd^C4-
log10(X[,1]))+rd^3}^(1/3))))*(1.257+0.4*exp(-0.55*(2*({((C1*rd^C2)/(C3*rd^C4-
log10(X[,1]))+rd^3}^(1/3)))/lambda))))/(18*dyn.vis))*(X[,5])^2)/kin.vis)^2)
)*(X[,7])/((((0.41*((X[,7])-(X[,8])))/((1+5*(z/(X[,3])))*((X[,7])-
(X[,8]))/((X[,3])))))))+(({(kx*(X[,6]))/(12*k_c^2*(1-(X[,8])/(X[,7]))^2)}^(1/3)*(1+5*(z/(X[,3])))^(2/3)*{((X[,7])-
(X[,8]))/((X[,3]))})/2)*tanh(((((kx*(X[,6]))/(12*k_c^2*(1-
(X[,8])/(X[,7]))^2)}^(1/3)*(1+5*(z/(X[,3])))^(2/3)*{((X[,7])-
(X[,8]))/((X[,3]))})^2/4+((X[,6])*((((X[,9])/(exp(({{kx*(X[,6]))/(12*k_c^2*(1-
(X[,8])/(X[,7]))^2)}^(1/3)*(1+5*(z/(X[,3])))^(2/3)*{((X[,7])-(X[,8]))/((X[,3]))})*((z)/(X[,7])-
```

```
1))))/(X[,5]))*((C_B*(((kin.vis/(((1+(2*lambda/(2*({(C1*rd^C2)/(C3*rd^C4-
log10(X[,1]))+rd^3}^(1/3))))*(1.257+0.4*exp(-0.55*(2*({(C1*rd^C2)/(C3*rd^C4-
log10(X[,1]))+rd^3}^(1/3)))/lambda)))*k_B*Temp)/(3*3.1416*dyn.vis*(2*({(C1*rd^C2)/(C3*rd^C4-
log10(X[,1]))+rd^3}^(1/3)))))))^(-2/3))*(((((X[,9])/(exp(({(kx*(X[,6]))/(12*k_c^2*(1-
(X[,8])/(X[,7]))^2)}^(1/3)*(1+5*(z/(X[,3])))^(2/3)*{((X[,7])-(X[,8]))/((X[,3]))})*((z)/(X[,7])-
1))))*L_obs)/(kin.vis))^(-1/2)))+(C_IN*((2*({(C1*rd^C2)/(C3*rd^C4-
log10(X[,1]))+rd^3}^(1/3)))/L_obs)*(2+log(4*L_obs/(2*({(C1*rd^C2)/(C3*rd^C4-
log10(X[,1]))+rd^3}^(1/3))))))+(C_IM*((((((X[,2])*(2*({(C1*rd^C2)/(C3*rd^C4-
log10(X[,1]))+rd^3}^(1/3)))^2*(1+(2*lambda/(2*({(C1*rd^C2)/(C3*rd^C4-log10(X[,1]))+rd^3}^(1/3))))*(1.257+0.4*exp(-
0.55*(2*({(C1*rd^C2)/(C3*rd^C4-log10(X[,1]))+rd^3}^(1/3)))/lambda))))/(18*dyn.vis)
)*((X[,9])/(exp(({(kx*(X[,6]))/(12*k_c^2*(1-(X[,8])/(X[,7]))^2)}^(1/3)*(1+5*(z/(X[,3])))^(2/3)*{((X[,7])-
(X[,8]))/((X[,3]))})*((z)/(X[,7])-1)))))/L_obs)/((((((X[,2])*(2*({(C1*rd^C2)/(C3*rd^C4-
log10(X[,1]))+rd^3}^(1/3)))^2*(1+(2*lambda/(2*({(C1*rd^C2)/(C3*rd^C4-log10(X[,1]))+rd^3}^(1/3))))*(1.257+0.4*exp(-
0.55*(2*({(C1*rd^C2)/(C3*rd^C4-log10(X[,1]))+rd^3}^(1/3)))/lambda))))/(18*dyn.vis)
)*((X[,9])/(exp(({(kx*(X[,6]))/(12*k_c^2*(1-(X[,8])/(X[,7]))^2)}^(1/3)*(1+5*(z/(X[,3])))^(2/3)*{((X[,7])-
(X[,8]))/((X[,3]))})*((z)/(X[,7])-1)))))/L_obs)+(beta_IM)))^2))+(2.5*10^-
3*C_IT*(((((X[,2])*(2*({(C1*rd^C2)/(C3*rd^C4-log10(X[,1]))+rd^3}^(1/3)))^2*(1+(2*lambda/(2*({(C1*rd^C2)/(C3*rd^C4-
log10(X[,1]))+rd^3}^(1/3))))*(1.257+0.4*exp(-0.55*(2*({(C1*rd^C2)/(C3*rd^C4-
log10(X[,1]))+rd^3}^(1/3)))/lambda))))/(18*dyn.vis))*(X[,5])^2)/kin.vis)^2)
)*(X[,7])/((((0.41*((X[,7])-(X[,8])))/((1+5*(z/(X[,3])))*((X[,7])-
(X[,8]))/((X[,3])))))))^0.5))/(((((kx*(X[,6]))/(12*k_c^2*(1-
(X[,8])/(X[,7]))^2)}^(1/3)*(1+5*(z/(X[,3])))^(2/3)*{((X[,7])-
(X[,8]))/((X[,3]))})^2/4+((X[,6])*((((X[,9])/(exp(({(kx*(X[,6]))/(12*k_c^2*(1-
(X[,8])/(X[,7]))^2)}^(1/3)*(1+5*(z/(X[,3])))^(2/3)*{((X[,7])-(X[,8]))/((X[,3]))})*((z)/(X[,7])-
1))))/(X[,5]))*((C_B*(((kin.vis/(((1+(2*lambda/(2*({(C1*rd^C2)/(C3*rd^C4-
log10(X[,1]))+rd^3}^(1/3))))*(1.257+0.4*exp(-0.55*(2*({(C1*rd^C2)/(C3*rd^C4-
log10(X[,1]))+rd^3}^(1/3)))/lambda)))*k_B*Temp)/(3*3.1416*dyn.vis*(2*({(C1*rd^C2)/(C3*rd^C4-
log10(X[,1]))+rd^3}^(1/3)))))))^(-2/3))*(((((X[,9])/(exp(({(kx*(X[,6]))/(12*k_c^2*(1-
(X[,8])/(X[,7]))^2)}^(1/3)*(1+5*(z/(X[,3])))^(2/3)*{((X[,7])-(X[,8]))/((X[,3]))})*((z)/(X[,7])-
1))))*L_obs)/(kin.vis))^(-1/2)))+(C_IN*((2*({(C1*rd^C2)/(C3*rd^C4-
log10(X[,1]))+rd^3}^(1/3)))/L_obs)*(2+log(4*L_obs/(2*({(C1*rd^C2)/(C3*rd^C4-
log10(X[,1]))+rd^3}^(1/3))))))+(C_IM*((((((X[,2])*(2*({(C1*rd^C2)/(C3*rd^C4-
log10(X[,1]))+rd^3}^(1/3)))^2*(1+(2*lambda/(2*({(C1*rd^C2)/(C3*rd^C4-log10(X[,1]))+rd^3}^(1/3))))*(1.257+0.4*exp(-
0.55*(2*({(C1*rd^C2)/(C3*rd^C4-log10(X[,1]))+rd^3}^(1/3)))/lambda))))/(18*dyn.vis)
)*((X[,9])/(exp(({(kx*(X[,6]))/(12*k_c^2*(1-(X[,8])/(X[,7]))^2)}^(1/3)*(1+5*(z/(X[,3])))^(2/3)*{((X[,7])-
(X[,8]))/((X[,3]))})*((z)/(X[,7])-1)))))/L_obs)/((((((X[,2])*(2*({(C1*rd^C2)/(C3*rd^C4-
log10(X[,1]))+rd^3}^(1/3)))^2*(1+(2*lambda/(2*({(C1*rd^C2)/(C3*rd^C4-log10(X[,1]))+rd^3}^(1/3))))*(1.257+0.4*exp(-
0.55*(2*({(C1*rd^C2)/(C3*rd^C4-log10(X[,1]))+rd^3}^(1/3)))/lambda))))/(18*dyn.vis)
)*((X[,9])/(exp(({(kx*(X[,6]))/(12*k_c^2*(1-(X[,8])/(X[,7]))^2)}^(1/3)*(1+5*(z/(X[,3])))^(2/3)*{((X[,7])-
(X[,8]))/((X[,3]))})*((z)/(X[,7])-1)))))/L_obs)+(beta_IM)))^2))+(2.5*10^-
3*C_IT*(((((X[,2])*(2*({(C1*rd^C2)/(C3*rd^C4-log10(X[,1]))+rd^3}^(1/3)))^2*(1+(2*lambda/(2*({(C1*rd^C2)/(C3*rd^C4-
log10(X[,1]))+rd^3}^(1/3))))*(1.257+0.4*exp(-0.55*(2*({(C1*rd^C2)/(C3*rd^C4-
log10(X[,1]))+rd^3}^(1/3)))/lambda))))/(18*dyn.vis))*(X[,5])^2)/kin.vis)^2)
)*(X[,7])/((((0.41*((X[,7])-(X[,8])))/((1+5*(z/(X[,3])))*((X[,7])-(X[,8]))/((X[,3])))))))^0.5))))))

N <- 100000
x1 = runif(1*N,0.1,1.0)           #RH
x2 = runif(1*N,1500,2000)         #rho
x3 = runif(1*N,10,100)            #L
x4 = runif(1*N,0.02,0.10)         #z0
x5 = runif(1*N,0.1,0.5)           #u_star
x6 = runif(1*N,1,4)               #LAI
x7 = runif(1*N,0.15,0.77)         #h
x8 = runif(1*N,0.10,0.49)         #d
x9 = runif(1*N,1,5)               #U

x_1 = runif(1*N,0.1,1.0)           #RH
x_2 = runif(1*N,1500,2000)         #rho
x_3 = runif(1*N,10,100)            #L
x_4 = runif(1*N,0.02,0.10)         #z0
x_5 = runif(1*N,0.1,0.5)           #u_star
x_6 = runif(1*N,1,4)               #LAI
x_7 = runif(1*N,0.15,0.77)         #h
x_8 = runif(1*N,0.10,0.49)         #d
x_9 = runif(1*N,1,5)               #U

Y1 = matrix(c(x1,x2,x3,x4,x5,x6,x7,x8,x9), nrow=N)
X1 = data.frame(matrix(Y1, nrow=N))
Y2 = matrix(c(x_1,x_2,x_3,x_4,x_5,x_6,x_7,x_8,x_9), nrow=N)
X2 = data.frame(matrix(Y2, nrow=N))
a = sobol2007(model = model, X1 = X1, X2=X2, nboot = 2000, conf= 0.95);a
```

Codes for Sobol' sensitivity test for Kouznetsov and Sofiev (2012) parameterization

```
#Dry deposition parameterization by Kouznetsov and Sofiev (2012)
#Sobol sensitivity test: Grass (the code is similar for other LUCs)
#Change LUC dependent parameters for other LUCs
#Change sensitivity ranges for other LUCs
set.seed(5)
library(sensitivity)
library(boot)
C1 = 0.2789
C2 = 3.115
C3 = 5.415*10^-11
C4 = -1.399
dp_a = 10
dp_i = dp_a*10^-6
rd = dp_i/2
k_B = 1.38*10^-23
Temp = 273.15+25
P = 101325
d_air = 3.7208*10^-10
lambda = (k_B*Temp)/(sqrt(2)*3.1416*P*d_air^2)
dyn.vis = ((5*10^-8)*Temp)+4*10^-6
kin.vis = ((9*10^-8)*Temp)+10^-5
a  =  2*10^-3
kin.vis = ((9*10^-8)*Temp)+10^-5
C_S = 0.003
C_R = 0.3
u.Uh = 0.3
eta_impSt.e2 = 0


model<-function(X) ((2*((((X[,3])*a)/kin.vis)^(-0.5))*(((kin.vis/(((1+(2*lambda/(2*({(C1*rd^C2)/(C3*rd^C4-
log10(X[,1]))+rd^3}^(1/3))))*(1.257+0.4*exp(-0.55*(2*({(C1*rd^C2)/(C3*rd^C4-
log10(X[,1]))+rd^3}^(1/3)))/lambda)))*k_B*Temp)/(3*3.1416*dyn.vis*(2*({(C1*rd^C2)/(C3*rd^C4-
log10(X[,1]))+rd^3}^(1/3))))))))^(-2/3))+(80*(X[,3])*(((2*({(C1*rd^C2)/(C3*rd^C4-
log10(X[,1]))+rd^3}^(1/3)))/(a))^2)*((((X[,3])*a)/kin.vis)^(0.5)))+(((2*((C_S+C_R/(X[,4]))^0.5))/(X[,3]))*(ifelse(
((((((X[,2])*(2*({(C1*rd^C2)/(C3*rd^C4-log10(X[,1]))+rd^3}^(1/3))))^2*(1+(2*lambda/(2*({(C1*rd^C2)/(C3*rd^C4-
log10(X[,1]))+rd^3}^(1/3))))*(1.257+0.4*exp(-0.55*(2*({(C1*rd^C2)/(C3*rd^C4-
log10(X[,1]))+rd^3}^(1/3)))/lambda))))/(18*dyn.vis))*(X[,3]))/a) - (((((C_S+C_R/(X[,4]))^0.5))^-
1)^2*(((X[,3])*a)/kin.vis))^(-0.5))>0.15,(exp((-0.1/(((((((X[,2])*(2*({(C1*rd^C2)/(C3*rd^C4-
log10(X[,1]))+rd^3}^(1/3))))^2*(1+(2*lambda/(2*({(C1*rd^C2)/(C3*rd^C4-log10(X[,1]))+rd^3}^(1/3))))*(1.257+0.4*exp(-
0.55*(2*({(C1*rd^C2)/(C3*rd^C4-log10(X[,1]))+rd^3}^(1/3)))/lambda))))/(18*dyn.vis))*(X[,3]))/a) -
(((((C_S+C_R/(X[,4]))^0.5))^-1)^2*(((X[,3])*a)/kin.vis))^(-0.5)) - 0.15 ) )-
(1/sqrt(((((((X[,2])*(2*({(C1*rd^C2)/(C3*rd^C4-
log10(X[,1]))+rd^3}^(1/3))))^2*(1+(2*lambda/(2*({(C1*rd^C2)/(C3*rd^C4-log10(X[,1]))+rd^3}^(1/3))))*(1.257+0.4*exp(-
0.55*(2*({(C1*rd^C2)/(C3*rd^C4-log10(X[,1]))+rd^3}^(1/3)))/lambda))))/(18*dyn.vis))*(X[,3]))/a) -
(((((C_S+C_R/(X[,4]))^0.5))^-1)^2*(((X[,3])*a)/kin.vis))^(-0.5))-
0.15)))),(eta_impSt.e2)))*((((((X[,2])*(2*({(C1*rd^C2)/(C3*rd^C4-
log10(X[,1]))+rd^3}^(1/3))))^2*(1+(2*lambda/(2*({(C1*rd^C2)/(C3*rd^C4-log10(X[,1]))+rd^3}^(1/3))))*(1.257+0.4*exp(-
0.55*(2*({(C1*rd^C2)/(C3*rd^C4-log10(X[,1]))+rd^3}^(1/3)))/lambda))))/(18*dyn.vis))*(X[,3]))/a)-
((C_S+C_R/(X[,4]))^0.5)*(((X[,3])*a)/kin.vis)^-0.5))+((((X[,2])*(2*({(C1*rd^C2)/(C3*rd^C4-
log10(X[,1]))+rd^3}^(1/3))))^2*(1+(2*lambda/(2*({(C1*rd^C2)/(C3*rd^C4-log10(X[,1]))+rd^3}^(1/3))))*(1.257+0.4*exp(-
0.55*(2*({(C1*rd^C2)/(C3*rd^C4-log10(X[,1]))+rd^3}^(1/3)))/lambda))))/(18*dyn.vis))*9.81))



N <- 100000
x1 = runif(1*N,0.1,1.0)            #RH
x2 = runif(1*N,1500,2000)          #rho
x3 = runif(1*N,0.1,0.5)            #u_star
x4 = runif(1*N,1,4)                #LAI
x_1 = runif(1*N,0.1,1.0)           #RH
x_2 = runif(1*N,1500,2000)         #rho
x_3 = runif(1*N,0.1,0.5)           #u_star
x_4 = runif(1*N,1,4)               #LAI
Y1 = matrix(c(x1,x2,x3,x4), nrow=N)
X1 = data.frame(matrix(Y1,nrow=N))
Y2 = matrix(c(x_1,x_2,x_3,x_4), nrow=N)
X2 = data.frame(matrix(Y2, nrow=N))
a = sobol2007(model = model, X1 = X1, X2=X2, nboot = 2000, conf = 0.95);a
```

Codes for Sobol' sensitivity test for Zhang and He (2014) parameterization

```
#Dry deposition parameterization by Zhang and He (2014)
#Sobol sensitivity test: Grass (the code is similar for other LUCs)
#Change LUC dependent parameters for other LUCs
#Change sensitivity ranges for other LUCs
set.seed(5)
library(sensitivity)
library(boot)
C1 = 0.4809
C2 = 3.082
C3 = 3.110*10^-11
C4 = -1.428
dp_a = 1
dp_i = dp_a*10^-6
rd = dp_i/2
k_B = 1.38*10^-23
Temp = 273.15+25
P = 101325
d_air = 3.7208*10^-10
lambda = (k_B*Temp)/(sqrt(2)*3.1416*P*d_air^2)
dyn.vis = ((5*10^-8)*Temp)+4*10^-6
z = 2
zR = 3.5
k_c = 0.41
# For PM2.5-10
b1= -7.9*10^-2
b2= 1.0*10^0
b3 = 6.6*10^-1
c1= 5.1*10^0
c2 = -4.2*10^0
c3 = 9.9*10^-1
LAImax = 4

model<- function(X) (1/(1/((((X[,2])*((2*({(C1*rd^C2)/(C3*rd^C4-
log10(X[,1]))+rd^3}^(1/3))))^2*(1+(2*lambda/(2*({(C1*rd^C2)/(C3*rd^C4-
log10(X[,1]))+rd^3}^(1/3))))*(1.257+0.4*exp(-0.55*(2*({(C1*rd^C2)/(C3*rd^C4-
log10(X[,1]))+rd^3}^(1/3)))/lambda))))/(18*dyn.vis))*9.81))+(1/(((log(zR/(X[,5]))-(ifelse((z/(X[,4])) <= 0,
(2*log(0.5*{1+(1-16*(z/(X[,4])))^0.5})),(-
5*(z/(X[,4])))))/(k_c*(X[,3])))+(1/((b1*(X[,3])+b2*(X[,3])^2+b3*(X[,3])^3)*(exp((c1*(X[,3])+c2*(X[,3])^2+c3*(X[,3
])^3)*(X[,6])/LAImax)-1))))))

N <- 100000
x1 = runif(1*N,0.1,1.0)           #RH
x2 = runif(1*N,1500,2000)         #rho
x3 = runif(1*N,0.1,0.5)           #u_star
x4 = runif(1*N,10,100)            #L
x5 = runif(1*N,0.02,0.10)         #z0
x6 = runif(1*N,1,4)               #LAI
x_1 = runif(1*N,0.1,1.0)           #RH
x_2 = runif(1*N,1500,2000)         #rho
x_3 = runif(1*N,0.1,0.5)           #u_star
x_4 = runif(1*N,10,100)            #L
x_5 = runif(1*N,0.02,0.10)         #z0
x_6 = runif(1*N,1,4)               #LAI
Y1 = matrix(c(x1,x2,x3,x4,x5,x6), nrow=N)
X1 = data.frame(matrix(Y1,nrow=N))
Y2 = matrix(c(x_1,x_2,x_3,x_4,x_5,x_6), nrow=N)
X2 = data.frame(matrix(Y2, nrow=N))
a = sobol2007(model = model, X1 = X1, X2=X2, nboot = 2000, conf = 0.95);a
```

Codes for Sobol' sensitivity test for Zhang and Sao (2014) parameterization

```
#Dry deposition parameterization by Zhang and Sao (2014)
#Sobol sensitivity test: Grass (the code is similar for other LUCs)
#Change LUC dependent parameters for other LUCs
#Change sensitivity ranges for other LUCs
set.seed(5)
library(sensitivity)
library(boot)
```

```
C1 = 0.2789
C2 = 3.115
C3 = 5.415*10^-11
C4 = -1.399
dp_a = 10
dp_i = dp_a*10^-6
rd = dp_i/2
k_B = 1.38*10^-23
Temp = 273.15+25
P = 101325
d_air = 3.7208*10^-10
lambda = (k_B*Temp)/(sqrt(2)*3.1416*P*d_air^2)
dyn.vis = ((5*10^-8)*Temp)+4*10^-6
kin.vis = ((9*10^-8)*Temp)+10^-5
Temp = 273.15+25
k =  0.41
z =  1
zd = 0.20
z0 = 0.3/1000
h_c = 0.3*z0
B1 = 0.45
d_c = 0.005
nB = 0.5
C_B = 0.467
beta_IM = 0.6
Ain = 150
b = 2
B2 = 3
Beta = 200
C_1 = 6
C_2 = 0.1
lambda_FAI = 0.4
n_FAI = (lambda_FAI)/(h_c*d_c)
q = (3.1416*d_c^2)/4
eta_BAI = n_FAI*q
lambda_FAIe = ((lambda_FAI)/(1-eta_BAI)^C_2)*exp((-C_1*lambda_FAI)/(1-eta_BAI)^C_2)
Tau_c_BY_Tau = (Beta*lambda_FAIe)/(1+Beta*lambda_FAIe)
Cd = 1/6
model<- function(X) ((((1/(((((X[,2])*(dp_i)^2*(1+(2*lambda/(2*({(C1*rd^C2)/(C3*rd^C4-
log10(X[,1]))+rd^3}^(1/3))))*(1.257+0.4*exp(-0.55*(2*({(C1*rd^C2)/(C3*rd^C4-
log10(X[,1]))+rd^3}^(1/3)))/lambda))))/(18*dyn.vis))*9.81)))+(((((exp(-
b*sqrt(((((X[,2])*(dp_i)^2*(1+(2*lambda/(2*({(C1*rd^C2)/(C3*rd^C4-log10(X[,1]))+rd^3}^(1/3))))*(1.257+0.4*exp(-
0.55*(2*({(C1*rd^C2)/(C3*rd^C4-
log10(X[,1]))+rd^3}^(1/3)))/lambda))))/(18*dyn.vis))*(X[,3]))/d_c)))*(((X[,3])/(X[,4])*h_c))*(((((C_B*((kin.vis
/(((1+(2*lambda/(2*({(C1*rd^C2)/(C3*rd^C4-log10(X[,1]))+rd^3}^(1/3))))*(1.257+0.4*exp(-
0.55*(2*({(C1*rd^C2)/(C3*rd^C4-
log10(X[,1]))+rd^3}^(1/3)))/lambda)))*k_B*Temp)/(3*3.1416*dyn.vis*(2*({(C1*rd^C2)/(C3*rd^C4-
log10(X[,1]))+rd^3}^(1/3)))))))^(-2/3)*(((X[,4])*d_c)/(kin.vis))^(nB-
1))+(((((((X[,2])*(dp_i)^2*(1+(2*lambda/(2*({(C1*rd^C2)/(C3*rd^C4-log10(X[,1]))+rd^3}^(1/3))))*(1.257+0.4*exp(-
0.55*(2*({(C1*rd^C2)/(C3*rd^C4-
log10(X[,1]))+rd^3}^(1/3)))/lambda))))/(18*dyn.vis))*(X[,3]))/d_c)/((((((X[,2])*(dp_i)^2*(1+(2*lambda/(2*({(C1*
rd^C2)/(C3*rd^C4-log10(X[,1]))+rd^3}^(1/3))))*(1.257+0.4*exp(-0.55*(2*({(C1*rd^C2)/(C3*rd^C4-
log10(X[,1]))+rd^3}^(1/3)))/lambda))))/(18*dyn.vis))*(X[,3]))/d_c)+beta_IM))^2)+(Ain*(X[,3])*(10^((-
((((X[,2])*(dp_i)^2*(1+(2*lambda/(2*({(C1*rd^C2)/(C3*rd^C4-log10(X[,1]))+rd^3}^(1/3))))*(1.257+0.4*exp(-
0.55*(2*({(C1*rd^C2)/(C3*rd^C4-
log10(X[,1]))+rd^3}^(1/3)))/lambda))))/(18*dyn.vis))*(X[,3]))/d_c)))*(2*(2*({(C1*rd^C2)/(C3*rd^C4-
log10(X[,1]))+rd^3}^(1/3)))/d_c))))*(Tau_c_BY_Tau/Cd))+(1+Tau_c_BY_Tau)*((kin.vis/(((1+(2*lambda/(2*({(C1*rd^C2
)/(C3*rd^C4-log10(X[,1]))+rd^3}^(1/3))))*(1.257+0.4*exp(-0.55*(2*({(C1*rd^C2)/(C3*rd^C4-
log10(X[,1]))+rd^3}^(1/3)))/lambda)))*k_B*Temp)/(3*3.1416*dyn.vis*(2*({(C1*rd^C2)/(C3*rd^C4-
log10(X[,1]))+rd^3}^(1/3)))))))^-1+10^((-3/(((((X[,2])*((2*({(C1*rd^C2)/(C3*rd^C4-
log10(X[,1]))+rd^3}^(1/3))))^2*(1+(2*lambda/(2*({(C1*rd^C2)/(C3*rd^C4-
log10(X[,1]))+rd^3}^(1/3))))*(1.257+0.4*exp(-0.55*(2*({(C1*rd^C2)/(C3*rd^C4-
log10(X[,1]))+rd^3}^(1/3)))/lambda))))/(18*dyn.vis))*(X[,3])^2)/kin.vis))))+((((X[,2])*((2*({(C1*rd^C2)/(C3*rd^
C4-log10(X[,1]))+rd^3}^(1/3))))^2*(1+(2*lambda/(2*({(C1*rd^C2)/(C3*rd^C4-
log10(X[,1]))+rd^3}^(1/3))))*(1.257+0.4*exp(-0.55*(2*({(C1*rd^C2)/(C3*rd^C4-
log10(X[,1]))+rd^3}^(1/3)))/lambda))))/(18*dyn.vis))*9.81))^-1)-
(1/(((((X[,2])*(dp_i)^2*(1+(2*lambda/(2*({(C1*rd^C2)/(C3*rd^C4-log10(X[,1]))+rd^3}^(1/3))))*(1.257+0.4*exp(-
0.55*(2*({(C1*rd^C2)/(C3*rd^C4-
log10(X[,1]))+rd^3}^(1/3)))/lambda))))/(18*dyn.vis))*9.81))))/(exp(((((1+(((((X[,2])*((2*({(C1*rd^C2)/(C3*rd^C4
-log10(X[,1]))+rd^3}^(1/3))))^2*(1+(2*lambda/(2*({(C1*rd^C2)/(C3*rd^C4-
log10(X[,1]))+rd^3}^(1/3))))*(1.257+0.4*exp(-0.55*(2*({(C1*rd^C2)/(C3*rd^C4-
log10(X[,1]))+rd^3}^(1/3)))/lambda))))/(18*dyn.vis))*9.81)^2/(X[,3])^2))^0.5)/(k*(X[,3])))*(log((z-zd)/(h_c-
zd))))/(1/(((((X[,2])*(dp_i)^2*(1+(2*lambda/(2*({(C1*rd^C2)/(C3*rd^C4-
```

```
log10(X[,1]))+rd^3}^(1/3))))*(1.257+0.4*exp(-0.55*(2*({(C1*rd^C2)/(C3*rd^C4-
log10(X[,1]))+rd^3}^(1/3)))/lambda))))/(18*dyn.vis))*9.81))))))))^-1)


N <- 100000
x1 = runif(1*N,0.1,1.0)            #RH
x2 = runif(1*N,1500,2000)          #rho
x3 = runif(1*N,0.1,0.5)            #u_star
x4 = runif(1*N,1,5)                #U
x_1 = runif(1*N,0.1,1.0)           #RH
x_2 = runif(1*N,1500,2000)         #rho
x_3 = runif(1*N,0.1,0.5)           #u_star
x_4 = runif(1*N,1,5)               #U
Y1 = matrix(c(x1,x2,x3,x4), nrow=N)
X1 = data.frame(matrix(Y1, nrow=N))
Y2 = matrix(c(x_1,x_2,x_3,x_4), nrow=N)
X2 = data.frame(matrix(Y2, nrow=N))
a = sobol2002(model = model, X1 = X1, X2=X2, nboot = 2000, conf= 0.95);a
```